INFORMATION TO USERS

This manuscript has been reproduced from the microfilm master. UMI films the text directly from the original or copy submitted. Thus, some thesis and dissertation copies are in typewriter face, while others may be from any type of computer printer.

The quality of this reproduction is dependent upon the quality of the copy submitted. Broken or indistinct print, colored or poor quality illustrations and photographs, print bleedthrough, substandard margins, and improper alignment can adversely affect reproduction.

In the unlikely event that the author did not send UMI a complete manuscript and there are missing pages, these will be noted. Also, if unauthorized copyright material had to be removed, a note will indicate the deletion.

Oversize materials (e.g., maps, drawings, charts) are reproduced by sectioning the original, beginning at the upper left-hand corner and continuing from left to right in equal sections with small overlaps.

ProQuest Information and Learning
300 North Zeeb Road, Ann Arbor, MI 48106-1346 USA
800-521-0600

University of Alberta

Numerical and Physical Simulation of the VAPEX Process

by

Xinjie Wu 

A thesis submitted to the Faculty of Graduate Studies and Research in partial fulfillment of the requirements of the degree of Master of Science

in

Petroleum Engineering

Department of Civil and Environmental Engineering

Edmonton, Alberta

Spring 2005

University of Alberta

Library Release Form

Name of Author: Xinjie Wu

Title of Thesis: Numerical and Physical Simulation of the VAPEX Process

Degree: Master of Science

Year this Degree Granted: 2005

.....

Signature

ABSTRACT

This research proposes an approach to simulate numerically the asphaltenes precipitation effect of the VAPEX process. The model built for the VAPEX process, which uses a commercial thermal reservoir simulation software package, was validated using published experimental data. The effect of the apparent dispersion coefficient on the performance was investigated. In addition, the model was used to design a physical experiment, which contains the main phenomena of the VAPEX process. The purpose of the physical experiment was to investigate the impact of asphaltenes precipitation on porous fluid flow under reservoir permeability conditions. On the basis of the results obtained in this study, it is concluded that the numerical model can reproduce the process very well. Moreover, it was found that, because of the significant viscosity reduction, no significant blockage of flow through the porous medium was observed.

ACKNOWLEDGEMENTS

I would like to express my appreciation and gratitude to my supervisors, Dr. Marcel Polikar and Dr. Luciane B. Cunha, for their support and guidance during the course of this study. I would also like to acknowledge the tremendous help I received from Dr. Ramon G. Bentsen in editing the thesis. Without their assistance, I would not have accomplished my goals.

I want to thank Mr. Ted Frauenfeld, as well as my classmates including Mr. Hyundon Shin and Dr. Oluropo Rufus Ayodele, for their valuable discussion and encouragement during the study.

Thanks are also extended to Sean Watt for his help on the experimental equipment supply and all my friends for their encouragement throughout this study.

This work is dedicated to my family. I want to express my sincere appreciation to my dear husband, Bing Han, for his generous support and understanding, and also to my parents and sister in China for their financial and moral support.

I am very grateful for the financial support from the National Science and Engineering Research Council (NSERC).

TABLE OF CONTENTS

LIST OF TABLES

LIST OF FIGURES

NOMENCLATURE

Ad	adsorbed component
c	concentration
C_s	concentration of solvent in the mixture
D	dispersion coefficient
g	acceleration due to gravity
h	thickness
HL	heat transfer rate
k	thermal transmissibility
K	permeability
L	length of the wells
N_s	dimensionless parameter that incorporates the effects of dispersive mixing
P	pressure
P_0	pressure right before the top of the core
P_1	pressure at the first pressure port along the core
P_2	pressure at the second pressure port along the core
P_3	pressure right after the bottom of the core
q	well flow rate
Q_o	oil production rate
r	solid rock matrix
s	solid and adsorbed components
S	saturation
T	transmissibility
U	internal energies as a function of temperature and phase composition
V	volume
V_c	critical velocity
W	water mole fraction
X	oil mole fraction
Y	gas mole fraction
ΔS_o	mobile oil saturation

$\Delta\rho$	difference in density between the solvent/oil mixture and the pure solvent
$\Delta\Phi$	potential
μ	viscosity of the mixture
ϕ	porosity

Subscripts

C	critical
f	fluid
g	gas
i	component
inj	injection
j	*phase type*
k	well layer number
l	liquid
m	solid (inert) rock matrix
n	upstream cell number
o	oil
r	relative
s	solvent
v	vapour
w	water

Abbreviations

AOSTRA	Alberta Oil Sands Technology and Research Authority
BT	Breakthrough
CMG	Computer Modeling Group
EOR	Enhanced Oil Recovery
EOS	Equation of State
GOR	Gas Oil Ratio

LV	Low Velocity
MRI	Magnetic Resonance Imaging
RC	Reservoir Condition
RF	Reaction Factor
RPM	Revolutions Per Minute
SC	Standard Condition
SAGD	Steam-Assisted Gravity Drainage
VAPEX	Vapour Extraction

1.0 INTRODUCTION

Canada is very rich in heavy oil and bitumen resources and most of them are located in Alberta with an estimated oil in place of 258.9 billion m^3 (Rahnama, 2003). Since 2001, total raw bitumen production has exceeded total conventional crude oil production even if only two per cent of the initial established crude bitumen reserve has been produced. The bitumen production in the overall Alberta crude oil and equivalent supply is expected to increase from 53 per cent in 2003 to some 80 per cent by 2013.

There are two different processes to recover heavy oil/bitumen: open pit mining and *in-situ* recovery through wells. Open pit mining can develop economically only those reserves with overburden formations of less than 70 m in thickness, which amount to less than 5% of the total resources (Jiang, 1997). *In-situ* recovery methods are used for much deeper reservoirs. These methods include thermal methods and non-thermal methods. Thermal methods recover the oil by introducing heat into the formation to reduce the oil viscosity and enhance the mobility of the oil. They are commonly used in heavy oil/oil sands recovery and include cyclic steam stimulation, steam flooding, *in situ* combustion and steam-assisted gravity drainage (SAGD) methods. Non-thermal methods, such as water flooding and gas injection, are mostly used for conventional oil recovery.

The vapour extraction (VAPEX) process, developed by Butler and Mokrys (1991), is a new non-thermal technology applied to heavy oil reservoirs. As is shown in Figure 1-1, the VAPEX process is very similar to the SAGD process (Figure 1-2) as they share the same gravity counter-current drainage concept. Two "parallel" horizontal wells are located one over the other (Butler and Mokrys, 1991). The upper horizontal well is the injector and the lower well is the producer. Injected solvents, such as butane and propane (Mokrys and Butler, 1993; Das and Butler, 1994a), rather than steam, are used to improve the mobility of the oil and to get higher oil recovery ratios.

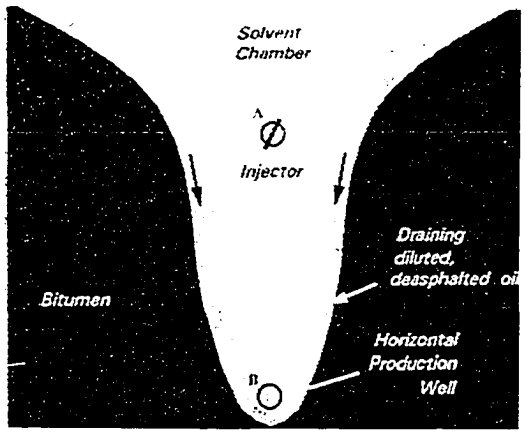

Figure 1-1: VAPEX Process (after Baytex Web)

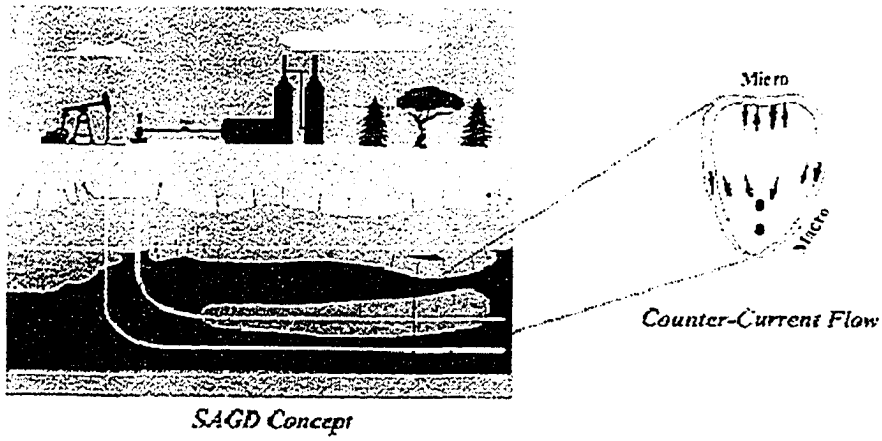

Figure 1-2: Steam-Assisted Gravity Drainage Concept (after World Energy Web)

Because the VAPEX process is a non-thermal recovery method, the steam generator, which is a must in current thermal recovery technologies, is not needed. Hence, the corresponding problems of carbon dioxide emissions, as well as water handling and disposal, are minimized significantly. The process also has the potential to upgrade the oil *in-situ* (Mokrys and Butler, 1993), and it has advantages for use in thin reservoirs and reservoirs with bottom water (Butler and Mokrys, 1991; Mokrys and Butler, 1993), where conventional thermal recovery methods are not economically or technically feasible.

This process is mechanistically complex and some questions regarding its expected performance are still pending (Das and Butler, 1994b; Oduntan et al., 2001; Dauba et al., 2002; Singhal et al., 2002; Boustani, 2002; Wen et al., 2004; Cuthiell and McCarthy, 2003; Cuthiell and Kissel, 2004). Thus, a numerical model is strongly needed to be able to predict the performance of this process, especially to predict the occurrence and effect of asphaltenes precipitation during the 'upgrading' process (Nghiem et al., 1993; Nghiem et al., 1998; Nghiem et al., 2000a, b; Nghiem et al., 2001).

The objective of this research is to find an approach to simulate numerically these types of solvent-based processes with acceptable accuracy, and to further the understanding of the effect of the operating strategy on VAPEX performance. A further objective is to study the effect of asphaltenes precipitation on fluid flow under reservoir permeability conditions using physical experiments.

2.0 REVIEW OF LITERATURE

2.1 VAPEX and its Main Mechanisms

Butler and Mokrys (1991) developed the VAPEX process, which is illustrated in Figure 1-1. The recovery concept is closely related to the steam-assisted gravity drainage (SAGD) process (Figure 1-2), but with the steam chamber replaced by a chamber containing hydrocarbon vapour (Butler and Mokrys, 1989, 1993b).

As suggested by Butler and Mokrys (Butler and Mokrys, 1993b; Mokrys and Butler, 1993), a solvent, such as propane, is injected at or near its dew point and the solvent forms a vapour chamber within the reservoir. The solvent vapour dissolves in the oil around the chamber and results in solution drainage, driven by gravity, to a horizontal production well placed lower in the formation. As in SAGD, the central feature is a pair of horizontal wells, shown in a cross-section in Figure 1-1.

2.1.1 Analytical Model

Butler and Mokrys (1989, 1991) have developed an analytic model describing the VAPEX process, which is very useful for understanding the key parameters affecting the process. The oil production rate, Q_o, is defined by:

$$Q_o = 2L\sqrt{2Kg\phi\Delta S_o hN_s} \qquad (1)$$

This model is very similar to that found for SAGD (Butler et al., 1979). The only difference is that, for SAGD, heat diffuses into the reservoir by thermal conduction (Butler and Mokrys, 1991), while, for VAPEX, the growth of the solvent chamber is controlled by molecular diffusion and convective dispersion (Butler and Mokrys, 1991; Cuthiell and McCarthy, 2003).

The factor 2 on the right hand side of Equation (1) accounts for drainage from both sides of the solvent chamber. The parameter N_s depends on the intrinsic dispersion of the solvent D_s (the model does not distinguish between transverse and longitudinal dispersion) as shown below (Butler and Mokrys, 1991; Cuthiell and McCarthy, 2003):

$$N_s = \int \frac{\Delta\rho(1-C_s)D_s}{\mu C_s} dC_s \qquad (2)$$

All of the quantities $\Delta\rho$, D_s and μ depend on the solvent fraction C_s.

2.1.2 Mass Transfer

Butler and Mokrys (1989) observed the boundary layer that is formed around a rising solvent finger by utilizing a vertical Hele-Shaw cell. They found that the boundary layer mechanism is relevant to miscible flooding in general.

As claimed by Shrivastava and Nghiem (2002), dispersive mixing is an important mechanism in a miscible displacement process. It determines the amount of the solvent that will mix with the *in-situ* oil and promote miscibility under favourable conditions. Bear (1988) studied the dynamics of fluids in porous media and claimed that mechanical dispersion and molecular diffusion are two basic elements of dispersive mixing. Mechanical dispersion is induced by variation in the convective velocity of the fluids and the tortuosity of the pores. Molecular diffusion, however, takes place solely due to the concentration gradient, with or without the presence of motion. Perkins and Johnston (1963) reviewed comprehensively the dispersion phenomena in porous media and assessed dispersive mixing using longitudinal and transverse dispersion coefficients. Nghiem et al. (2001) compared VAPEX simulation cases with both longitudinal and transverse dispersion, and with transverse dispersion only using a compositional simulator. Their conclusion was that transverse dispersion is the main mechanism for fluid mixing during the VAPEX process as the solvent-oil front moves in the direction perpendicular to the velocity.

2.1.3 Asphaltenes Precipitation

Asphaltenes are probably the components of crude oils that have been researched the most thoroughly, yet are the least understood (AOSTRA, 1998). They are not specific chemical components. There are two main ways to define asphaltenes. Hirschberg et al. (1984) and Leontarieis and Mansoori (1988) defined asphaltenes as the heavy hydrocarbon molecules that are suspended in the oil, and that are stabilized by resins adsorbed on their surface. The Alberta Oil Sands Technology and Research Authority (AOSTRA, 1998) defined asphaltenes as the components of bitumen which are soluble in toluene and which precipitate from solutions of normal paraffins under specified test conditions. A number of analytical methods are listed in the AOSTRA Technical Publication Series No. 5 (AOSTRA, 1998) to describe quantitatively the amount of asphaltenes in an oil sample.

Hirschberg et al. (1984) and Leontarieis and Mansoori (1988) suggested that asphaltenes precipitation results from changes in pressure, temperature and composition. These authors and Nghiem et al. (1993), Nghiem et al., (2000a, b), and Nghiem et al. (2001) also indicated that asphaltenes precipitation might occur during primary depletion or during the displacement of oil by rich gas or CO_2 in the upstream petroleum industry. After precipitation has occurred inside the reservoir, the asphaltenes precipitate can remain in suspension and flow within the oil phase, or it can deposit onto the rock surface (Leontarieis and Mansoori, 1988). Nghiem et al. (2000a, b) also clarified the definitions for precipitation and deposition. The term "precipitation" refers to the formation of asphaltenes precipitate as a result of thermodynamic equilibrium, and "deposition" refers to the settling of the precipitated asphaltenes onto the rock surface in a porous medium. The main deposition mechanisms are adsorption and mechanical entrapment. The deposited asphaltenes may cause plugging of the formation and alteration of rock wettability (from water-wet to oil-wet), which is undesirable for any oil recovery process because of the blockage of the pore-throats; that is, reduction of reservoir permeability (Leontarieis and Mansoori, 1988; Nghiem et al., 2000a, b; Nghiem et al., 2001).

Butler and Mokrys (1993b), Mokrys and Butler (1993) and Das and Butler (1994b) observed asphaltenes bands deposition in the VAPEX process in their Hele-Shaw experiments and later in their sand-pack experiments. The formation of the asphaltenes bands was caused by the solvent concentration gradient across the oil-solvent interface. No asphaltenes precipitate when the solvent contacts fresh bitumen because the solvent concentration is too low. When the solvent concentration builds up beyond a certain value, asphaltenes precipitate. The highest concentration of solvent occurs only in the outer section of the boundary. The pattern of deposition would not be the same in bitumen reservoirs as observed in the Hele-Shaw model, and the pressure conditions required for precipitation to occur will change because deasphalting is a thermodynamics phenomenon (Das and Butler, 1994b). However, the mechanism is expected to be similar.

Mokrys and Butler (1993) and Das and Butler (1994b) demonstrated that deasphalting takes place when the injected propane pressure is close to the vapour pressure of propane at the same temperature. Das and Butler further investigated the extent of the *in situ* deasphalting process in a large, scaled, physical model with Lloydminster-type heavy oil. They found (Das and Butler, 1994b) that the oil viscosity was lowered by a factor as high as 50 in scaled model experiments, which is the same extent of viscosity reduction as which occurs in benchtop mixing experiments.

The significant viscosity reduction of the oil by the solvent makes the VAPEX process very energy efficient. According to the correlations of Shu (1984), Mehrotra and Svreck (1986), and Das and Butler (1994b), a 0.18 propane fraction generates almost the same viscosity reduction as the one generated with a temperature of 80°C.

Mokrys and Butler (1993) and Das and Butler (1994b) addressed the issues of permeability reduction and lower production rate. Their investigation (Das and

Butler, 1994b) of these issues in a Hele-shaw cell, using propane and several heavy crudes, demonstrated that deasphalting does not stop oil flowing out of the reservoir. On the contrary, flow rate is enhanced due to reduction of viscosity by deasphalting. Also, the lower production rates for VAPEX as compared to SAGD may be compensated by the advantages of oil upgrading.

2.1.4 Viscous Fingering and Criterion of Instability in Miscible Displacement

For the miscible displacement of one fluid by another in porous media, the stability of the interface depends on the mobility ratio between the displacing and displaced fluids. If the displacing fluid is less viscous than the displaced fluid, any perturbation at the front may cause the displacing fluid to penetrate into the displaced fluid region to form fingers (Cuthiell and Kissel, 2004). Fingering will affect the success of the miscible drive and the recovery efficiency of the process by leading to an early breakthrough of displacing solvent, so the stability of a miscible displacement is of particular importance. A good deal of research (Dumoré, 1964; Coskuner and Bentsen, 1990; Cuthiell and McCarthy, 2003) has gone into the question of stability limits for viscous fingering; that is, the conditions under which fingers are suppressed. Miscible fingering is suppressed by transverse dispersion and by gravity. For example, vertical downwards displacement of oil by gas will help the gas-oil interface become stable as a consequence of the gravity difference (Cuthiell and Kissel, 2004).

Dumoré (1964) presented a criterion for predicting the instability of vertical flow in a homogeneous permeable medium saturated with oil, which is displaced downwards by a less viscous solvent. In the development of such a criterion, Dumoré assumed that a horizontal interface divided the oil and solvent initially, and that the pressure at the interface was distributed evenly. The interface is unstable when the pressure gradient in the solvent is greater than that in the oil. By applying Darcy's law, a critical velocity was obtained as follows:

$$V_c = \frac{\rho_o - \rho_s}{\mu_o - \mu_s} Kg \qquad (3)$$

Practically, the horizontal interface will be stable if the velocity has a lower value than the critical velocity. A similar determination of instability applies to the case of immiscible flow.

2.2 Experimental Investigation of the VAPEX Process

Many interesting experimental works regarding VAPEX have been published. Hele-Shaw cells (Butler and Mokrys, 1989; Mokrys and Butler, 1993; Das and Butler, 1994b), 2-D scaled models (Mokrys and Butler, 1993; Butler and Mokrys, 1993b; Luhning and Luhning, 1999 and Oduntan et al., 2001) packed with glass beads or synthetic medium, and even a 3-D physical model have been used (Jha et al., 1995). These studies were dedicated to furthering the understanding of the main mechanisms, assessing influential factors on the performance of the process and building a bridge between laboratory results and field prediction.

Butler and Mokrys (1991) studied the VAPEX process by conducting experiments with a line source cell, a point source cell (Hele-Shaw cell) and a packed cell, respectively. They recognized that the mechanisms involved in the VAPEX method are molecular diffusion, solvent dilution and gravity drainage. Propane was the solvent adopted.

Butler and Mokrys (1991) adopted the terms "displacement stage" and "drainage stage" to describe the VAPEX process. The displacement stage refers to the period when the dominant mechanism is solvent vapour pushing the oil. The drainage stage refers to the period when the solvent-oil drainage interface has been established and gravity drainage of diluted oil has taken over as the main mechanism. The gas displacement rate is always higher than the drainage rate Q_o. Moreover, it plays a significant role because it lasts 0.5 to 1.5 years in a field with a 10 m thick pay zone and longer in thicker reservoirs. This represents an opportunity for an early recovery of capital.

Asphaltenes deposition was observed in almost all the physical experiments that Butler and his colleagues performed (Butler and Mokrys, 1991, 1993a, 1993b; Butler and Jiang, 1997; Mokrys and Butler, 1993; Das and Butler, 1994a, 1994b). All of these experiments were carried out in cells with permeabilities ranging from 220 Darcies to 81,030 Darcies and pressures ranging from 700 kPa to 1,000 kPa under room temperature conditions. However, other researchers observed less asphaltenes deposition in their experiments.

In a joint industry project with 16 participants (Luhning et al., 2003), experiments in 2-D physical models for three different reservoir types were carried out. A low-pressure (700 kPa) model for the Athabasca Oil Sands reservoir and a high-pressure (12,000 kPa) model for the Cold Lake Oil sands and Southeast Alberta Heavy Oil Basin were used. Core material was used for all the experiments. Contrary to the previous references, the deasphalting effect was observed in only one of the experiments. Oduntan et al. (2001) only observed the phenomenon of deasphalting in the region near the production end of his 2-D scale-up model.

Dauba et al. (2002) performed a core flood experiment under reservoir conditions (4,500 kPa, 45 °C, 6.72 Darcy). Solvent (80% C_2 and 20% C_3) was injected top-down into an unconsolidated 35-cm long core. After conducting solubility and deasphaltenes tests, they concluded that, in the oil studied, the main mechanism, which causes the viscosity reduction, was the dilution effect and not asphalthene flocculation. The latter occurs only for an amount of gas injection that was not technically feasible (molar fraction of solvent 0.934) to reach.

Singhal et al. (2002) conducted VAPEX experiments to investigate the compositional changes in the produced oil and in the remaining oil within the model. They only detected a subtle reduction in asphaltenes content in the produced oil. And the oil production rates shown for Athabasca bitumen indicated that complete deasphalting is not necessary for significant viscosity reduction to occur. They also conducted some 30 VAPEX physical experiments over the past

6 years to check the possibility of plugging in a porous medium with low permeability. No evidence of plugging was observed with sand packs having a permeability exceeding one Darcy. Because of the strong effect of operating conditions on the asphaltenes deposition and the absent information of operating conditions they used, this conclusion need further validation with more experiments by other researchers.

Fisher et al. (2002) obtained an important finding through their physical experiment combined with the Magnetic Resonance Imaging (MRI) technique; that is, the presence of connate water seems to promote the deasphalting process. It can be seen clearly in the images for the Athabasca oil-propane system that no deasphalting was apparent in the no connate water series, while in the series with connate water, asphaltenes streaks were apparent at a low concentration and the vapour chamber had advanced much farther. However, the role of connate water was not well understood yet.

In addition to the experiments directed towards investigating the main recovery mechanisms of the VAPEX process, some experiments concentrated on the effect of the operating strategy on the performance of the process. Mokrys and Butler (1993) discussed the effect of factors such as injected/produced gas oil ratio (GOR), different saturation pressures and vapour chamber temperatures on the rate of oil production based on scaled physical experiment results. Das and Butler (1994a) carried out a scaled packed cell experiment using butane instead of propane as a solvent and recognized that the production rate is different though the mechanism of the VAPEX process is basically the same for propane and butane. Additionally, they found out that the flow rates in a packed cell are higher than those obtained by scaling up the results of Hele-Shaw cell experiments carried out with butane using identical conditions of temperature and pressure. The reason for the higher flow rate was believed to be the extended interfacial area of contact (Das and Butler, 1994a).

Jiang and Butler (1996) carried out experimental studies on the effects of reservoir heterogeneity on the VAPEX process using a 2-D packed model. These authors investigated the effects of low-permeability layers and lenses on the VAPEX process. Low permeability layers or lenses result in a lower oil production rate than that achieved using a homogeneous model with high permeability. Low permeability layers or lenses result in a wider vapour chamber and oil is extracted from a larger area.

Jiang (1997) carried out experiments in a scaled packed model in which Tangleflags heavy oil was extracted by co-injection of solvent (n-butane) and non-condensable gas (nitrogen) at a pressure above the vapour pressure of the injected solvent. The effect of well configuration on the initial displacement, profiles of the vapour chamber in the formation, and deasphalting and its effect on the flow of diluted oil were studied. The results showed that, for conventional heavy oil, top injection was better than bottom injection for both homogeneous and heterogeneous reservoirs. This was particularly the case when an injector was placed horizontally apart from a producer. The major finding has been that wider lateral well spacing allows for higher production rates and makes the process more economic.

Currently, the majority of the physical experiments are focusing on the determination of the scale dependence of dispersion so that the laboratory results obtained in sand-packed models can be scaled-up reasonably to field scale (Boustani, 2002; Yazdani et al., 2004; and Wen et al., 2004).

2.3 Numerical Simulation of the VAPEX Process

To simulate numerically the VAPEX process, one must be able to simulate the two most important mechanisms in the VAPEX process (Nghiem et al., 2001), which are (1) mixing of fluid through convective dispersion and (2) asphaltenes precipitation. These two aspects posed new challenges for compositional reservoir simulation development.

2.3.1 Numerical Simulation of Dispersive Mixing

Nghiem et al. (2000a) modeled effectively the mixing mechanisms with a total dispersion coefficient. The total dispersion coefficient represents the combined effect of molecular diffusion and convective dispersion. They discussed the sensitivity of the simulation results to different dispersivity levels and concluded that dispersivity could be used as a parameter for matching laboratory and field observations.

Nghiem et al. (2001) implemented a new method to handle the full dispersion tensor. The molecular diffusion was calculated from Sigmund's (1976) correlation. The effect of dispersivity on the simulation of the VAPEX process was investigated using Lindbergh oil, and it was found that the use of zero longitudinal dispersivities and non-zero transverse dispersivities improved the simulation results as compared to the use of isotropic dispersivities. It was assumed that the dispersivities for the oil and the gas were the same.

2.3.2 Numerical Simulation of Asphaltenes Precipitation

A model that is able to correlate and predict asphaltenes precipitation is highly desirable for the VAPEX process because it would allow the optimal design of injection/production schemes to control asphaltenes precipitation at the expected level. Nghiem et al. (1993) have summarized many thermodynamic models that describe the phase behaviour of asphaltenes precipitation in the literature, which include a liquid solubility model, a thermodynamic colloidal model, a thermodynamic micellization model, and a pure solid model. They also proposed their incorporation approach of the pure solid model into an equation of state (EOS) compositional simulator (Nghiem et al., 1993). Some of these models are described briefly as follows:

Solubility model

This is the first approach to model asphaltenes precipitation in petroleum engineering, which was developed by Hirschberg et al. (1984). The mixture was

split into a vapour and a liquid phase by vapour-liquid equilibrium calculations with a cubic equation of state. The liquid was then divided into three components: asphaltenes, resin and a component for the remaining oil and solvent. The performance of the model depended on the molar volumes and solubility parameters of the oil, resins and asphaltenes. Burke et al. (1990), Novosad and Costain (1990) and Kokal et al. (1992) used this approach to match their experimental data with a limited degree of success, because this model can only reproduce the asphaltenes behaviour qualitatively, not quantitatively.

Solid model

The simplest model for the asphaltenes precipitation is the single-component solid model tried by Gupta (1986) and Thomas et al. (1992). The precipitated asphaltenes were represented as a pure solid while the oil and gas phases were modelled with a cubic equation of state. The shortcoming of this model is that a large number of empirical parameters and excessive tuning are required to match experimental data; for example, compositional dependence for interaction coefficients and solid fugacity. These operations made the model highly empirical and difficult to use. Thomas et al. (1992) also observed that this model did not exhibit the correct behaviour with increasing solvent concentration.

Nghiem et al. proposed approach

Nghiem et al. (1993) proposed a model for asphaltenes precipitation during solvent injection, which overcomes the shortcoming of the previous models. It has the ability to make quantitative predictions, has a small number of adjustable parameters, is compatible with flash calculations with an equation of state, and is computationally efficient for potential inclusion in a compositional model.

The asphaltenes precipitate was modeled as a pure solid that may flow as a suspension in the oil phase or deposit on the rock surface. This model was demonstrated to be able to make quantitative predictions of experimental data from the literature as well as additional data from industry (Nghiem et al., 2000b).

The success of the approach was based on the approach for characterizing the asphaltenes component-- splitting the heaviest component in the oil (e.g. C31+) into a non-precipitating component (C31A+) and a precipitating component (C31B+). These two components have identical critical properties and acentric factors, but different interaction coefficients with the light components. This approach resolves most of the modelling deficiencies associated with the solid model (Gupta, 1986; Thomas et al., 1992) reported in the literature.

Nghiem et al. (1998) described the incorporation of an asphaltenes deposition and plugging model in an equation-of-state (EOS) compositional simulator. The deposition was considered as an adsorption process, and the permeability reduction (plugging) resulting from it was modeled with a resistance factor. The adsorption process is assumed to follow a Langmuir isotherm. This thermodynamic model showed a good match of the asphaltenes precipitation for a North Sea oil with hydrocarbon gas, for a Canadian crude with CO_2, and for a heavy oil with propane and reproduced the asphaltenes precipitation behaviour of the VAPEX process observed in the laboratory.

Nghiem et al. (2001) enhanced the model described above. The enhanced model accounts for the fact that the precipitated components (asphaltenes and resins) may form associations, resulting in larger aggregates. The enhanced model also includes the formation of a second solid through a chemical reaction that addresses this issue, so that the asphaltenes precipitate is modeled as two solids: Solid 1 (S1), which is in equilibrium with the asphaltenes component in the oil phase, and Solid 2 (S2), which is formed from Solid 1 through a chemical reaction (the association of asphaltenes and resins molecules) and its precipitation can be made irreversible.

Nghiem et al. (2001) have run a model that accounts for both reversible and irreversible asphaltenes precipitation. Both S1 and S2 are allowed to flow with the oil and do not deposit through adsorption or mechanical entrapment. The modeled

results showed that the region of reversible asphaltenes (S1) precipitation moves with the front, whereas a large amount of irreversible solid (S2) is left in the residual oil left behind the front. The component flow equations, the water flow equation, and the solids S2 flow equation together with the phase equilibrium equation and the reaction rate equation provide the necessary equations for compositional simulation of the VAPEX process.

2.4 Selection of the Simulator Type

Most of the numerical simulation methods discussed above make use of a fully compositional simulator (Computer Modeling Group Ltd., GEM Manual, Version 2002), while several published papers use a semi-compositional and thermal reservoir simulator (Computer Modeling Group Ltd., STARS Manual, Version 2002) operated in a non-thermal mode (Dauba et al., 2002; and Cuthiell and McCarthy, 2003; Luhning et al., 2003). Dauba et al. (2002) undertook simulations of their core-flood experiment with both a semi-compositional and a fully compositional model and compared the difference in the results. They concluded that STARS could reproduce the BT time, pressure profile at the injector, and the cumulative oil and gas production of the VAPEX process as well as GEM.

The joint industry project led by Luhning et al. (2003) carried out lab-scale numerical simulations of the VAPEX process on Athabasca/Cold Lake Oil sands using the STARS simulator. The commercial scale forecasts are also going to be done using STARS. The simulations showed that the experimentally determined VAPEX front agreed with that predicted numerically. Cuthiell and McCarthy (2003) also employed STARS to verify the mechanisms present in their VAPEX experiments. They determined that the numerical simulations were able to match some of the fingering features, as well as the later VAPEX –like stages of the displacements. All of the above researchers did not consider the asphaltenes deposition effect in their simulations.

The ability of STARS to simulate asphaltenes deposition in the solvent process

has not been published; rather, a template for the used of a reaction model to simulate asphaltenes deposition during pressure depletion was provided in the STARS software package. Consequently, it is concluded to try STARS to simulate the VAPEX process including asphaltenes precipitation mechanism.

3.0 STATEMENT OF THE PROBLEM

Numerical simulation is a useful tool for understanding the mechanisms and performance of the VAPEX process. Currently, work is being carried out on the development and validation of simulation techniques using a compositional simulator (GEM) or a semi-compositional simulator (STARS) for reproducing the VAPEX process properly. Although previous research has indicated that STARS has the ability to simulate reliably the VAPEX process, more work is needed to confirm that the main mechanisms and phenomena of the process can be represented properly by STARS.

In this research, it is planned to develop a non-thermodynamic simulation approach for describing asphaltenes precipitation in the VAPEX process by combining the theory of asphaltenes precipitation modeling developed for a compositional simulator and the advantages of STARS. Qualitative and quantitative validation as well as the simulation results of the simulation model will be presented and discussed. Finally, the numerical model built will be used to design operating strategies for a physical experiment.

It is plausible that asphaltenes precipitation during the VAPEX process might plug the pore throats under reservoir conditions. Most of the investigations of this issue were performed on scaled physical models with significant permeability. Only one set of experiments (Singhal et al., 2002) was conducted with reservoir permeability. The researchers concluded that no evidence of plugging was found with the sand pack permeability exceeding one Darcy. It is therefore necessary to conduct more physical experiments with reservoir permeability (less than 5 Darcies) to investigate this issue.

4.0 NUMERICAL INVESTIGATION OF THE VAPEX PROCESS

4.1 Numerical Model Design

STARS (CMG Ltd. manuals, version 2002), a computer software model released by the Computer Modeling Group, is an advanced multicomponent thermal reservoir simulator useful for simulating thermal recovery processes. The mathematical and numerical models used in STARS are described briefly in Appendix A. It has been reported (Cuthiell and McCarthy, 2003; Luhning et al., 2003) that STARS can also simulate the VAPEX process, a non-thermal process, successfully and quickly, when operated in the isothermal mode. In the simulations conducted here, STARS was used in all the runs. The reservoir geometry, fluid/rock parameters and operation conditions used for this study were based on the 2-D scaled physical experiment published by Mokrys and Butler (1993). Each of the factors affecting the simulation is discussed below.

4.1.1 Geometry, Well Position and Grid System

The numerical model, as does the physical experiment model (Mokrys and Butler, 1993), has a width (x-direction) of 69.8 cm, a thickness (y-direction) of 3.5 cm and a height (z-direction) of 21.7 cm, corresponding to a 15*1*6 grid number. The two-dimensional (x-z) numerical model was developed to represent the 2-D scaled VAPEX physical experiment.

As was with the well configuration in the physical model, the injector was placed at the right top of the model and the producer was located at the left bottom of the model. The well positions and grid system are shown in Figure 4-1.

In multidimensional models, numerical dispersion leads to an interesting and sometimes troublesome phenomenon in which calculated performance is influenced by the orientation of the grid relative to the location of the injection and production wells (CMG Ltd. manuals, version 2002). The grid orientation effect is usually important in simulations in which the displacing phase is much

more mobile than the displaced phase (as in thermal or solvent processes involving heavy oil).

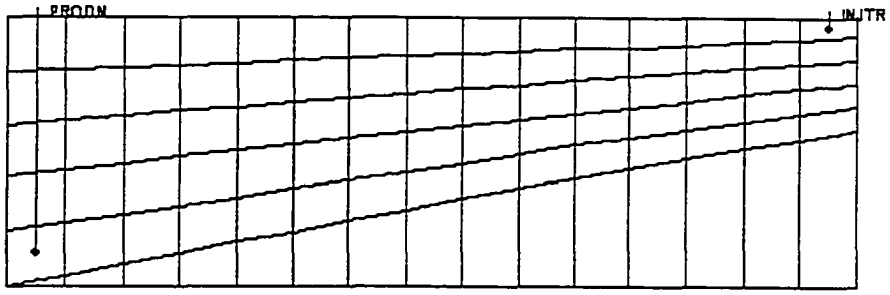

Figure 4-1: Grid System for History Match

To reduce the numerical dispersion to the maximum extent, the grid system was built as shown in Figure 4-1 to try to follow better the evolution of the solvent – oil interface in the simulation of the VAPEX process (Shrivastava and Nghiem, 2002). As a result, the grid lines of the top five layers dip from right to the left. That is, the grid height for the top 5 grid layers decreases in the z-direction from a constant 4.35 cm on the left side to a low of 1.52 cm on the right side. The bottom layer, the 6^{th} grid layer, has a thickness of zero on the left and thickness as large as 12.71 cm on the right. That is, this layer pinches out and has the shape of a triangle. This approach is believed to be adequate for hard-to-be-reached locations. Its utility will be checked by analyzing the recovery results obtained during the course of the study.

In the x-direction, a constant grid size of 4.65 cm divides the total width of 69.8 cm into 15 grid blocks. In the y-direction, there is only one block of 3.5 cm, which is the thickness of the physical model. A corner point, instead of a center block gridding system, is used to describe the z-direction of this complicated system.

4.1.2 Reservoir/Fluid Properties and Fluid Definition

The reservoir properties used in the simulation are the same as those of the physical experiment that is going to be matched. The fluid properties (coefficients

of liquid heat capacity correlations, coefficient in vapourization enthalpy correlation and KV values and so forth) are obtained from the template data file of 'Stars Test Bed No. 5' attached to the STARS simulator package. The viscosity of Lloyd-O (representing the deasphalted oil component) is obtained based on the viscosity of upgraded Lloydminster oil, while the viscosity of asphaltenes is calculated using the logarithmic mixing rule. The rock properties (relative permeability curves) were taken from the data file mentioned above. The capillary pressure was assumed to be 0 kPa because of its originally low value and the demonstrated miscible effect (Butler and Mokrys, 1989). The rock properties are reported in Appendix B (see Figure B-1).

Table 4-1: Reservoir and Fluid Properties

Reservoir Pressure	847.2 kPa
Reservoir Temperature	20 °C
Reference Pressure	101.3 kPa
Reference Temperature	20 °C
Capillary Pressure	0 kPa
Permeability	1,135 Darcy
Porosity	39.1%
Water Saturation	0.1%
Oil API	11°
Asphaltenes content	15.6%
Oil viscosity @ 20°C	10,000 cp

The reservoir and injected fluid were defined in two different ways to try to check the effect of different mechanisms on the final performance of the process, as well as to match the published physical experimental results. The Model 1 system adopts four components named as water, Lloyd-O, asphalt, and propane. Initially, this defined asphalt component is dissolved in the component Lloyd-O at 15.6% by volume to form the original oil. The Model 2 system adopts six components

named as water, Lloyd-O, C31A+, C31B+, asphalt and propane. This system was chosen to consider the reaction from C31B+ to asphaltenes according to the solid model theory. (Nghiem et al., 2000a, 2000b, 2001) and also to check the effect of reactant combination on the final performance.

4.1.3 Gas Type, Initial Pressure, Operating Control and Boundary Conditions

Because the physical experiment that was going to be matched was performed under a pressure of 847.2 kPa with propane injection, the numerical simulation was also run under the same conditions. The gas type and initial/operating pressure were chosen as follows.

As the critical operating characteristic for the VAPEX process was injecting hydrocarbon at or near its dew point, the optimal condition to obtain the deasphalting effect, the gas type was chosen as propane, which made it easier to reach the dew point pressure under normal room temperature conditions (20-23°C). The relationship of propane vapour pressure with temperature is shown in Appendix C (see Figure C-1). The experiment was conducted at 20°C, which corresponded to a vapour pressure of 859 kPa. Consequently, the initial pressure was chosen as 847.2 kPa to give some pressure difference for gas injection.

Because the physical experiment that was going to be matched was to be operated by controlling the oil and gas production rate instead of the gas injection rate and production pressure, the numerical simulation was conducted under the same conditions. A no flow boundary was used for all sides of the model because the experiment was operated in a cell isolated to the outside.

4.1.4 Conditions of Numerical Runs

The detailed descriptions of the numerical runs are listed in Table 4-2. The case number, model type, reaction factor, operation condition and so forth are given in the Table. Also, the related data files are listed in Appendices E, F and G.

Table 4-2: Conditions of Numerical Runs

Case No.	Model Type	Component No.	Reactant	Reaction Factor	Explicit Dispersion Coefficient (m^2/s)	Gas Production Rate Control (cm^3/min)	Oil Production Rate Control (cm^3/min)	Injection Well	Production Well	Well Distance(cm)	Initial Pressure(kPa)	Injection Pressure(kPa)	Comment
1	No Reaction Considered	4	N/A	N/A	0	50	10.6	Right top	Left bottom	67.42	847.2	848	Linear Kr curves
2		4	N/A	N/A	0	50	10.6	Right top	Left bottom	67.42	847.2	848	non-linear Kr curves
3		4	N/A	N/A	0	50	10.6	Right top	Left bottom	67.42	847.2	848	rectangular grid
4		4	N/A	N/A	0	40	10.6	Right top	Left bottom	67.42	847.2	848	Linear Kr curves
5		4	N/A	N/A	0	30	10.6	Right top	Left bottom	67.42	847.2	848	
6		4	N/A	N/A	0	50	3	Right top	Left bottom	67.42	847.2	848	
7		4	N/A	N/A	0	50	10.6	Direct top of producer	Left bottom	4.35	847.2	848	
8		4	N/A	N/A	0	50	10.6	Left top	Left bottom	17.35	847.2	848	
9		4	N/A	N/A	0	50	10.6	Right top	Left bottom	67.42	750	790	
10		4	N/A	N/A	0	50	10.6	Right top	Left bottom	67.42	700	740	
11		4	N/A	N/A	0	50	10.6	Right top	Left bottom	67.42	600	640	
12		4	N/A	N/A	0	50	10.6	Right top	Left bottom	67.42	200	240	
13		4	N/A	N/A	0	50	10.6	Right top	Left bottom	67.42	2000	2040	
14		4	N/A	N/A	0	50	10.6	Right top	Left bottom	67.42	840	880	
15		4	N/A	N/A	0	50	10.6	Right top	Left bottom	67.42	890	930	
16	Reaction Considered	6	C31B+	0.0004	0	50	10.6	Right top	Left bottom	67.42	847.2	848	
17		6	C31B+	0.0008	0	50	10.6	Right top	Left bottom	67.42	847.2	848	
18		6	C31B+	0.002	0	50	10.6	Right top	Left bottom	67.42	847.2	848	
19		6	C31B+	43.2	0	50	10.6	Right top	Left bottom	67.42	847.2	848	
20		6	C31B+, C3H8	0.0004	0	50	10.6	Right top	Left bottom	67.42	847.2	848	
21		6	C31B+	0.0004	5.00E-05	50	10.6	Right top	Left bottom	67.42	847.2	848	
22		6	C31B+	0.0004	0	50	3.3	Right top	Left bottom	67.42	847.2	848	

4.2 Numerical Simulation Results and Discussion

4.2.1 Quantitative Validation

4.2.1.1 Relative Permeability Curve Effect

Linear relative permeability curves (Appendix B, Figure B-1) and non-linear relative permeability curves (Appendix B, Figure B-2, Donnelly, 1997) were used in Cases 1 and 2 and run to match the shape of the physical experimental data from Mokrys and Butler (1993). The performance comparison is shown in Figure 4-2. It can be seen clearly that Case 1 with linear relative permeability curves matched the physical experiment. This supports the opinion of Butler and Mokrys (1989) that the boundary layer mechanism of the VAPEX process is a miscible process. Consequently, linear relative permeability curves were used in all the following numerical simulation runs.

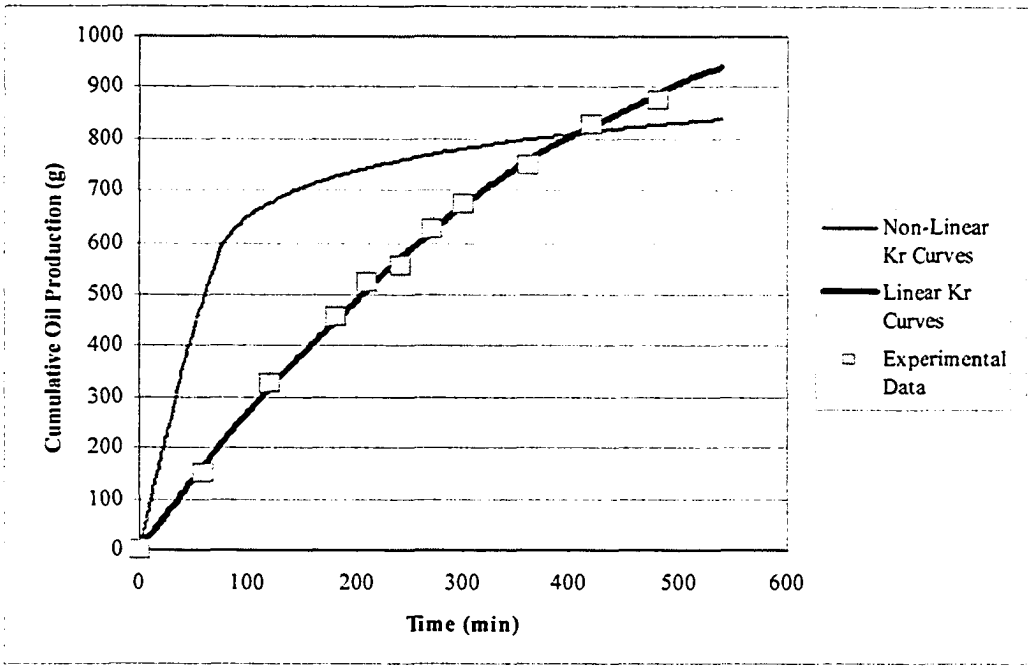

Figure 4-2: Comparison of the Oil Production Performance with Different Relative Permeability Curves

4.2.1.2 Reaction Frequency Factor

The Reaction frequency factor (RF) is the constant in the expression for the reaction

rate. It must be non-negative. A reaction with a reaction frequency factor equal to zero will not react or produce any components. For the reader's convenience, the section on the reaction factor was taken from the STARS manual (Version 2002) and is shown in Appendix D.

Case 1, with non-reaction model, and Cases 16-19, with various reaction factors (0.0004, 0.0008, 0.002 and 43.2), were run and the results are shown in Figures 4-3, 4-4 and 4-5. The reaction factors were selected arbitrarily to try to match the oil production curve. In Figure 4-3, the amount of asphaltenes deposition is plotted with time for the same location (8,1,2) of the grid system. As is apparent, the amount of asphaltenes deposition increases with time for all the cases and more asphaltenes deposit with a higher reaction factor. Case 19, with a reaction factor of 43.2, reached the 15% deposition level too fast to be able to be shown on the graph. The results presented in Figure 4-3 demonstrate that the numerical model constructed is able to simulate the asphaltenes deposition quantatively. Significant

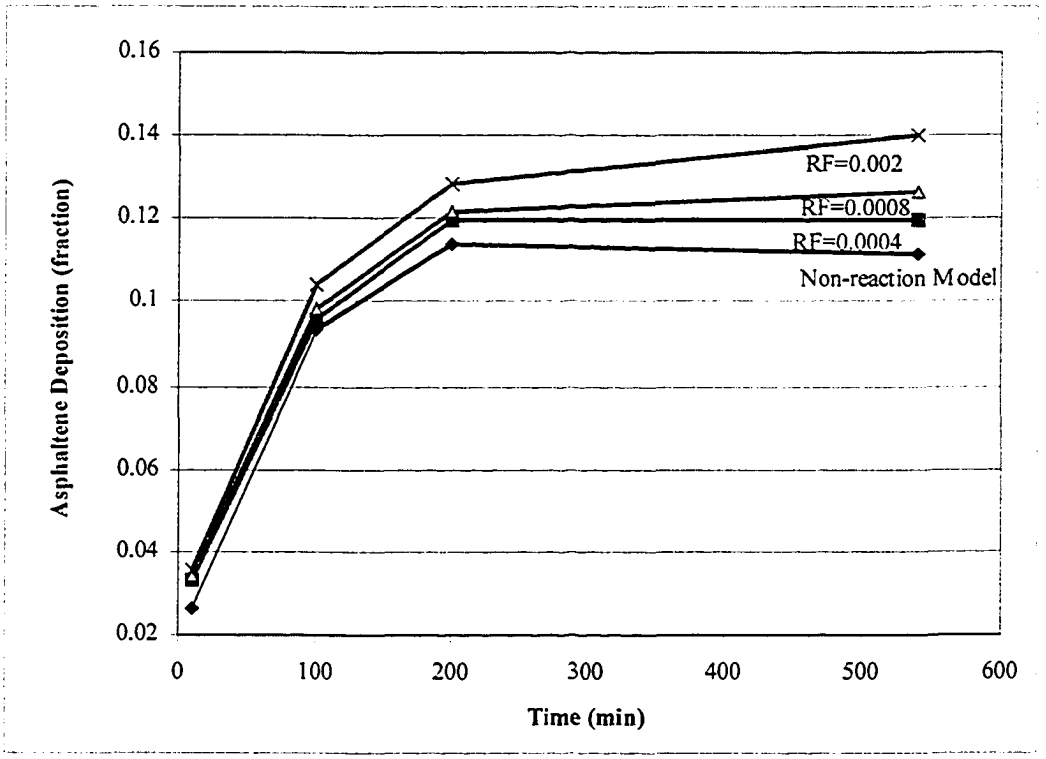

Figure 4-3: Asphaltenes Deposition for Varied Reaction Rates

asphaltenes deposition takes place during 0-100 minutes, where the asphaltenes deposition increase from 2.65% to around 10%. The asphaltenes deposition only increases from 1% to 4% over the next 440 minutes. At 540 minutes of running time, the case with a RF of 0.002 resulted in 14% asphaltenes deposited out of 15.6% original asphaltenes in the oil; that is, the oil was close to being fully upgraded.

In Figure 4-4, the cumulative oil production decreases as the reaction factor increases. Of particular interest is the fact that the drop in the cumulative oil production curve starts earlier for larger values of the reaction factor. This phenomenon can be explained using the definition of the reaction factor; that is, as the reaction rate increases, the asphaltenes are "produced" from C31B+ faster and earlier. This drop in production is significant during the 0 to 100 minutes time period, where significant asphaltenes deposition occurs. The most significant drop appears for the case with a RF of 43.2 at the very beginning of the process. The question then arises as to whether the fluid flow was impaired during this period of time.

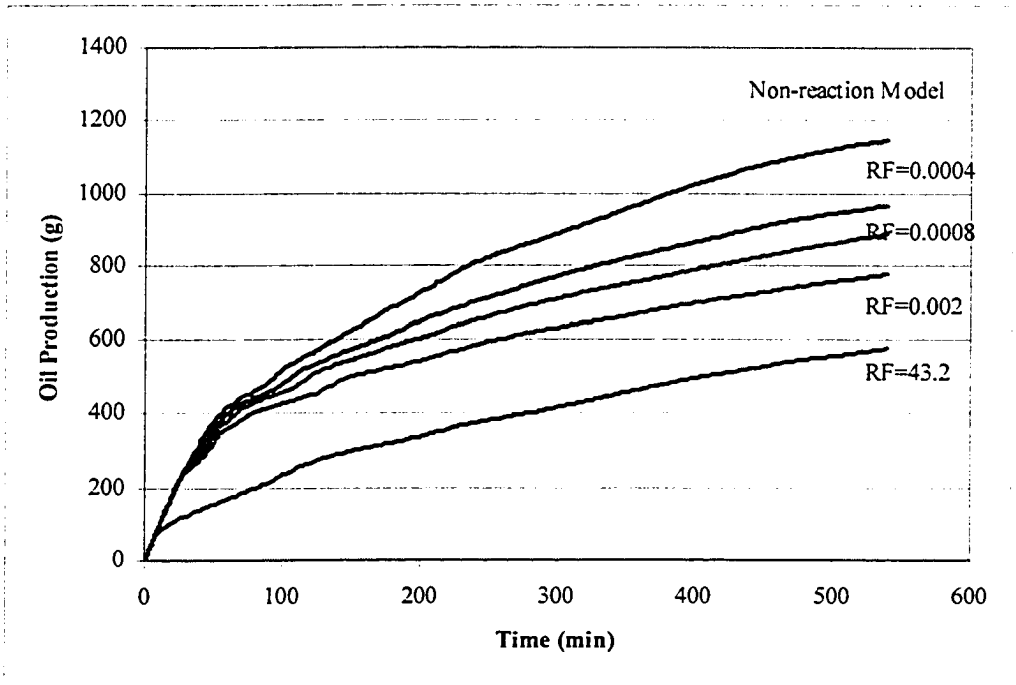

Figure 4-4: Reaction Factor Effect on Oil Production

Whether asphaltenes deposition impairs fluid flow through the porous medium or not is illustrated in Figure 4-5. Figure 4-5 shows that the oil production rate decreases significantly with time during the early displacement period and tends to stabilize later. The drop in the oil production rate starts earlier for the cases with bigger values of the reaction factor. The maximum difference in oil rates is 8 cm^3/min for the 0 to 100 minute period. For the period after 100 minutes, the differences in the oil rate among the cases were not significant, the maximum difference being 1 cm^3/min for all the cases. It can be seen that the oil rate curve for a RF of 43.2 overlaps that for a RF of 0.0002. Also, all of the oil rate curves meet at the same point at 540 minutes.

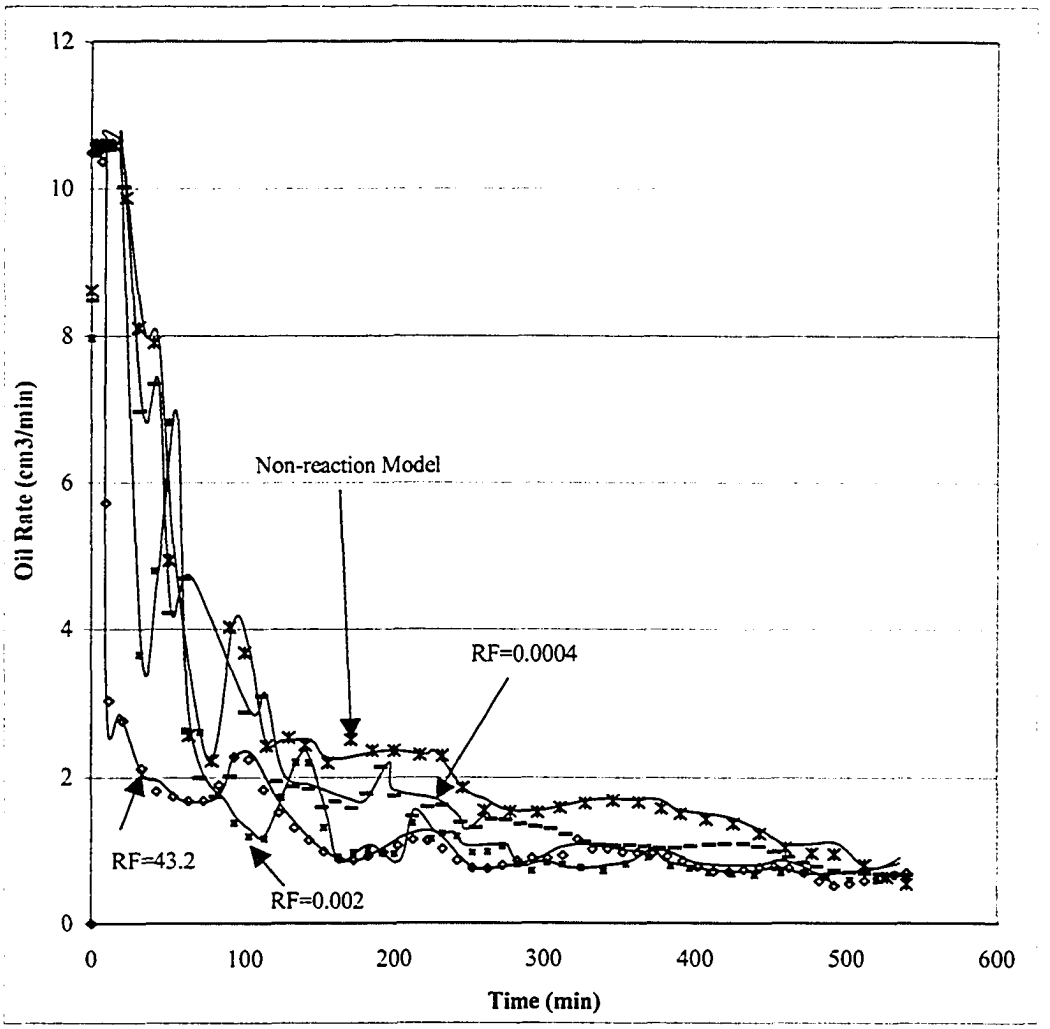

Figure 4-5: Reaction Factor Effect on Oil Production Rate

The investigation presented above demonstrates that asphaltenes deposition might impair fluid flow during the early displacement stage of the process, while it would not affect flow very much during the later drainage stage. That is, the displacement process may benefit from the gravity drainage mechanism and from viscosity reduction. In addition, this investigation suggests that one can infer the production rate of asphaltenes in the physical experiment/field pilot by matching the numerical simulation to the physical/pilot results by using trial and error to determine the value of the reaction factor.

4.2.1.3 Reactant

Based on the solid model developed by Nghiem et al. (1993), the asphaltenes precipitation process is based on the transformation between C31B+ and the asphaltenes component. However, for the solvent injection process, it is unknown if propane also helps or gets involved in this transformation. This issue was investigated numerically, and the results are illustrated in Figure 4-6. In Case 20,

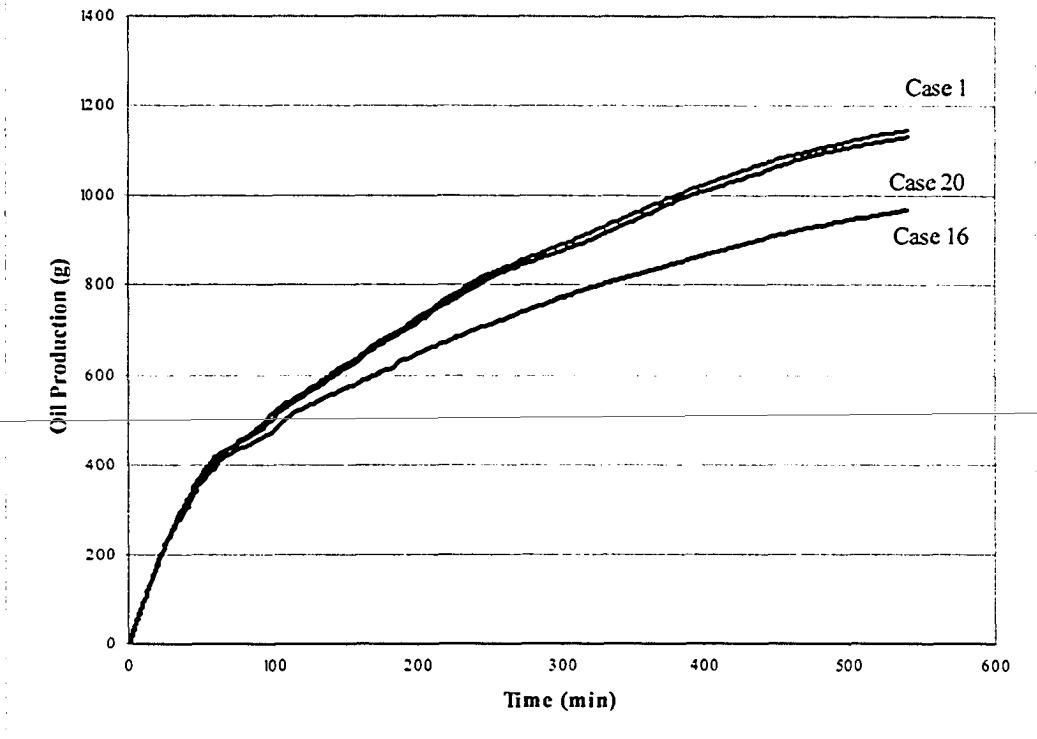

Figure 4-6: Reactant Combination Effect on Simulation Performance

propane, together with C31B+, act as the reactants. In Case 1, no reaction was considered, and in Case 16, only reaction from C31B+ to the asphalt component was considered. Both Case 16 and Case 20 have a reaction factor of 0.0004. In Case 16, 1 mol of C31B+ produces 1 mol of asphaltenes. In Case 20, 1 mol of propane and 0.9265mol of C31B+ produce 1 mol of asphaltenes according to mass conservation.

As can be seen from Figure 4-6, the cumulative production curve for Case 20 is higher than that of Case 16 and close to that for production without considering asphaltenes reaction (Case 1). The reason for this phenomenon is investigated by checking the oil mole fractions of propane for these cases.

Oil mole fractions of propane for Cases 1, 16 and 20 were investigated for the same location (8,1,2) of the grid system. The results are shown in Figure 4-7 and Table 4-3.

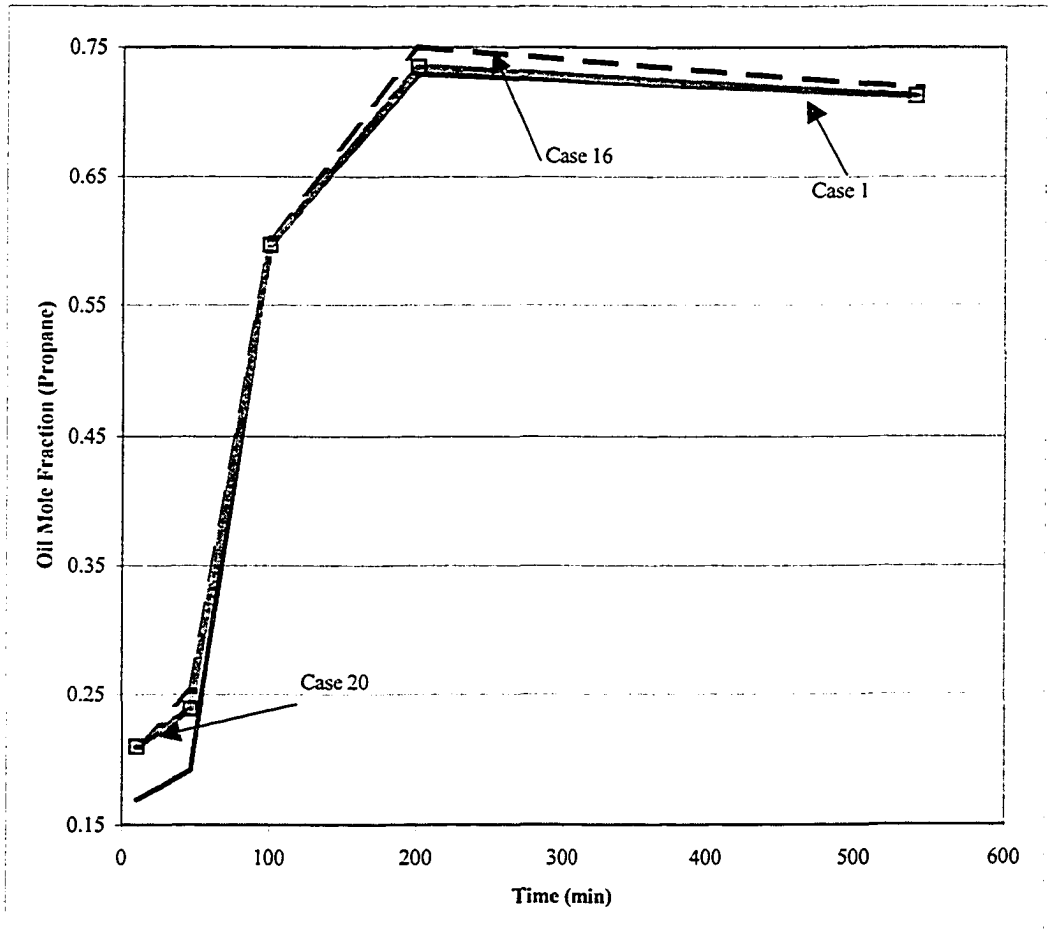

Figure 4-7: Oil Mole Fraction (Propane) for Various Cases

Table 4-3 is the data set for Figure 4-7. Figure 4-7 shows that the propane mole fraction increases with time and reaches a high concentration of around 75% for all the cases. The numerical results are consistent with the experimental results that asphaltenes precipitation occurs when the propane concentration is approximately 30-50%. A significant increase of propane mole fraction occurs during the 0-100 minute time period corresponding to the time when the asphaltenes precipitate heavily (see Figure 4-3). Similar to the performance of the cumulative oil production curve, the propane mole fraction for Case 16 is a little higher than the other two cases corresponding to the lower oil production curve as shown in Figure 4-6. The propane mole fraction curves for Cases 1 and 20 basically overlap each other, which is the same as the results shown in Figure 4-6. The propane mole fraction curves obtained for the three cases demonstrated that the involvement of propane in the transformation to asphaltene affected the concentration of propane in the oil phase.

Table 4-3: Oil Mole Fraction (Propane) for Various Cases

Case 1		Case 16		Case 20	
Time (min)	Oil Mole Fraction (Propane)	Time (min)	Oil Mole Fraction (Propane)	Time (min)	Oil Mole Fraction (Propane)
10	0.1694	10	0.2092	10	0.2095
46	0.1919	46	0.2526	46	0.2386
100	0.5977	100	0.602	100	0.5964
200	0.7298	200	0.7503	200	0.7351
540	0.7136	540	0.7194	540	0.713

4.2.1.4 Dispersion Coefficient and Numerical Dispersion

Traditionally, finite-difference methods with upstream weighting of fluxes have been used in reservoir simulators because of their simplicity. However upstream weighting leads to the smearing of sharp fronts, which is called numerical dispersion (Mattax, 1990). In the simulation of miscible displacement problems with finite-difference single-point upstream methods, numerical dispersion can be greater or of the same order of magnitude as physical dispersion. Thus, unless

numerical dispersion is controlled, the effect of physical dispersion would not be represented correctly. This is the case for STARS simulator (See Appendix A).

Cases 16 and 21 were run and are compared in Figure 4-8. In Case 16, no dispersion coefficient is presented to a component/phase combination. Because the apparent dispersion coefficients would be viewed as the actual physical dispersion coefficients minus the numerical dispersion in STARS, zero apparent dispersion coefficients actually means that the numerical dispersion represented the actual physical dispersion. In Case 21, an apparent dispersion coefficient of 5E-5 m^2/s (which is 100 times the general scale of a dispersion coefficient) is applied to propane in all the directions (I, J, K).

The cumulative oil production curves (See Figure 4-8) show that two curves overlap each other, which means that the magnitude of numerical dispersion is greater than that of the apparent dispersion. Consequently, the numerical dispersion dominated the physical dispersion effect.

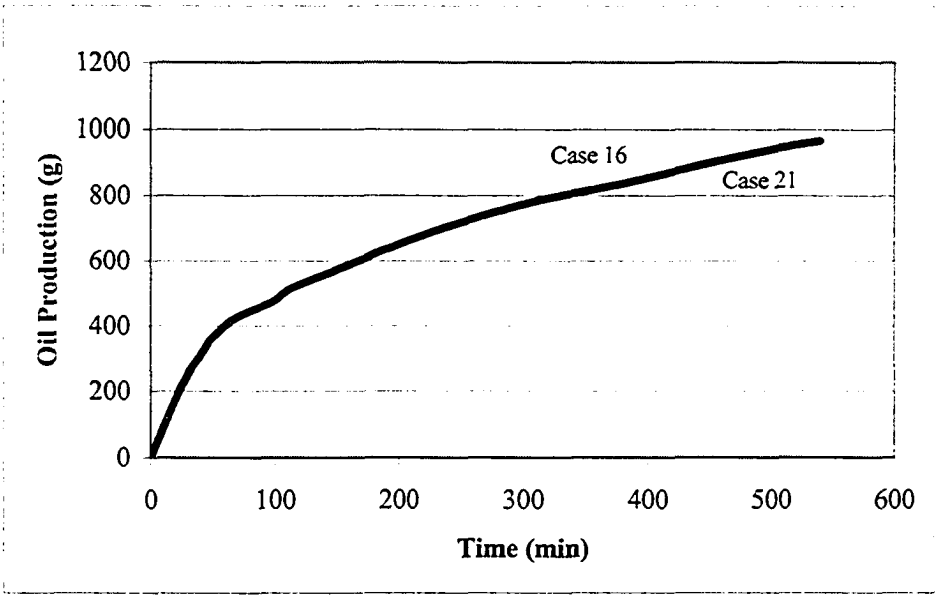

Figure 4-8: Effect of Dispersion Coefficient Involvement on the Simulation Performance

4.2.1.5 Gas Production Control

Propane, or other Natural Gas Liquid (NGL), is much more expensive than steam (water). This is one of the reasons for researchers to vapourize the injected NGL and develop a processing flow line to recover the NGL from the production well as much as possible. Similar to steam production control in a thermal project, gas production control in a solvent process is one of the important aspects to performing the field project economically.

Cases 1, 4 and 5 were run using Model 1 to compare the effect of different gas production rate (50, 40, 30 cm^3/min) control. To investigate the effect of dissolved gas on oil production, the term "consumed GOR" is introduced. It is defined as the difference in the injected gas volume and the produced gas volume divided by the produced oil volume. Figure 4-9 shows that the consumed GOR through the core decreased significantly with time at the beginning of the process and tended to stablize later at a lower level. This indicates that most of the solvent injected was used for diluting and displacing the oil at the beginning of the process, while the demand for solvent decreased when the drainage mechanism became the dominant oil production mechanism. Figure 4-9 also

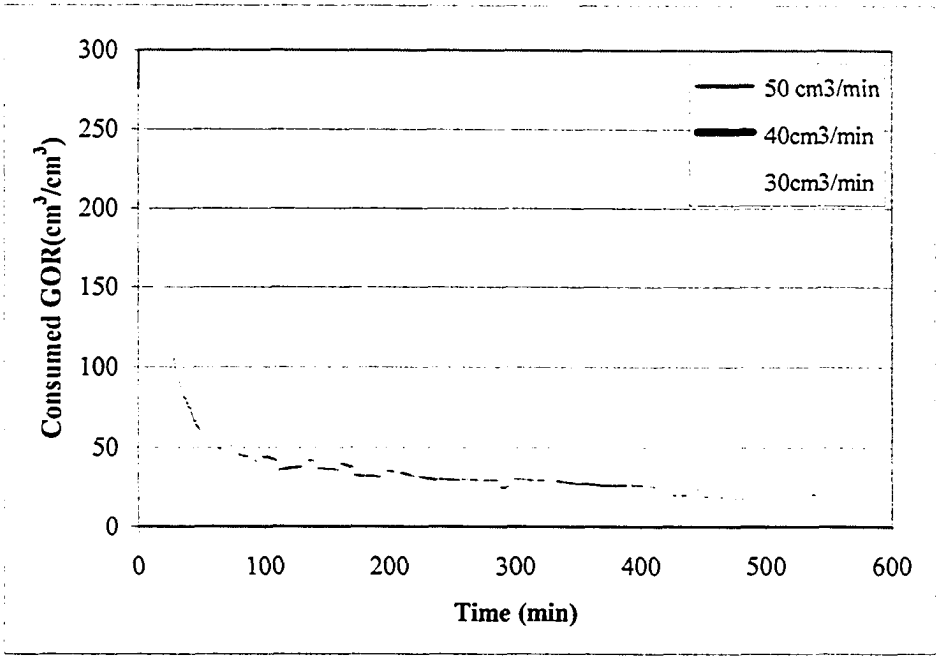

Figure 4-9: Effect of Gas Production Control on Consumed GOR

shows that the consumed GOR for all the cases basically overlap each other. This suggests that there is a determinable amount of solvent needed for the VAPEX process. One part of the solvent required is determined by the solubility of the solvent in the oil, and the second part is determined by the extent of the displacement stage. If extra solvent were injected, it would pass through the core without affecting oil production. This conclusion is supported by the performance curves shown in Figures 4–10 and 4-11. Increasing the gas production rate had no benefit with respect to cumulative oil production, while it increases the produced

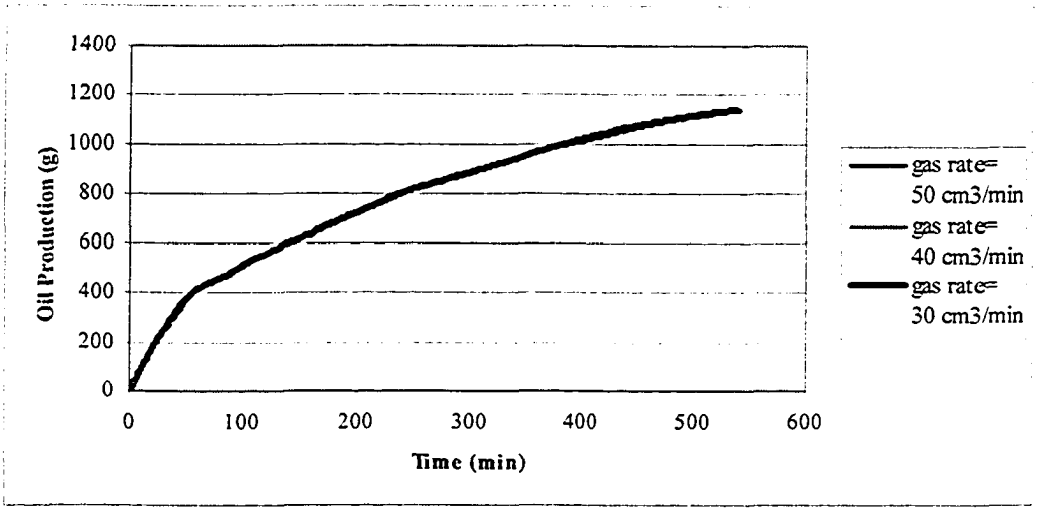

Figure 4-10: Effect of Gas Production Rate Control on Cumulative Oil Production

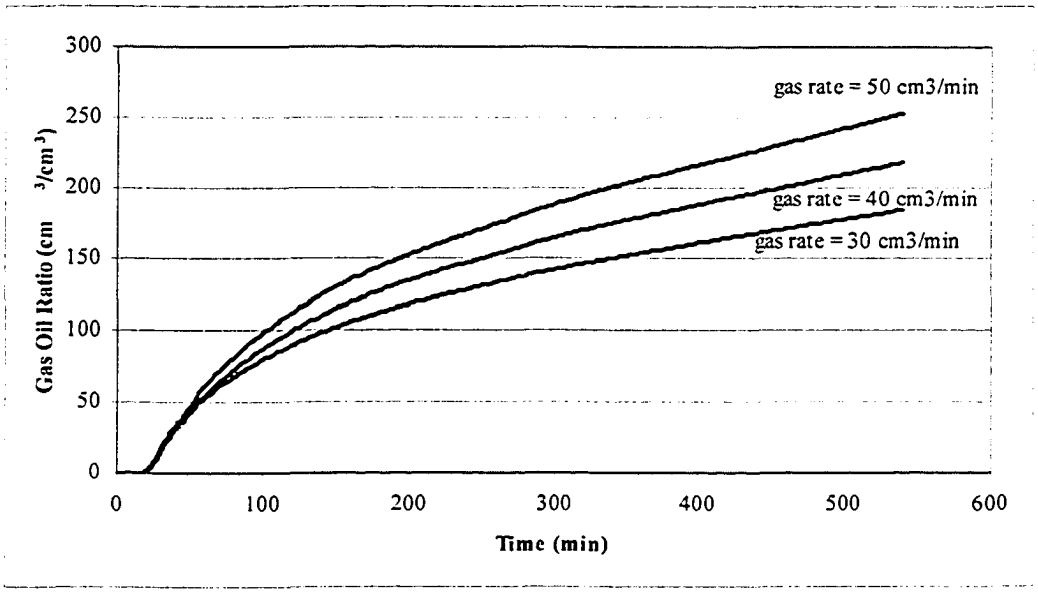

Figure 4-11: Gas Production Rate Control Effect on GOR

gas oil ratio significantly. So in future physical experiments or pilot projects, gas production rate control is one of the most important parameters controlling the economical potential of the project.

4.2.1.6 Oil Production Rate Control

Cases 1 and 6 are compared in Figure 4-12. The oil production rate was controlled at 10.6 cm^3/min in Case 1, while it was decreased to 3 cm^3/min in Case 6. Both runs did not consider the asphaltene precipitation effect. Obviously, the cumulative oil production curve of Case 6 is significantly lower.

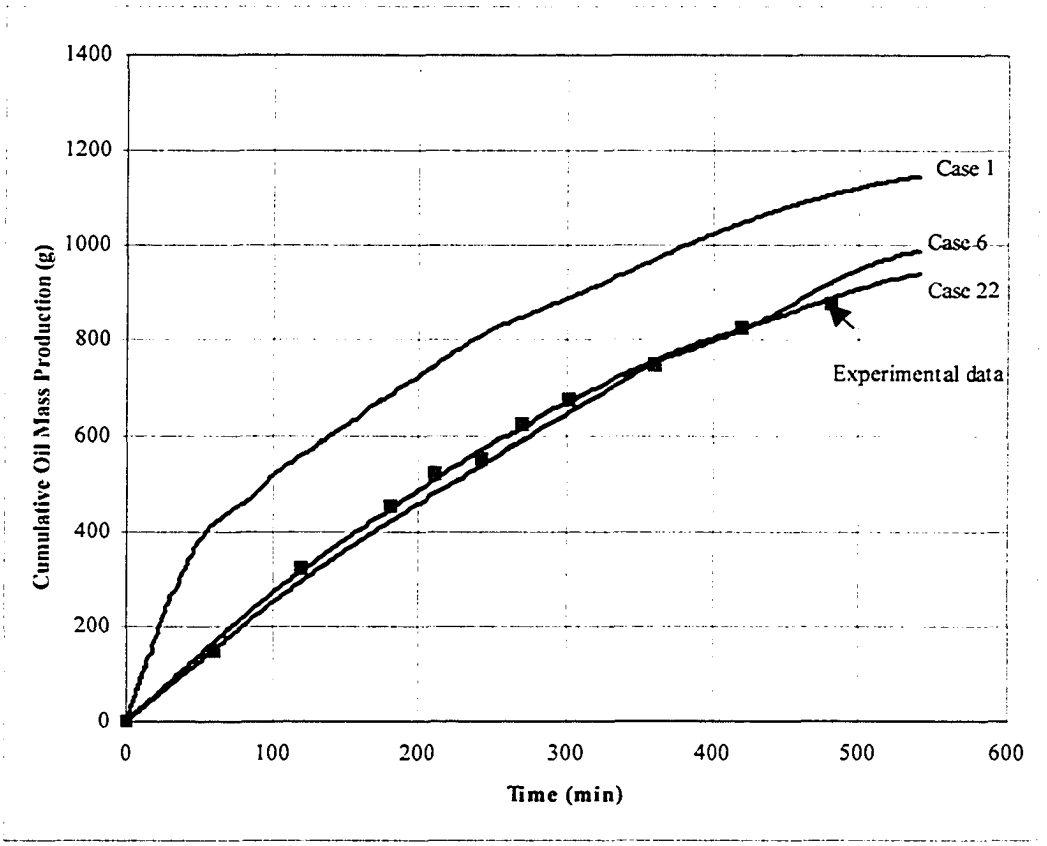

Figure 4-12: Performance Comparison of Various Model Systems

4.2.1.7 Validation

Based on an understanding of the effect of each parameter on the simulation performance, the cumulative oil production curve for Butler's physical experiment (Mokrys and Butler, 1993) is matched in Case 22 using Model 2

(Figure 4-12). The important conditions for Case 22 are: only C31B+ was allowed to transfer to the asphaltenes, a reaction factor of 0.0002, and an oil production rate of 3.3 cm^3/min. No apparent dispersion was used in Case 22, instead, the numerical dispersion from the coarse grid block provides the same magnitude dispersion to the model. The performances are shown in Figures 4-12 and 4-13. In Figure 4-13, Case 22, with linear relative permeability curves, matched very well with the oil production rate from the physical experiment, while Case 2, with non-linear relative permeability curves, showed a significant difference with the experimental data. This result confirms the opinion of Butler and Mokrys (1989) that the boundary layer mechanism of the VAPEX process is a miscible process.

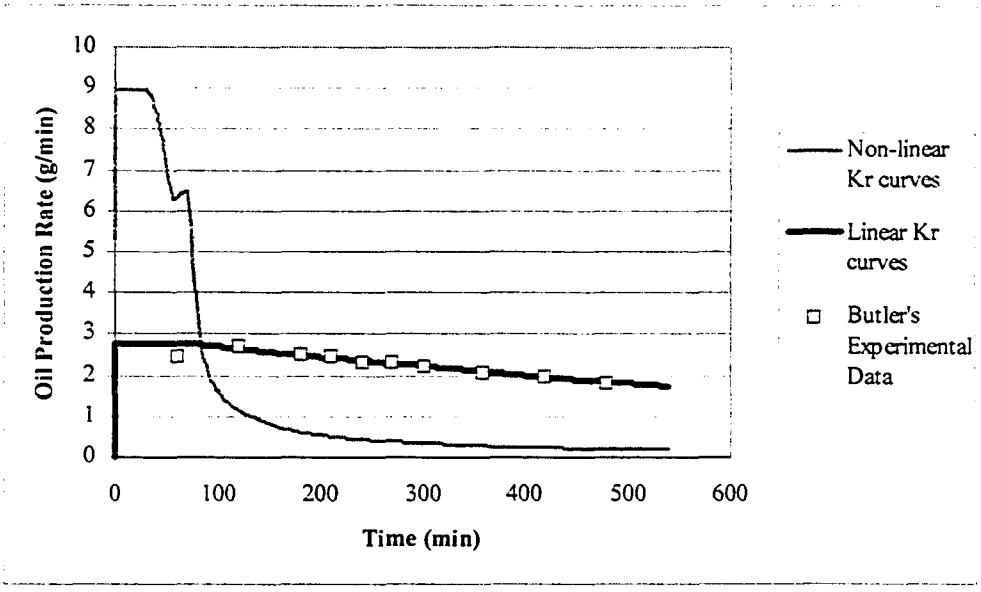

Figure 4-13: Production Rate History Match Curve

4.2.2 Qualitative Validation

In addition to matching the cumulative oil production curve of the physical experiment, efforts were made to study the sensitivity of grid type, well configuration, operating pressure and relative permeability curve selection. These results will also be used for qualitative comparison with known conclusions from Butler's physical experiments.

4.2.2.1 Grid Type

Case 3, with a 15*1*5 Cartesian rectangular grid, and the same geometry and operating conditions as used in Case 1, was run and compared with the result of Case 1. As shown in Figure 4-14, the use of a rectangular grid system resulted in a higher cumulative oil production, which is consistent with the idea that a grid system that follows better the evolution of the solvent-oil interface gives lower numerical dispersion.

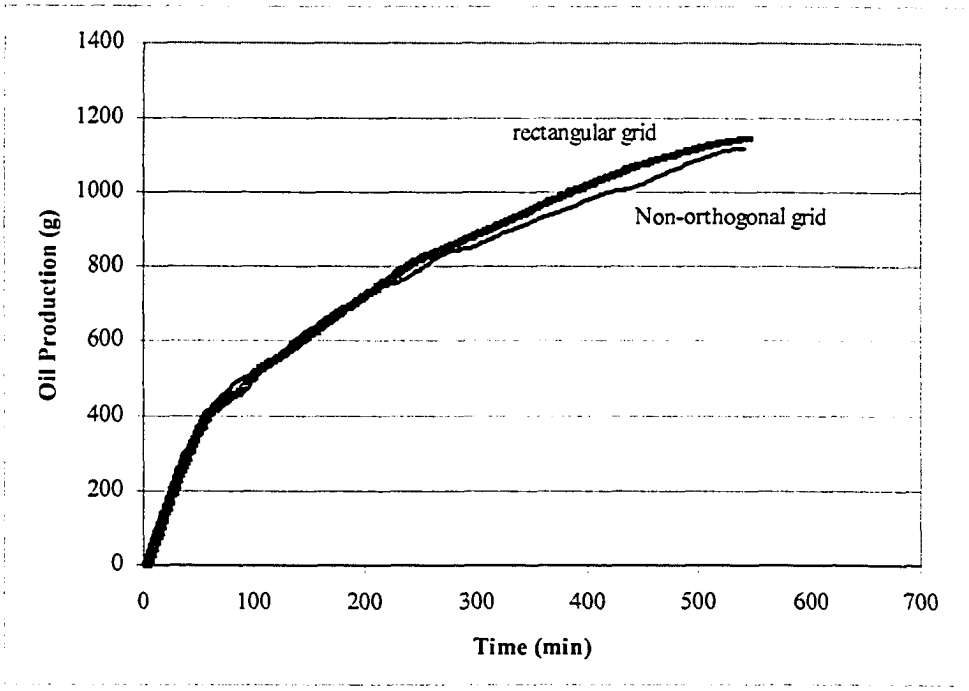

Figure 4-14: Grid Type Effect on Oil Production

4.2.2.2 Well Configuration

Cases 1, 7 and 8 were run with various well configurations and their performances are shown in Figure 4-15. The results show that the widely spaced well configuration (Case 1) resulted in higher oil production than the closely spaced well configurations (Cases 7 and 8). This conclusion is consistent with that of Butler and Jiang (1997), which was based on their physical experiments.

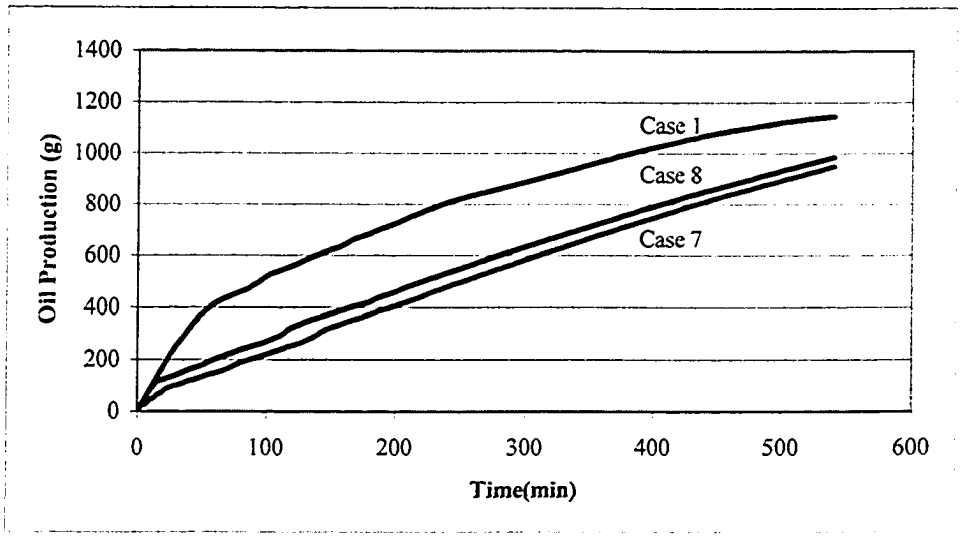

Figure 4-15: Well Configuration Effect on Production

4.2.2.3 Operating Pressure

Various initial reservoir pressures were tried with the same pressure difference of 40 kPa with the injection pressure. Cases 9 to 15 were run and the results are shown in Figures 4-16 and 4-17.

From Figure 4-16, it can be seen that the highest oil production is obtained when the injection pressure is close to the vapour pressure (882 kPa @ 21°C), either slightly above or below. This conclusion is the same as that from Butler and Mokrys (1993b). The only difference between Cases 14 and 15 is that the propane was injected as gas in Case 14 (P_{inj} = 840 kPa), and as a liquid in Case 15 (P_{inj} = 890 kPa). Case 14, where propane was injected as a gas, has the lowest GOR and a little better oil production performance than Case 15, which is consistent with the idea that the solvent should be vapourized when it is first injected into the reservoir. On the other hand, as the increase in production was not significant over a limited range of initial pressures, the production loss would not be significant if the injection condition was not exactly as expected.

Another interesting phenomenon is that Case 13 with an initial pressure of 2,000 kPa, which is much higher than the vapour pressure at this temperature, had much

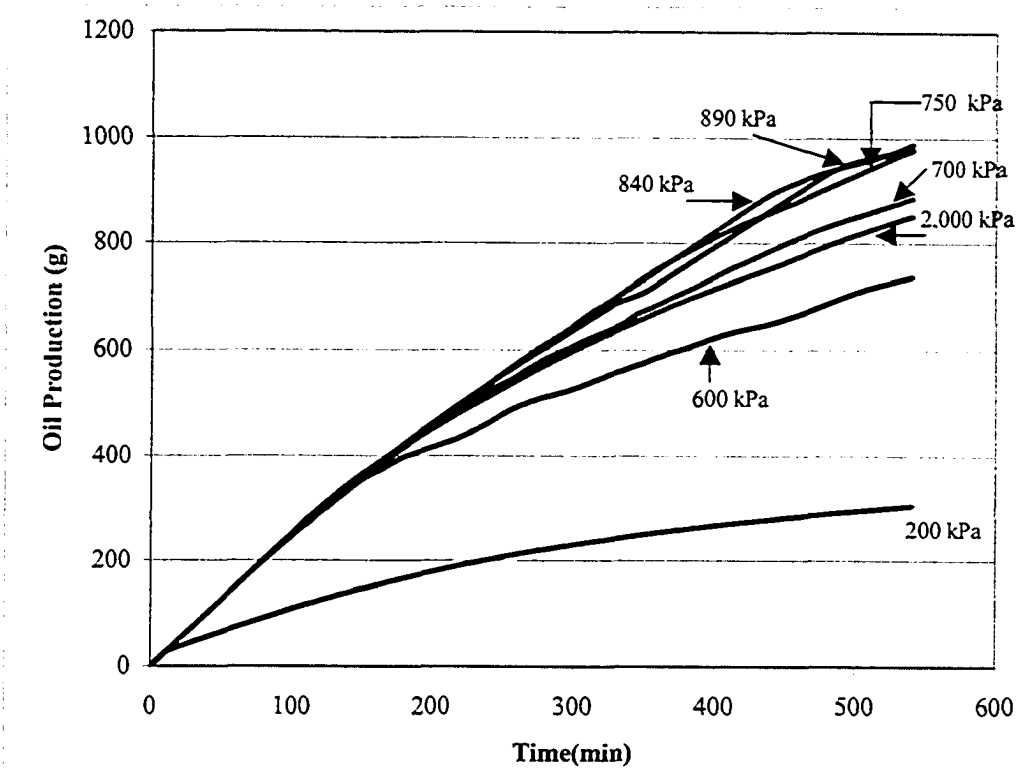

Figure 4-16: Effect of Initial Reservoir Pressure on Oil Production

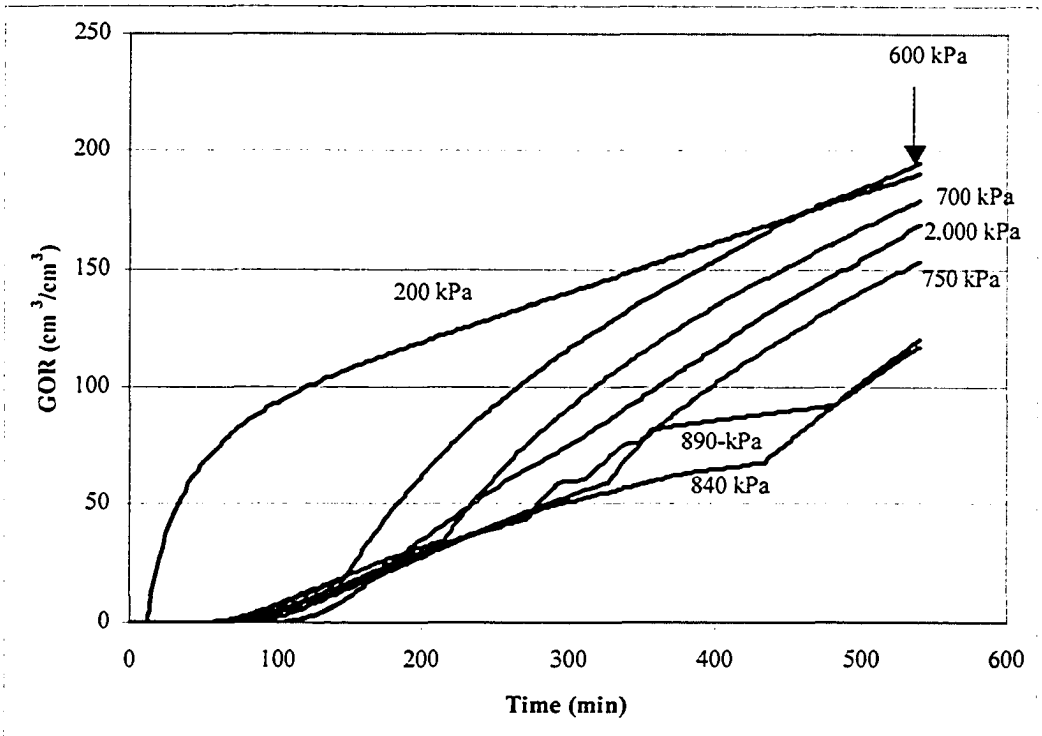

Figure 4-17: Effect of Initial Reservoir Pressure on GOR

more production than Case 11 with an initial pressure of 600 kPa. Moreover, the production for Case 13 was a little less than Case 10 with an initial pressure of 700 kPa. At the same time, Case 13 has a lower GOR than both Cases 10 and 11. This shows that a higher pressure difference between the vapour pressure and the reservoir initial pressure does not always give a worse performance.

4.3 Summary

1. Linear relative permeability curves are demonstrated as being suitable for the numerical simulation of the VAPEX process.
2. An approach that considers chemical reactions can be used successfully to represent the process of asphaltenes precipitation during the solvent injection process.
3. The reaction occurs between the precipitating component (C31B+), which is split from the heaviest component (for example, C31+) in the oil phase, and the asphaltenes.
4. The process of asphaltenes precipitation can be controlled by the reaction rate.
5. The analysis of the oil production rate, which is based on numerical simulation results, demonstrated that asphaltenes deposition might impair fluid flow during the displacement stage of the process, while it would not affect the flow very much during the drainage stage.
6. Propane dissolution concentration is not affected by the reaction model.
7. Numerical dispersion is higher than the physical dispersion in the model adopted.
8. Gas production rate control is an important economic parameter.
9. The consumed GOR curve did not change with the operating conditions.
10. The reaction model with a reaction factor of 0.0002 matched the oil rate profile of Butler's 2-D physical experiment.
11. The numerical simulations led to the same conclusions about the operating strategies of VAPEX as the physical experiments, such as the well configuration and operating pressure.
12. The simulation model built can quantitatively and qualitatively match the experimental results.

5.0 EXPERIMENTAL DESIGN USING THE VALIDATED NUMERICAL MODEL

5.1 Numerical Model Construction

A numerical model for experimental design purposes has been constructed. The geometry, well location and grid system used in the numerical model are described below. STARS and the four component model (Model 1) were used in all the following numerical runs; that is, no asphaltenes reaction is considered because the reaction rate matched is as low as 0.0002.

5.1.1 Geometry, Injecting/Producing Position and Grid System

The core used in this study is one foot long and two inches in diameter. To represent this core simply, a two-dimensional (x-z) Cartesian model was developed. The model had a width (x-direction) of 4.5 cm, a thickness (y-direction) of 4.5 cm and a height (z-direction) of 34 cm, corresponding to a 63*1*34 grid number. Consequently, the core in the physical model and the core in the numerical simulation have the same cross sectional area.

The injection port was placed in the middle of the top of the core, while the production port was placed in the middle of the bottom of the core. This configuration was the same as that in the physical model in order to be able to investigate the gravity drainage mechanism through the longest part of the core. The grid system, which is shown in Figure 5-1, has only 11 grid blocks in the x-direction to improve the clarity of the graphical presentation.

5.1.2 Reservoir/Fluid Properties and Fluid Definition

The reservoir/rock/fluid properties used in this simulation are the same as those used in the validated numerical model, except that the field permeability (5 Darcies) is adopted. The injected and reservoir fluids are defined as in Model 1.

5.1.3 Gas Type, Initial Pressure, and Boundary Conditions

Propane was selected as the solvent to be injected, because its vapour pressure could be reached easily at room temperature. The initial pressure was set at 810 kPa and 830 kPa for different cases. The top and bottom of the cell were flow boundaries, while the sides of the cell were no flow boundaries.

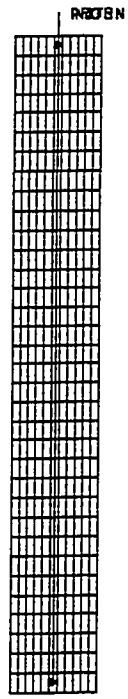

Figure 5-1: Grid System for Core Flooding Experiment

5.1.4 Conditions of Numerical Runs

Detailed descriptions of numerical runs for the experimental design are given in Table 5-1. The related data files are listed in Appendix H.

5.2 Numerical Simulation Results and Discussion

5.2.1 Grid Size Optimization

Numerical dispersion is a well-known problem, which can cause serious difficulties in simulating the movement of a sharp saturation front (Mattax, 1990). Among the many parameters that control dispersion and mixing problems, cell

size is one of the most important. It is usually recognized that the smaller the grid size, the smaller the dispersion and mixing error.

Table 5-1: Numerical Runs for Experimental Design

Case No.	Grid	Initial Pressure (kPa)	Injector Pressure (kPa)	Injection Rate (cm^3/min)	Production control	Water Saturation (%)
Case 23	5,1,34	810	900	N/A	Bhg*=0.05, Bhl*=0.025	0.1
Case 24	11,1,34		900	N/A	Bhg=0.05, Bhl=0.025	0.1
Case 25	15,1,34		900	N/A	Bhg=0.05, Bhl=0.025	0.1
Case 26	21,1,34		900	N/A	Bhg=0.05, Bhl=0.025	0.1
Case 27	25,1,34		900	N/A	Bhg=0.05, Bhl=0.025	0.1
Case 28	31,1,34		900	N/A	Bhg=0.05, Bhl=0.025	0.1
Case 29	35,1,34		900	N/A	Bhg=0.05, Bhl=0.025	0.1
Case 30	63,1,34		900	N/A	Bhg=0.05, Bhl=0.025	0.1
Case 31	63,1,34	830	840	N/A	N/A	0.1
Case 32	63,1,34		855	N/A	N/A	0.1
Case 33	63,1,34		870	N/A	N/A	0.1
Case 34	63,1,34		885	N/A	N/A	0.1
Case 35	63,1,31		855	5	N/A	0.1
Case 36	63,1,32		855	10	N/A	0.1
Case 37	63,1,33		855	15	N/A	0.1
Case 38	63,1,34		855	20	N/A	0.1
Case 39	63,1,34		855	30	N/A	0.1
Case 40	63,1,34		855	N/A	Bhg=1	0.1
Case 41	63,1,34		855	30	N/A	15

Bhg*: Bottom Hole Gas Rate

Bhl*: Bottom Hole Liquid Rate

For EOR processes like the VAPEX method, the transport of fluids (and energy) at the vapour-oil boundary due to diffusive and/or dispersive flows controls the movement of the vapour chamber in the reservoir. An accurate representation of fluid flow near the internal boundaries is required when attempting to evaluate the main phenomena of the process such as viscous fingering (which is likely to occur when the mobility ratio between the oil and the miscible gas is adverse. The more

mobile gas will finger through the oil leading to an early solvent breakthrough). Because the interfacial regions are relatively thin, the grid size required to represent properly the fluid physics at the interfaces should also be small. As the injection rate in the physical experiment is much less than that in the field, the grid size should also be much less to represent adequately the mixing effect.

Cases 23 to 30 were run to assess the effects of grid refinement. The breakthrough time was selected as the indicator to investigate the effect of grid size. Figure 5-2 shows that decreasing the grid size results in an earlier solvent breakthrough time. This is because a smaller grid enables a more detailed description of the component exchanges taking place during the process. Also it was found that the breakthrough time tended to stabilize with increasing grid number, which means that an optimal grid number exists. A grid number of 63 for a 2-inch diameter core, referred to as a 0.07cm/grid, was selected to do all of the rest of the simulations.

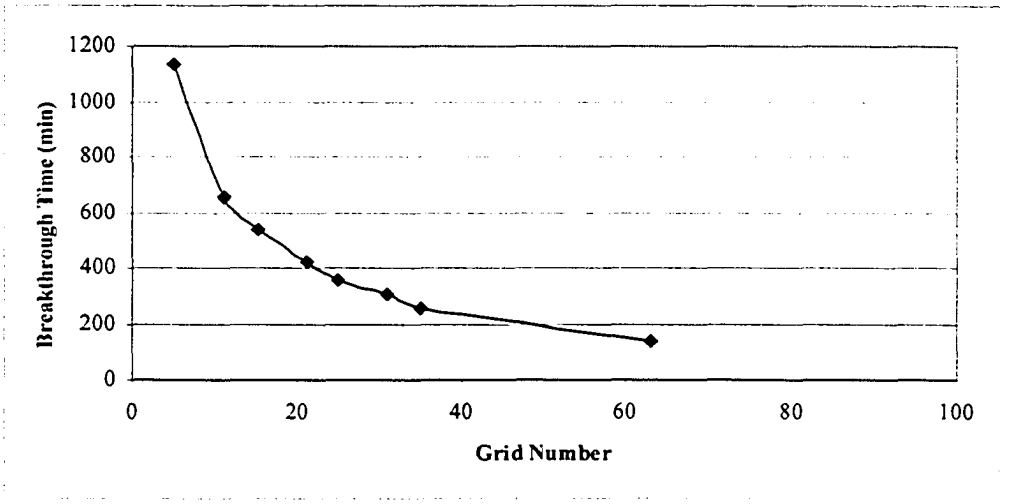

Figure 5-2: Effect of Grid Refinement on Breakthrough Time

It is also obvious that the recovery obtained when using a grid number of 63 in the x- direction is a little bit lower than the same simulation performed using a smaller grid number (see Figure 5-3).

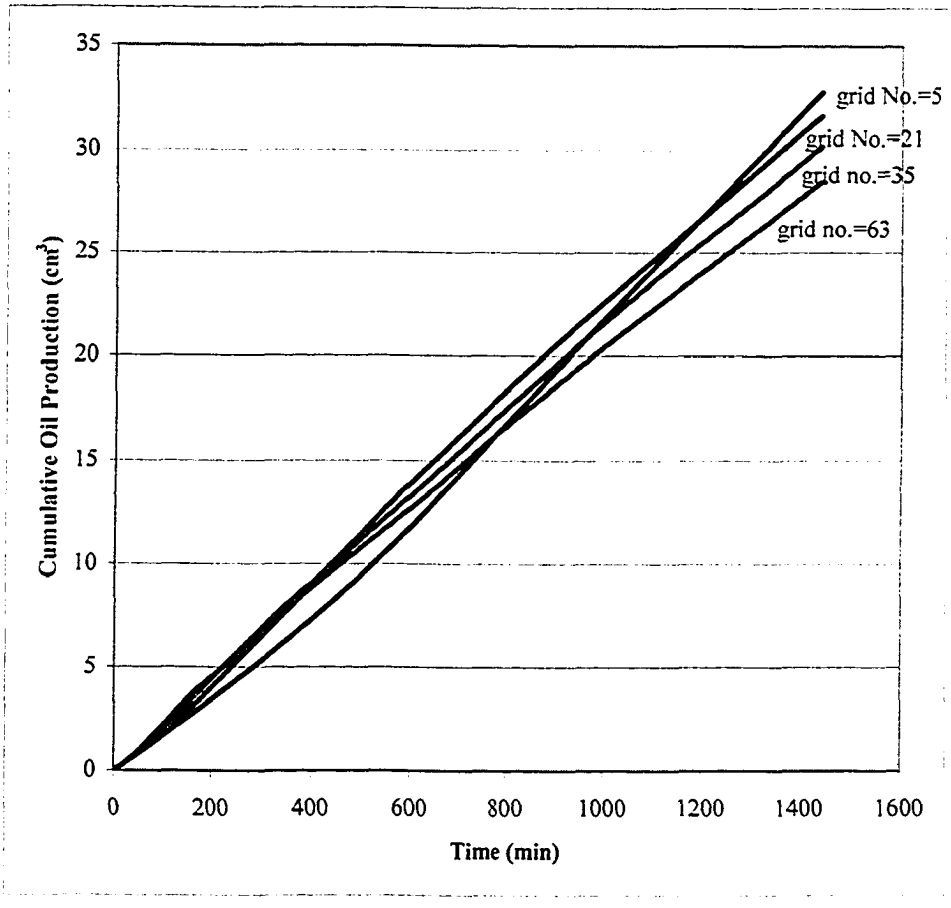

Figure 5-3: Effect of Grid Refinement on the Oil Production

5.2.2 Operating Strategy

Two different series of operating strategies are capable of representing the VAPEX process. The first involves controlling the injection/production pressure and the injection rate. The second one involves controlling the oil/gas production rate. In this study, the performance of each operating strategy is investigated, and the difference between them is compared.

5.2.2.1 Injection Pressure Control

As can be seen in Figures 4-16 and 4-17, the cumulative oil production was the highest and the GOR was the lowest when the initial pressure of the reservoir was close to (either slightly above or slightly below) the solvent vapour pressure. In the core flooding experiments to be performed, a reservoir pressure lower than the solvent vapour pressure is preferred. When such is the case, less effort is needed to compare the liquid solvent injection volume and the gaseous solvent production

volume. An initial reservoir pressure of 830 kPa was chosen to make sure that the injection pressure was lower than the vapour pressure, as well as to give enough pressure difference between the injection pressure and the initial pressure.

Cases 31 to 34 were run to investigate the effect of the pressure difference between the injection pressure and the initial core pressure on the performance of the VAPEX process. The results are shown in Figures 5-4, 5-5 and 5-6.

Figure 5-4 shows that the consumed GOR through the core has a performance similar to that shown in Figure 4-9; that is, the consumed GOR decreases with time at the beginning of the process and tends to stabilize at a lower level later. The curves for the consumed GOR are almost the same for most of the cases, except for the case with an injection pressure of 840 kPa. The higher consumed GOR for the latter case is because the lower pressure drop through the core resulted in a longer contacting time between the solvent and the oil. Thus more solvent is being dissolved, while the produced oil did not increase very much because of the low pressure drop.

In Figures 5-5 and 5-6, one can notice that the highest pressure difference (55 kPa, 885-830) gives the second lowest oil production and the highest GOR during the course of the runs, which means that some of the injected solvent just passed through the core and did not dissolve in the oil. It is clear in Figures 5-5 and 5-6 that pressure differences of 25 kPa and 40 kPa give the highest cumulative oil production and relatively low GORs. The pressure difference of 40 kPa resulted in higher production during the displacement period, while the pressure difference of 25 kPa resulted in higher production during the drainage period. Both the cumulative oil production and the GOR are the lowest in all the runs when the difference between the injection pressure and the initial pressure is 10 kPa (840-830). The reason for this behaviour is believed to be that the amount of solvent injected by the lower pressure difference limits the amount of oil dissolved by the solvent reaching a given mobility.

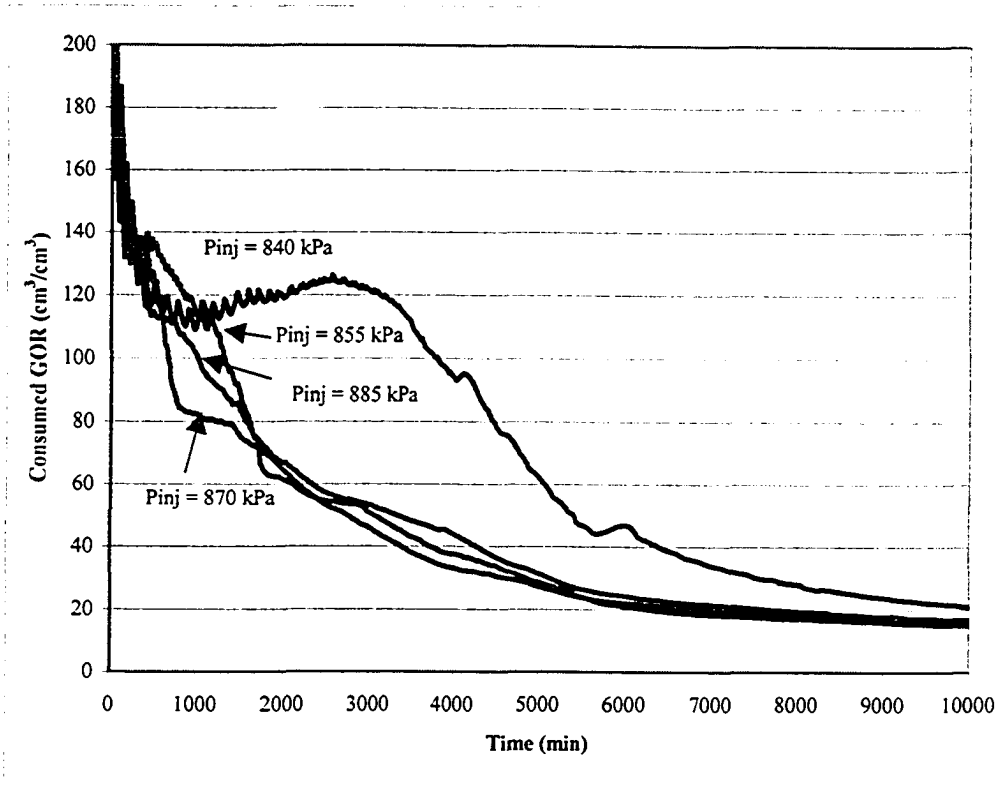

Figure 5-4: Effect of Injection Pressure on the Consumed GOR

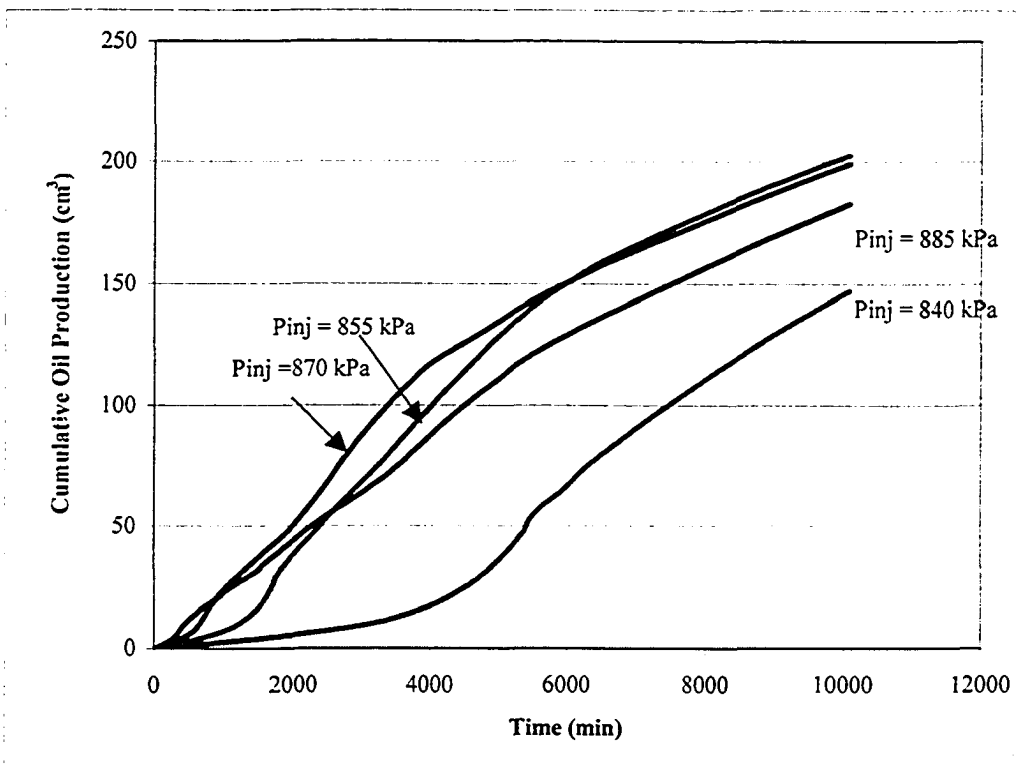

Figure 5-5: Effect of Injection Pressure on Core Production

Because the GOR is one of the more important economic factors, and because the drainage period is the period of more concern, a pressure difference of 25 kPa was selected as the optimal pressure drop through the core.

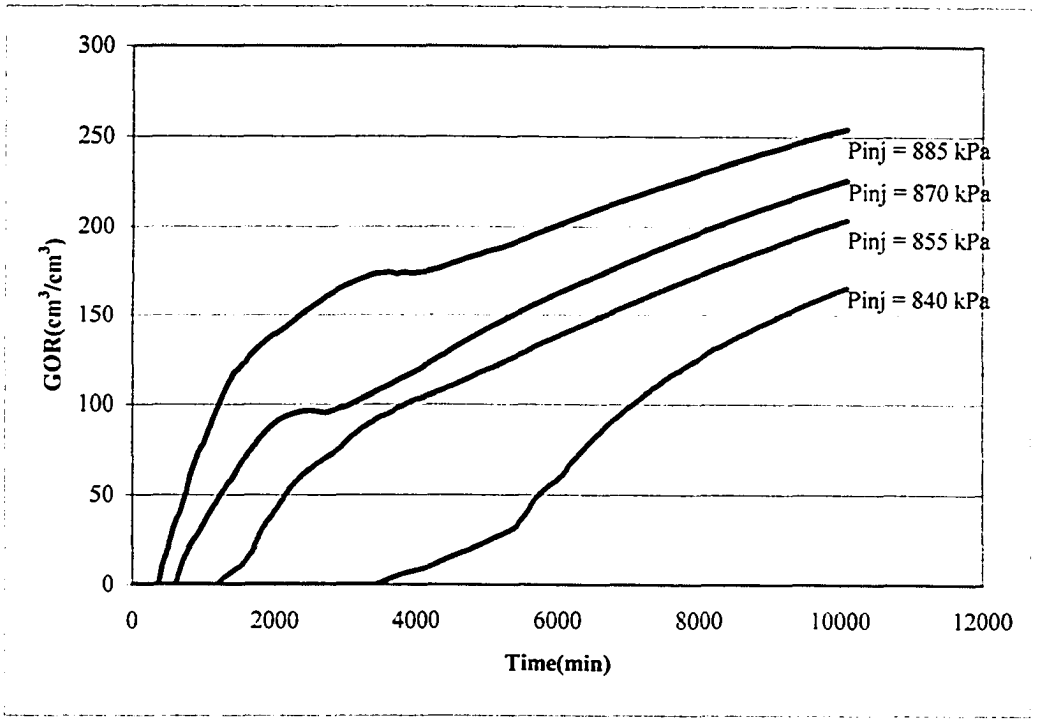

Figure 5-6: Effect of Injection Pressure on GOR

5.2.2.2 Viscous Fingering and Critical Velocity Calculation

To inspect the fingering phenomena and instability issue for the current oil and core system, some simulations were run and BT times were compared as one indicator of fingering and instability phenomena (Table 5-2, Figure 5-7). The injection

Table 5-2: Core Length and Radius Effect on BT Time (63 grids for cross section)

Core Length (ft)	Core Diameter (inch)	BT Time (min)
0.5	2	30.18
	1	12.07
1	2	136
	1	86.15
1.5	2	405.1
	1	263.1

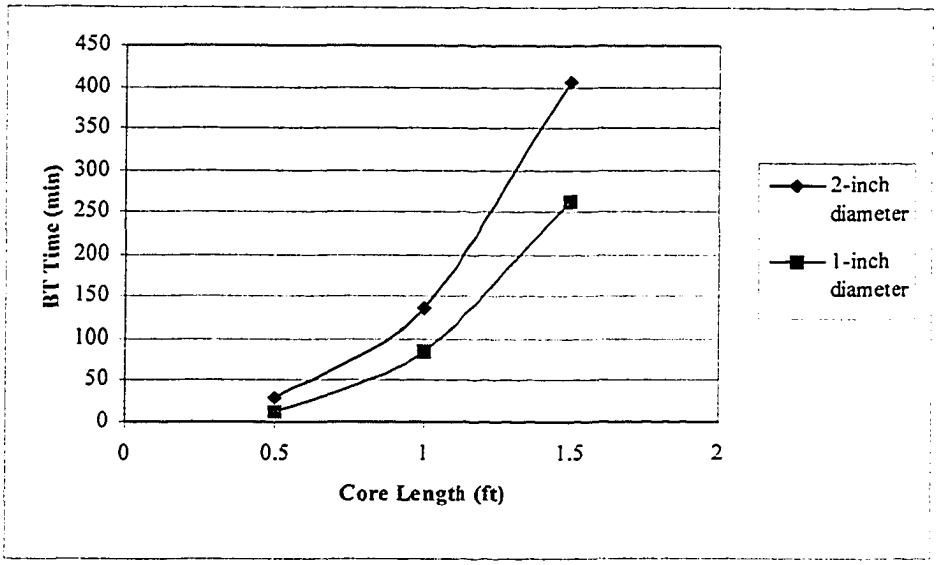

Figure 5-7: Core Length and Diameter Effect on BT Time

rate is constant for all the runs in this section. Table 5-2 is the data used in Figure 5-7. It is clear in Figure 5-7 that the BT time increases significantly with core length and that, for a given core length, BT time increases with core diameter. This demonstrates the suppression effect of transverse dispersion and gravity on viscous fingering.

Also some calculations were made to check the critical velocity for stability (Tables 5-3, 5-4). Table 5-3 shows the properties used in the calculation. The results of calculations of V_c (the critical injection rate) to achieve a stable process with Lloydminster heavy oil and gaseous propane using the Dumoré (1964) formula are shown in Table 5-4. Dumore's equation is based on the assumption that there is a sharp front between the gas such as propane and the oil. In reality, there will be a transition zone between the gas (propane) and the oil. This gradation

Table 5-3: Density Data for Liquid and Gaseous Propane

	Density lb/ft^3		Density g/cm^3	
	60 °F	70 °F	60 °F	70 °F
Liquid C_3H_8	31.74603	31.162	0.5085	0.49917
Gaseous C_3H_8	1.01626	1.1709	0.0162	0.0187

Table 5-4: Critical Velocity Calculations for Different Oil and Propane System

	3-inch Diameter Area = 45.56 cm^2		2-inch Diameter Area = 20.25 cm^2		1-inch Diameter Area = 5.05 cm^2	
	Critical Injection Rate (cm^3/min)	V_c (cm/min)	Critical Injection Rate (cm^3/min)	V_c (cm/min)	Critical Injection Rate (cm^3/min)	V_c (cm/min)
Liquid C_3H_8, μ_o = 10,000 cp	0.107348	0.002356	0.04771	0.002356	0.002356	0.0023560
Liquid C_3H_8, μ_o = 6,000 cp	0.178914	0.003926	0.079517	0.003926	0.003927	0.0039267
gaseous C_3H_8, μ_o = 10,000 cp	0.214604	0.004710	0.095379	0.004710	0.023786	0.0047100
gaseous C_3H_8, μ_o = 6,000 cp	0.357673	0.007850	0.158966	0.007850	0.039643	0.0078501

of concentrations will increase the stability of the process. However, as the injection rate has to be as low as 0.09379 cm^3/min (shown in Table 5-4) to reach a stable condition; it is easy to form viscous fingers. Consequently, fingers in a process such as VAPEX are unlikely to be suppressed, due to the very large viscosity contrast between typical solvents and heavy oil. This is in agreement with the general opinion that miscible displacements with a low viscosity fluid displacing a more viscous oil are likely to be unstable, leading to the development of viscous fingers.

5.2.2.3 Injection Rate Control

Viscous fingering reduces the oil recovery of the VAPEX process, so it is good to reduce the impact of fingering as much as possible, even under unstable conditions, in order to reach a higher final recovery. Injection rate is an important factor in controlling viscous fingering. One way to investigate the impact of the fingering is to check if the interface between the gas phase and the oil phase is close to horizontal. If so, then the corresponding injection rate is the one that ensures a stable interface. As mentioned above, the VAPEX process is difficult to stabilize. But it is still good to have a stable interface early in the life of the process. The distribution of the phases (gas, oil, water) for Cases 35 to 39 shows that 5 and 10 cm^3/min are the rates that ensure a stable interfacial front (see Figure 5-8) for early displacement times. An example of viscous fingering is shown in Figure 5-9.

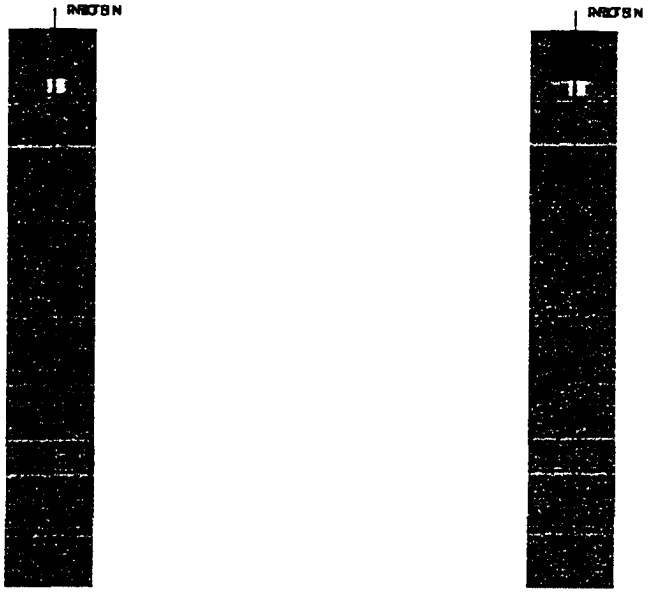

gas rate= 5 cm^3/min at 1,440 minutes gas rate =10 cm^3/min, at 1,440 minutes

Figure 5-8: Interfacial Front in the Core Flooding Simulation

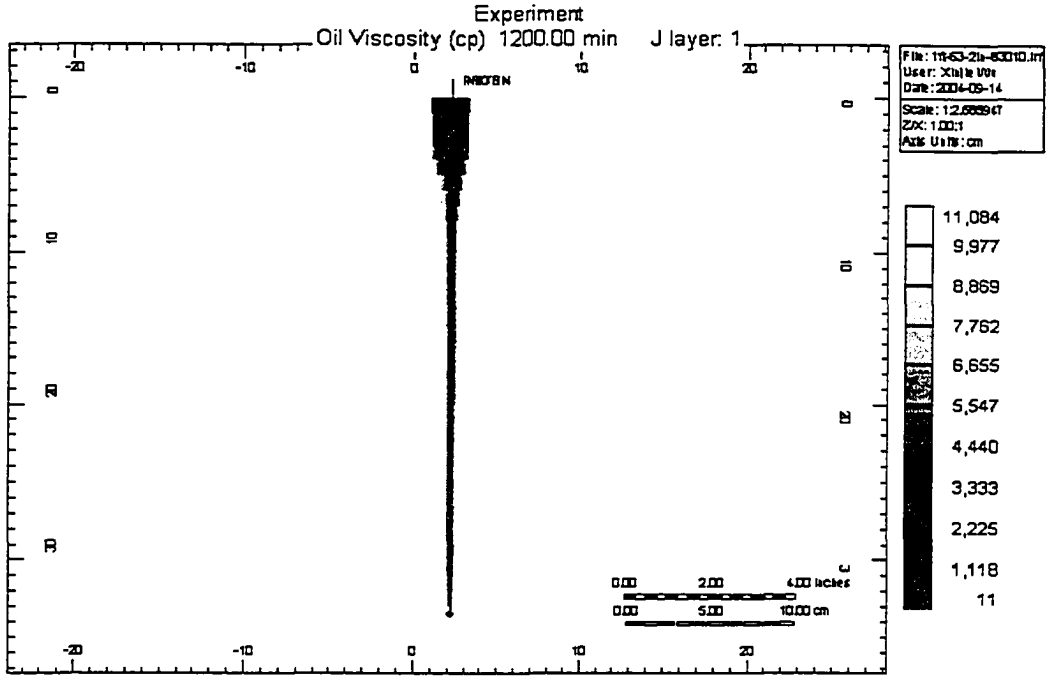

Figure 5-9: Viscous Fingering

Cases 35 to 39 were run with different injection rates, and the results are shown in Figures 5-10, 5-11and 5-12. It is clear from Figure 5-10 that the consumed

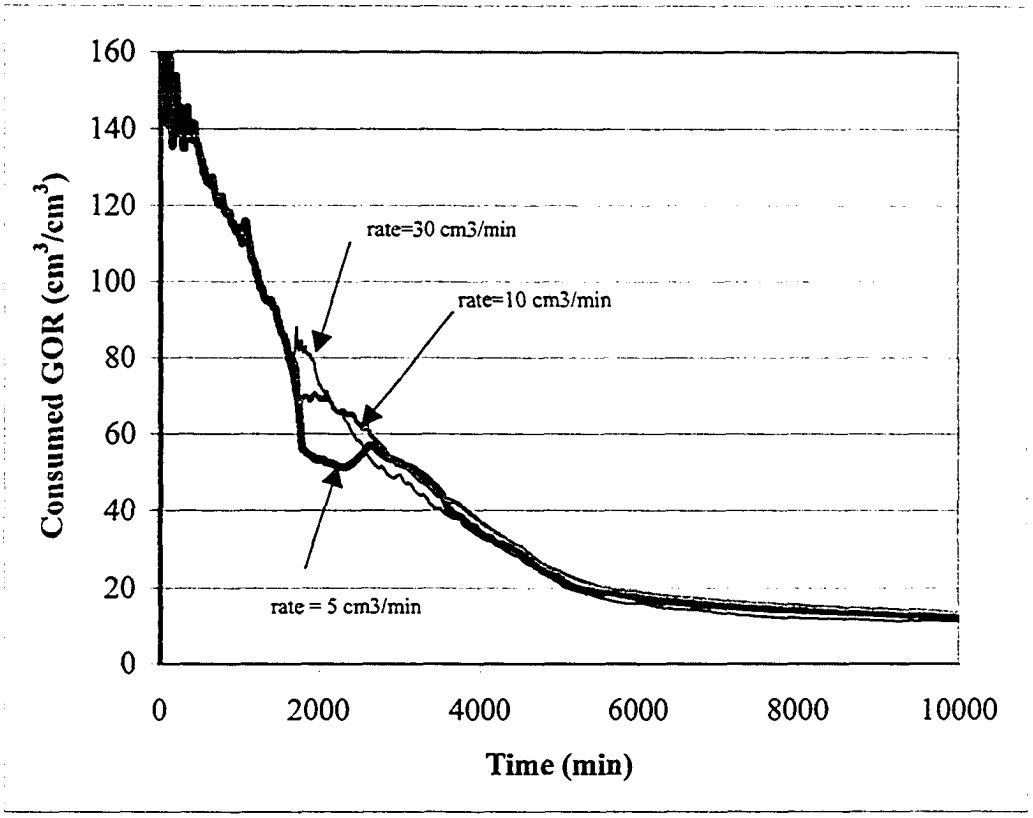

Figure 5-10: Effect of Gas Injection Rate on Consumed GOR

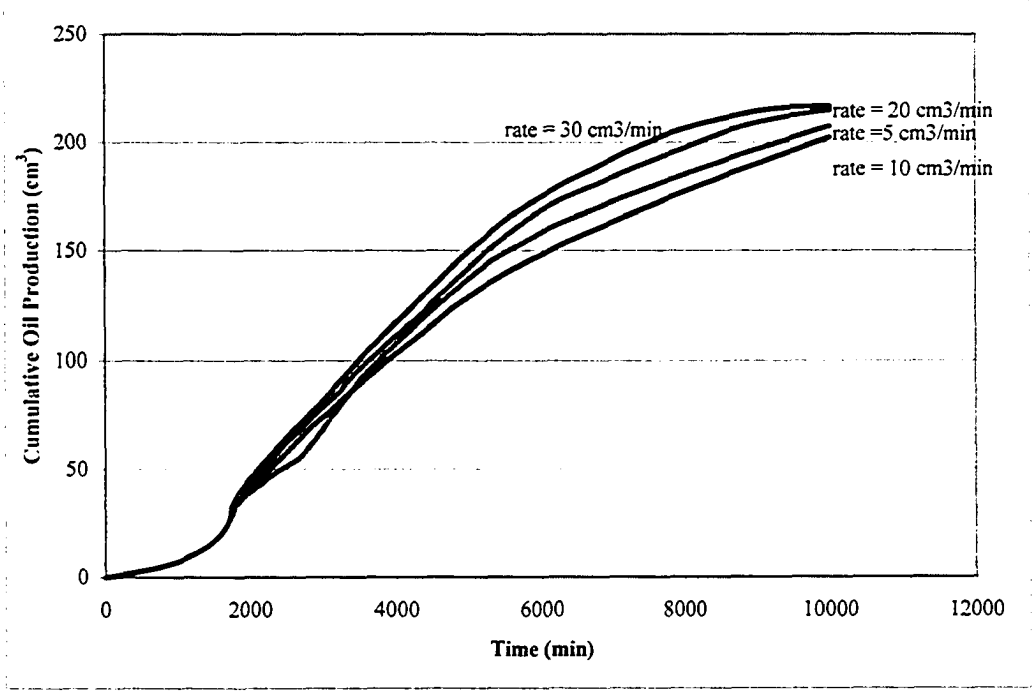

Figure 5-11: Effect of Injection Rate on Oil Production

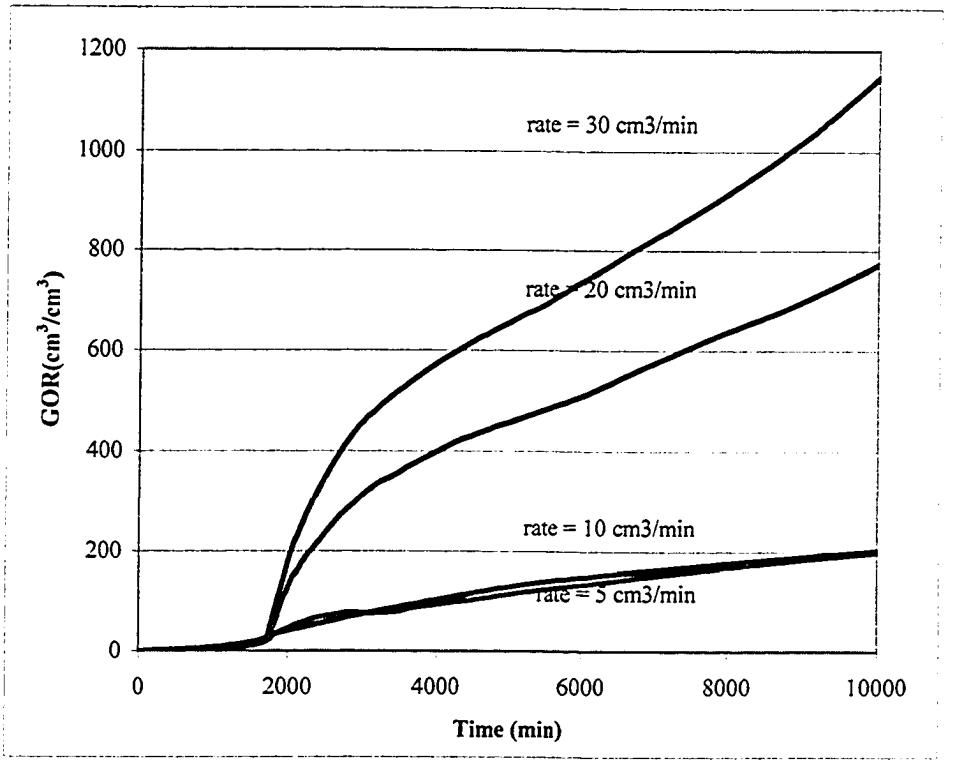

Figure 5-12: Effect of Injection Rate on the GOR

GOR is consistent with the performance depicted in Figures 4-9 and 5-4. This confirms the idea that there is a specific amount of solvent needed for the VAPEX process. Figure 5-12 shows that the produced GOR increased significantly with injection rate while Figure 5-11 shows that the cumulative oil production increased just a little. This indicates that the increased injection rate did not help the oil production very much; however, it did promote the solvent passing by the oil. As can be seen in Figures 5-11 and 5-12, injection rates of 5 cm^3/min and 10 cm^3/min give the lowest GOR and a little smaller cumulative oil production. Hence, these rates are the optimal injection rates for the core flooding process. Because of easier operating conditions, 10 cm^3/min was selected to do the experiments.

5.2.2.4 Production Rate Control

Cases 36 and 40 are compared in Figures 5-13 and 5-14 to see if production rate control has the same effect as injection rate control. In Case 36, the injection rate is 10 cm^3/min at standard conditions, while, in Case 40, the bottom hole gas

production rate is 1 cm^3/min under 830 kPa production pressure (around 10 cm^3/min under standard conditions). The figures show that production rate control gives a little higher cumulative oil production, as well as a higher GOR, as compared to injection rate control. As both methods follow similar performance

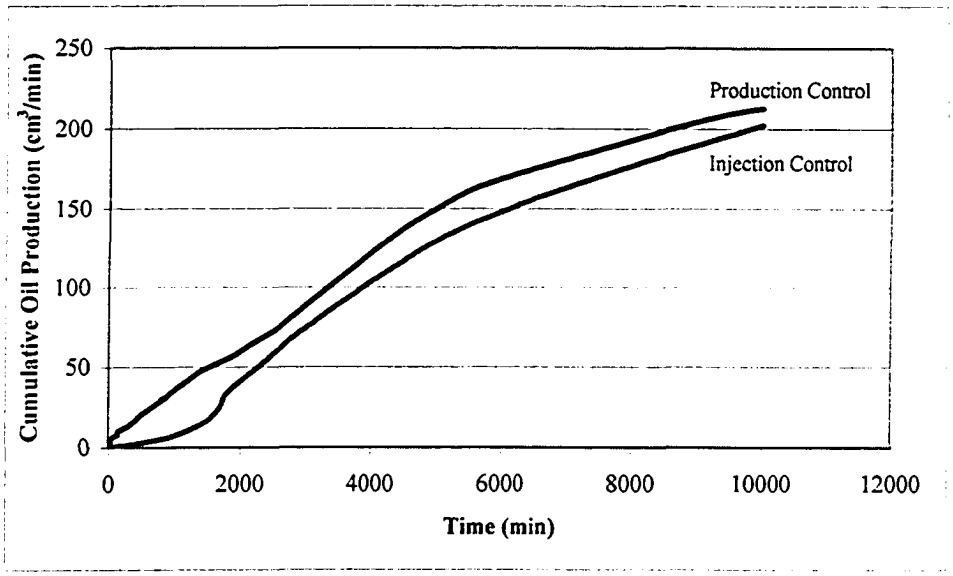

Figure 5-13: Effect of the Operating Strategy on the Oil Production

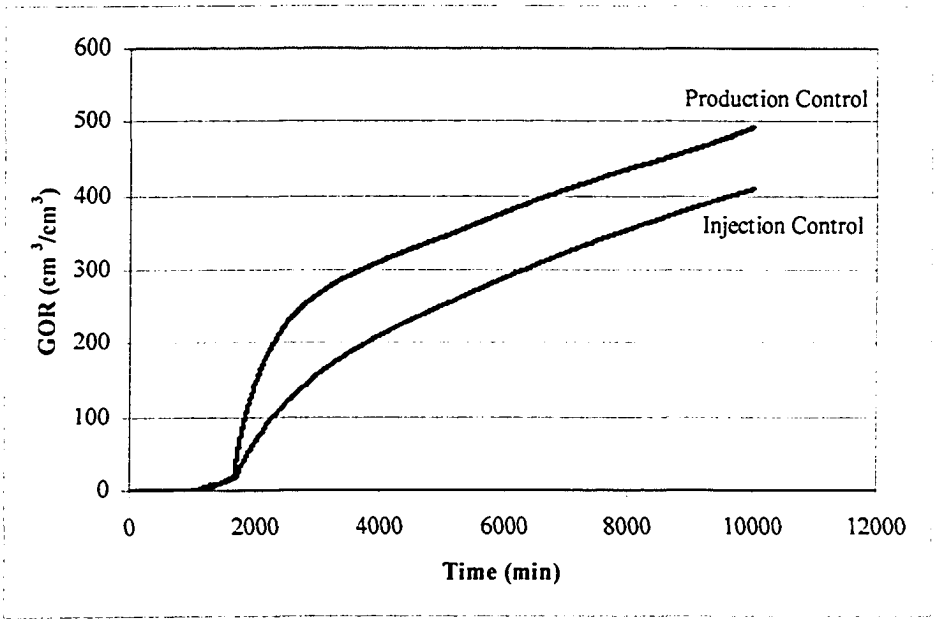

Figure 5-14: Effect of Operating Strategy on GOR

trends, it is concluded that both methods are able to control the performance of the process; however, injection rate control is preferred because of the lower GOR.

5.2.3 Water Saturation

Some researchers (Singhal et al., 2002) have claimed that the existence of water would benefit asphaltenes precipitation. A numerical investigation was conducted on this issue. Cases 36 and 41 were run and the asphaltene deposition values at the same location (35, 1, 32) are compared in Table 5-5 and Figure 5-15. In Case 36, the water saturation is 0.1%, while it is 15% in Case 41. As can be seen in Figure 5-15, the case with less water (0.1%) had lower asphaltenes deposition for the whole process period. Also the starting point of the asphaltenes deposition for the case with the smaller water saturation is later than the case with the greater water saturation. This conclusion is consistent with the results provided by Singhal et al. (2002).

Table 5-5: Effect of Water Saturation on Asphaltenes Deposition

Time (min)	With Water	No Water
10	0.0025	0
30	0.0371	0
60	0.106	0.0002
100	0.1197	0.0009
200	0.1201	0.0084
300	0.1203	0.056
400	0.1196	0.0804
600	0.1183	0.11
720	0.1179	0.1099
840	0.156	0.1117
960	0.156	0.1123
1200	0.156	0.1263
1440	0.156	0.1257
2000	0.156	0.1178
3000	0.156	0.1133
4000	0.156	0.1107
10000	0.156	0.1055

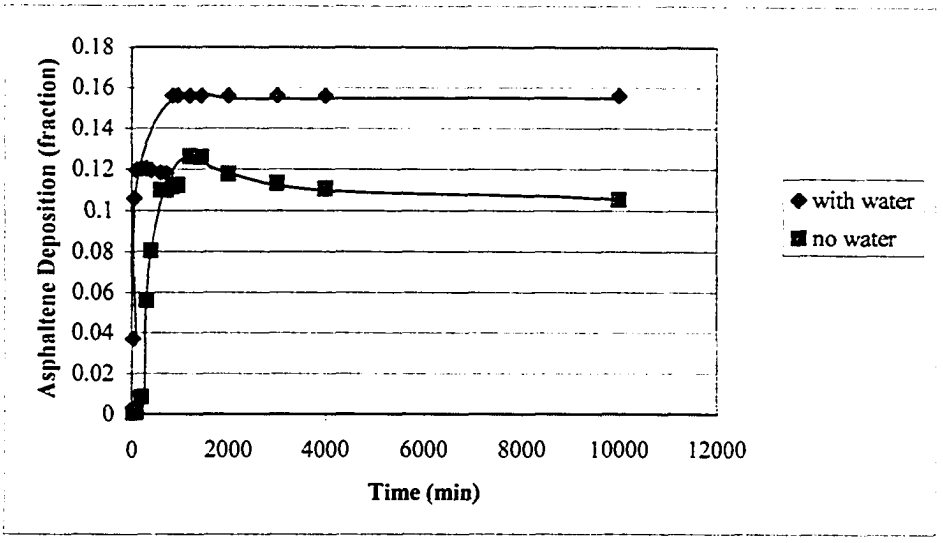

Figure 5- 15: Effect of Water Saturation on Asphaltenes Deposition

5.3 Summary

1. The grid number for the numerical model was optimized for numerical dispersion.
2. The optimal difference between the injection pressure and the production pressure was found to be 25 to 40 kPa and the optimal gas injection rate was found to be 5 to 10 cm^3/min in order to suppress viscous fingering.
3. The VAPEX process can be performed using gas injection rate control or gas production rate control.
4. Numerical simulation results and physical experimental results both suggest that the existence of water enhances asphaltenes precipitation.

6.0 EXPERIMENTAL INVESTIGATION OF THE EFFECT OF ASPHALTENES DEPOSITION ON FLUID FLOW

6.1 Construction of Physical Model

The schematic representation of the experimental set-up for core flooding is shown in Figure 6.1. Three essential systems are included in the experimental system: the injection system, the sand-pack and the production system.

The injection system consisted of the propane high-pressure cylinder, the mass flow controller and the pressure transducer right before the top of the sand pack. The propane used had a purity of 99.99% in order to be able to calculate its vapour pressure easily and quickly. The maximum pressure that the cylinder could supply was 896 kPa (130 psig), which is higher than the vapour pressure of propane at room temperature (859 kPa at 20°C). Consequently, the propane cylinder was connected directly to the sand pack without a booster. The mass flow controller has a range of 0 to 100 cm^3/min. It was planned to control and measure the gas injection rate.

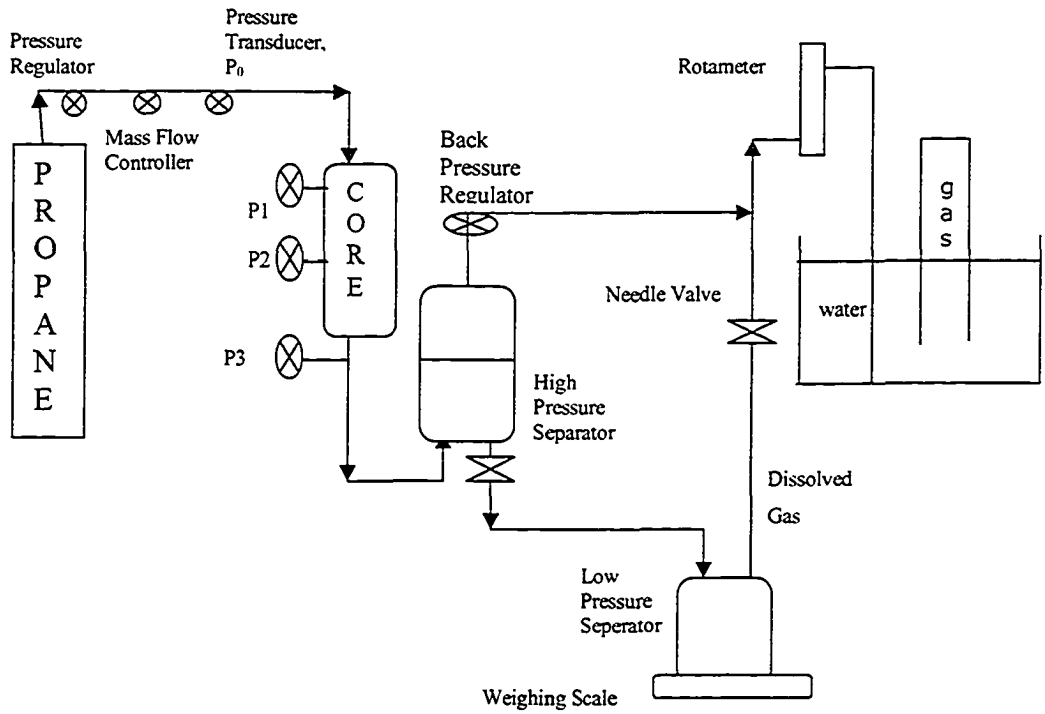

Figure 6-1: Schematic of the Experimental Set-Up

The sand-pack, the porous medium in which the flooding would be taking place, was a cylinder with one-foot length and two inches diameter. It was packed with glass beads (90 mesh) to obtain the expected reservoir permeability of 5 Darcies. The sand-pack was installed vertically to permit oil gravity drainage to take place. The sand-pack was designed to inject gas at the top and produce oil from the bottom so that the gravity difference of the injected gas and the original oil in the core is able to help stabilize the gas-oil interface. Two pressure transducers were calibrated and installed along the side of the core to measure the pressure difference between each section. Another pressure transducer was installed right below the end of the core in order to measure the pressure drop along the whole length of the core.

The production system consisted of the backpressure regulator, the high-pressure separator, the low-pressure separator, the needle valve, the weighing scale, the controllable gas rotameter and an inverted cylinder in the water bath for small gas rate measurement. The backpressure regulator was used for controlling the pressure through the core. A high-pressure separator was used because the backpressure regulator could be used only for the gas phase and because it could not be installed right below the sand-pack, where multiphase flow occurs. The low-pressure separator was used to separate the dissolved gas from the oil under ambient conditions. The needle valve was installed in case the produced gas rate exceeded its designed value, for example 10 cm^3/min for this experiment. Both the free gas and the dissolved gas were measured and controlled by the controllable gas rotameter. The rotameter had the lowest rate range (0-56 cm^3/min) obtainable and its calibration curve is shown in Appendix I.

6.2 Experimental Procedure

The experimental procedure included four steps: 1) packing, assembling and testing the tubular connections; 2) measuring pore properties of the sand-pack; 3) displacing *in-situ* oil by solvent at the desired constant rate and taking samples

during the displacement; and 4) measuring the produced free and dissolved gas volume as well as the asphaltenes content in the produced oil.

6.2.1 Packing

The core holder used for the experiments was mounted vertically with the bottom end sealed and the top end open. After the core holder was filled with water, a plastic tube with the same diameter and length as the core holder was installed on the top end of the core to allow relatively the same amount of weight to be on the upper layers of the sand. Small amounts of sand after having been soaked in water were poured into the core holder each time. This procedure was repeated until the level of the sand rose to a height 30% greater than the original height of the core holder. Then the core holder was set to vibrate so that the sand in the core could be packed tighter. The period of vibration time was about 20 hours.

6.2.2 Determination of Pore Properties

Porosity

The porosity of the sand pack was determined by measuring the amount of fluid used to saturate the core completely. In order to achieve a better accuracy in each measurement, the following steps were used: First, the core holder was set vertically with the bottom end sealed. After that, the core was filled with water. Finally the bottom end was opened and the water was displaced with air. The total water volume gathered can be considered as one pore volume. The porosity can be calculated using the known core holder volume.

Before measuring the permeability, water is injected once again to push most of the enclosed air from the pore space. Afterwards, CO_2 was injected to displace the remaining air. Then water was injected once again to displace the CO_2. Because CO_2 can be dissolved in water, it does not matter if the water can displace the CO_2 completely or not.

Permeability

The absolute permeability of the sand-pack was determined using the maximum flow rate (560 cm^3/hr) of the positive displacement pump. Water was injected from one end to the other end with the core in the horizontal mode. The pressure drop between the first pressure port and the third pressure port was measured. This pressure drop, together with the cross-sectional area and the distance between the pressure ports, and the viscosity of the injected fluid, was used in conjunction with Darcy's law to estimate the absolute permeability of the sand-pack. The arithmetic average value of three measurements for each pack was used as the permeability of the sand pack.

Saturation

To saturate the cores, oil was injected at a rate of 100 cm^3/hr into the bottom end of the core until about two pore-volumes of fluid were produced. The oil saturation then can be obtained by calculating the amount of oil injected divided by the pore volume.

6.2.3 Oil Properties Measurement and Analysis

Oil Viscosity

A digital viscometer was used to obtain the oil viscosity. The #3 low velocity spindle was chosen for the viscosity measurement of the Lloydminster oil that would be used in the experiment, because the measurement range is 2,000 cp to 400,000 cp. The spindle was attached to the viscometer's lower shaft and centered in the test oil until the meniscus of the fluid was at the center of the immersion groove on the spindle's shaft. Then the motor was turned on and a reading was recorded once stabilization was reached. This reading was then multiplied by the factor appropriate to the viscometer model/spindle/speed combination and the

viscosity was obtained. This process was repeated three times and the average was used as the final viscosity of the oil.

Asphaltenes Analysis Method (AOSTRA, 1998)

The method used was selected on the basis of the published information on the repeatability, equipment availability and operational difficulties. The method that was chosen for asphaltenes analysis was designated as ASTM D893. The procedure is: A 10 g sample is weighed and mixed with n-pentane to give a total volume of 100 cm^3. The mixture is centrifuged at a relative centrifugal force of 600* to 700* g and the oil solution decanted. The precipitate is washed twice with n-pentane, dried and weighed. The precision that the ASTM has published about this method is a repeatability of 10% and the ARC published repeatability for bitumen is 11.3%.

6.2.4 Experimental Conditions and Procedure

Two experiments were performed with different operating conditions. In Experiment #1, the gas injection pressure was adjusted and maintained at a constant value of 827 kPa (120 psig, the unit conversion is because the pressure transducer was calibrated in psig) by a regulator on the high-pressure gas cylinder. This gas injection pressure was set close to the propane vapour pressure of 876-924 kPa (127-134 psia) at room temperature (21°C-23°C) considering the average atmospheric pressure to be 100 kPa (13.4 psia). The injection rate was controlled in the range of 2 RC cm^3/min to 10 RC cm^3/min (under an injection pressure of 827 kPa (120 psig), the transformation between reservoir conditions and standard conditions is based on the gas equation of state). It was not possible to use the optimal injection rate (10 SC cm^3/min) because the measurement range of the mass flow meter is 0 to 100 cm^3/min. Consequently, it is difficult and not accurate to set the injection rate at low values such as 1 cm^3/min (corresponding to around 10 SC cm^3/min). It was not possible to control the production pressure as planned because the backpressure regulator only works for the gas phase and

could not be installed to control the oil production. Diluted oil was produced at the bottom of the model and accumulated in a separator connecting to atmospheric pressure. The produced oil was weighed offline. The production rate of gas from the top portion of the separator was measured using an inverted water cylinder via the displacement of water.

In Experiment #2, the main problems in Experiment #1 were solved. The gas production rate was controlled and measured by the controllable rotameter rather than by controlling the gas injection rate. The gas injection pressure was set at 758 kPa (110 psig). A high-pressure separator was used so that the backpressure regulator could be installed on the top of it to control the production pressure indirectly. The backpressure was set at 724 kPa (105 psig). With the installation of the high-pressure separator, the free gas could be vented or measured right after the backpressure regulator. The collected oil in the high-pressure separator was not allowed to release to the low-pressure separator very often because that would reduce the production pressure to atmospheric pressure. Then the oil production rate was measured by an online weighing scale. The solution gas from the produced oil was separated in a low-pressure separator connecting to atmospheric pressure and its volume was measured by the rotameter. At the beginning of the experiment, both the free gas and the solution gas were directed to a bottle of water to check the gas breakthrough time. The injection/production parameters were recorded every hour. The main operating parameters of these two experiments are summarized in Table 6-1.

Table 6-1: Operational Conditions for Physical Experiments

	Injection Pressure (psig)	Production Pressure (psig)	Backpressure Regulator	Separator Type	Pressure-Drop Measurement	Injection/Production Gas Rate Control	Oil Production Measurement
Core 1	120	14.7	Not Installed	Low-Pressure	Differential Pressure	Injection Rate	Offline Weighing
Core 2	110-120	105	Installed	Both High and Low Pressure	Absolute Pressure	Production Rate	Online Weighing

6.3 Physical Model Results and Discussion

6.3.1 Core and Oil Properties

The core and oil properties were measured following the method described in Section 6.2. The porosity measurements are shown in Table 6-2, the permeability measurements in Table 6-3, the oil viscosity measurements in Table 6-4, and a summary of the core and oil properties in Table 6-5.

The measurements of the porosity and the permeability (see Tables 6-2 and 6-3) show a very good consistency between the tests. The porosity is as low as 29%, which means that the core was packed tightly and successfully. The permeability measurements are consistent with what is predicted using the mesh size of the sands. The oil viscosity is a little less than the value of 10,000 cp used in the previous numerical simulation. The oil density data were obtained from Husky Energy. The displaced water volume during the water saturation measurement is 189 cm^3, which means only a very tiny (1 cm^3) amount of water remained in the core. This might be because the oil used is very viscous and the injection rate during

Table 6-2: Porosity Measurements

	Pore Volume (cm^3)	Diameter (cm)	Length (cm)	Core Volume (cm^3)	PV%
Core 1	190	5.3	30.48	672.1038	0.29
Core 2	190	5.3	30.48	672.1038	0.29

Table 6-3: Permeability Measurements

	P_{in} (volt)	P_{out} (volt)	P_{in} (atm)	P_{out} (atm)	Distance between Pressure Ports (cm)	Permeability (Darcy)	Average Permeability (Darcy)
Core 1	1.65	0.55	0.057188	0.019579	13.5	5.064	5.081
	1.67	0.57	0.057882	0.020291	13.5	5.066	
	1.64	0.55	0.056842	0.019579	13.5	5.111	
Core 2	1.7	0.51	0.058921	0.018155	13.5	4.672	4.730
	1.73	0.56	0.059961	0.019935	13.5	4.758	
	1.74	0.57	0.060308	0.020291	13.5	4.759	

Table 6-4: Oil Viscosity Measurements

Spindle No.	Spindle Speed (RPM)	Factor	Reading	Oil Viscosity (cp)	Average Oil Viscosity (cp)
LV 3#	3	400	22.2	8,880	8960
	6	200	45	9,000	
	3	400	22.5	9,000	

Table 6-5: Summary of Core and Oil Properties

	Length (cm)	Cross SectionalArea (cm^2)	Permeability (Darcy)	Porosity	Sw (%)	Oil Viscosity (cp)	Asphaltenes Content * (%)	Oil Density *(g/cm^3)
Core #1	30.48	20.25	5.08	0.29	0.5	8,960	14.5	0.963
Core #2	30.48	20.25	4.73	0.29	0.5	8,960	14.5	0.963

* data from Husky Energy

the displacing process was low enough so that the water was displaced completely. Consequently, the water saturation was as low as 0.5%.

6.3.2 Pressure Drop along the Core

The pressure drop along the core is a very important parameter to monitor the VAPEX process. It can indicate directly if the asphaltenes precipitation is blocking the fluid flow through the porous medium. The pressure drops along the core for the two experiments are shown in Tables 6-6, 6-7 and Figures 6-2, 6-3 and 6-4.

In Experiment #1, the pressure drop was measured by differential pressure between the top and the bottom of the core. The pressure drops before and after 50 hours were measured under the same and increasing injection rates, respectively. The results in Table 6-6 and Figures 6-2, 6-3 show that the differential pressure drops significantly with time and also at the same injection rate before 50 hours. After 50 hours, the pressure drop tends to be stable with the increasing gas injection rate. No pressure build up was ever noticed with the measurement accuracy of 0.1 psig. It indicates that no significant blockage of flow through the porous medium was observed.

Table 6-6: Pressure Drop along the Core for Experiment #1

Time (hr)	Injection Rate (cm^3/min)	Pressure Drop (psig)	Oil Production rate (g/hr)
0	2	5	
5	2	2.8	0.25
28	2	2-2.2	0.32
30	2	1.8-2	0.3
49	4	1.8	0.21
57	6	1.8	0.22
60	8	1.6	0.2
62	10	1.8	0.22

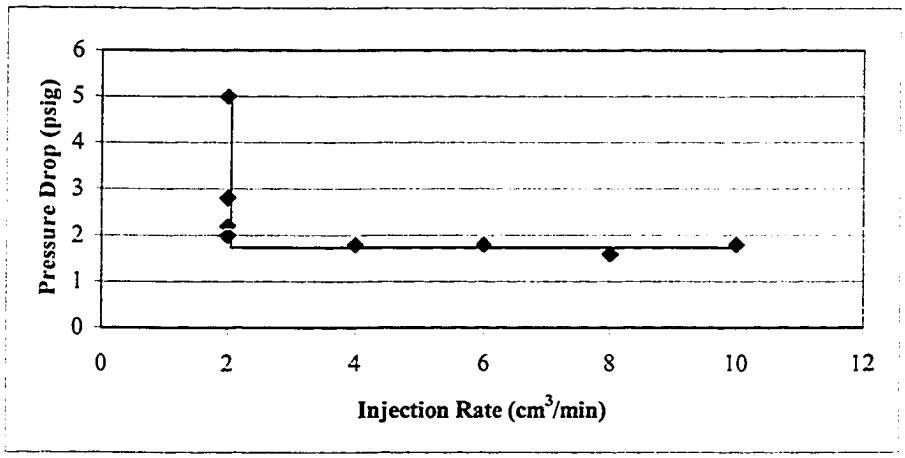

Figure 6-2: Pressure Drop along the Core for Experiment #1

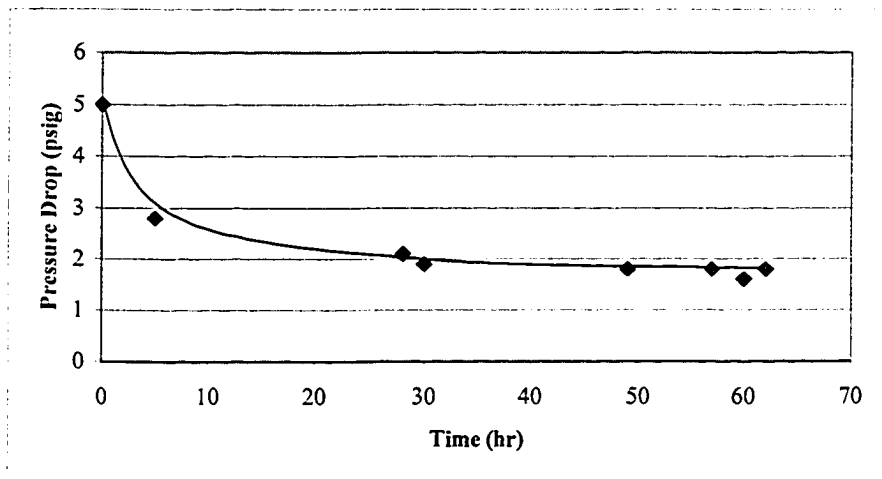

Figure 6-3: Pressure Drop with time for Experiment #1

In Experiment #2, the pressure drop was measured as the difference of the pressures at various locations. P_0 is the pressure right before the top of core; P_1 and P_2 are the pressures at the first and second pressure ports along the core; and P_3 is the pressure right after the bottom of the core. Table 6-7 and Figure 6-4 show clearly that both the difference between the first and second pressure ports, and the pressure drop through the whole core length, keep decreasing with time. This is consistent with the results obtained in Experiment #1.

Table 6-7: Pressure Drop along the Core for Experiment #2

Time (hr)	P_0 (volt)	P_1 (volt)	P_2 (volt)	P_3 (volt)	P_0 (psig)	P_1 (psig)	P_2 (psig)	P_3 (psig)	P_0-P_3	P_1-P_2
0	5.6	4.37	4.3	N/A	112	0			2.82656	
4.5	5.54	4.28	4.21	5.37	110.8	110.006	108.076	107.999	2.80073	1.93019
5	5.5	4.27	4.21	5.37	110	108.953	107.823	107.452	2.54815	1.13019
6	5.5	4.26	4.2	5.36	110	108.902	107.571	107.455	2.54528	1.33092
8	5.49	4.24	4.18	5.34	109.8	108.598	107.066	107.26	2.53954	1.53238
10.5	5.5	4.24	4.19	5.34	110	108.798	107.066	107.71	2.28983	1.73238
19.5	6.16	4.78	4.75	6.05	123.2	121.385	120.705	121.255	1.94539	0.68055
20	6.24	4.84	4.83	6.13	124.8	122.895	122.22	123.337	1.46319	0.67471
23	6	4.63	4.6	5.86	120	118.211	116.916	118.098	1.90234	1.29442
25	5.98	4.64	4.61	5.87	119.6	117.862	117.169	117.695	1.90521	0.69369
27	5.8	4.51	4.48	5.72	116	113.99	113.885	114.132	1.8679	0.10464
28	5.77	4.47	4.44	5.66	115.4	113.584	112.875	113.544	1.85642	0.70902
30	5.63	4.35	4.32	5.52	112.6	110.563	109.844	110.778	1.82198	0.71924
31	5.56	4.3	4.26	5.45	111.2	109.305	108.581	109.143	2.05734	0.72435
33	5.58	4.32	4.28	5.47	111.6	109.809	109.086	109.537	2.06308	0.72289
35	5.6	4.34	4.3	5.49	112	110.313	109.591	109.931	2.06882	0.72143
46.5	5.71	4.42	4.38	5.6	114.2	112.325	111.612	112.108	2.09178	0.7134
48	5.72	4.43	4.38	5.61	114.4	112.577	111.865	112.056	2.34436	0.71267
49.5	5.63	4.35	4.31	5.53	112.6	110.362	109.844	110.528	2.07169	0.51851
50.5	5.59	4.32	4.28	5.49	111.8	109.608	109.086	109.737	2.06308	0.52143
51.5	5.55	4.29	4.25	5.45	111	108.853	108.328	108.946	2.05447	0.52435
52.5	5.51	4.26	4.22	5.41	110.2	108.098	107.571	108.154	2.04586	0.52727
53.5	5.47	4.23	4.19	5.37	109.4	107.343	106.813	107.363	2.03725	0.53019
55.5	5.39	4.16	4.12	5.28	107.8	105.782	105.045	105.783	2.01716	0.73676
57.5	5.45	4.2	4.16	5.35	109	106.587	106.055	106.971	2.02864	0.53165
59	5.39	4.16	4.12	5.29	107.8	105.581	105.045	105.783	2.01716	0.53603
71	5.75	4.45	4.41	5.66	115	112.679	112.37	112.9	2.10039	0.30902
73	5.59	4.32	4.28	5.49	111.8	109.608	109.086	109.737	2.06308	0.52143
75	5.61	4.34	4.29	5.51	112.2	110.111	109.591	109.881	2.31853	0.51997
77	5.63	4.36	4.31	5.53	112.6	110.615	110.096	110.276	2.32427	0.51851
79	5.65	4.38	4.33	5.55	113	111.119	110.602	110.67	2.33001	0.51705
81	5.67	4.4	4.35	5.57	113.4	111.622	111.107	111.064	2.33575	0.51559
83	5.69	4.42	4.37	5.59	113.8	112.126	111.612	111.459	2.34149	0.51413

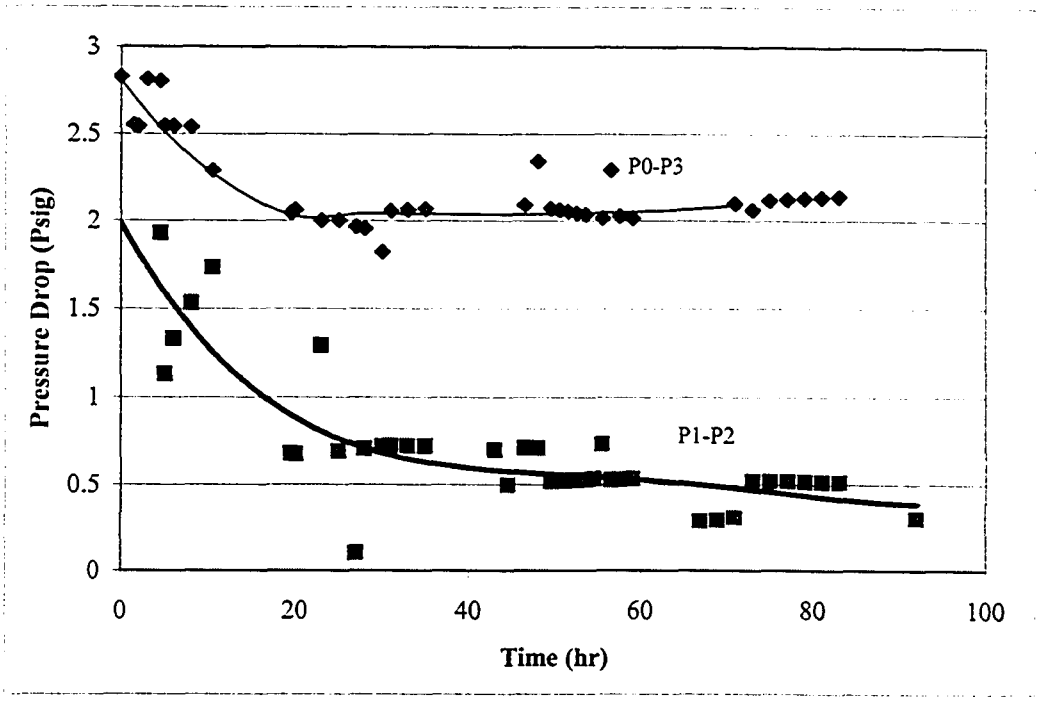

Figure 6-4: Pressure Drop along the Core for Experiment #2

6.3.3 Oil Production and Gas Breakthrough

In Experiment #1, the oil production was measured using the weighing scale because the production rate was too low to tell from the volume. The weighing scale was operated offline. The measured oil production rate is shown in Table 6-6 and presented in Figure 6-5. These data are compared with the expected oil production rate under optimal operating conditions (Cases 35 and 39) from the numerical simulation. A density of 0.963 g/cm^3 was used to change the volume oil rate of Cases 35 and 39 to a mass oil rate. It can be seen (Figure 6-5) that the oil production rates in the physical experiment and the numerical simulation share a similar decreasing trend, while the physical experiment result is one order lower in magnitude than the numerical simulation. The reason for this result was considered to be the uncontrolled production pressure in the physical experiment. The very high pressure drop without proper injection or production rate control resulted in a very high propane injection rate along the core, which increases the possibility of gas channeling and further leads to much less oil dissolved by the solvent to reach mobility. As a result, the oil production

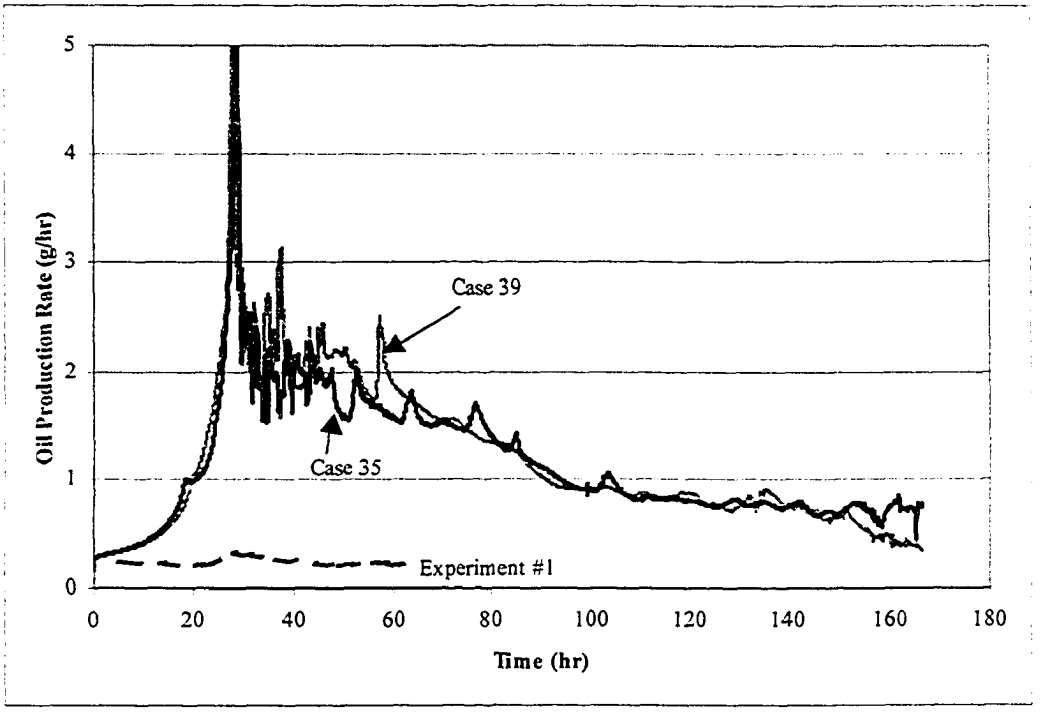

Figure 6-5: Comparison of Experimental and Expected Oil Production Rate from Numerical Simulation

rate was less than what was expected. The gas channeling claimed above was observed by the early gas breakthrough at 5 hours in the experiment, rather than at 30 hours in the numerical simulation which had the production pressure controlled. The breakthrough time of 30 hours is indicated as the peak oil production rate shown in Figure 6-5.

In addition, a numerical simulation under similar operating conditions as Experiment #1 (Case 41) was run and is shown in Figure 6-6. It is obvious that the oil rate curve in the numerical simulation matches that in the physical experiment. The experimental results are stabler than the numerical results because the experimental oil production rate was measured as average rate for a period rather than instantaneous rate. It demonstrates once again that the numerical model can simulate the process successfully. The first oil production rate peak of Case 41 indicates an early breakthrough time of 5 hours. The second oil rate peak indicates the start of the drainage stage.

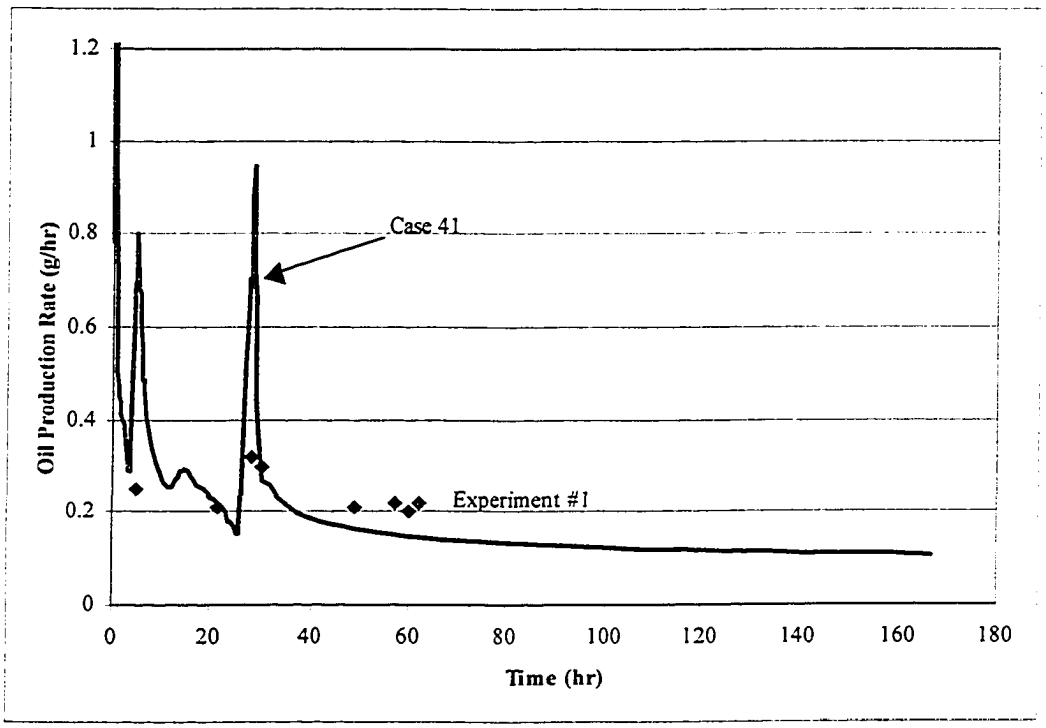

Figure 6-6: Oil Production Rate under Uncontrolled Production Pressure

In Experiment #2, the backpressure regulator was installed at the downstream end of the core. It was planned to measure the oil production on the weighing scale online so that the oil production rate could be obtained easily and the gas did not have to be released when trying to measure the oil production offline. Unfortunately, this approach did not work as well as expected. The scale used for oil production measurement kept jumping from negative to positive and in no way recorded reasonable values. The total amount of oil production was found to be too small after being transferred from the high-pressure separator. One of the reasons for this is considered to be the large volume of the flow line tubes, which is approximately 20 cm^3. That is, only volumes exceeding 20 cm^3 can be collected in the sample bottle. Another factor that may have affected the performance of the experiment is that the rotameter could not be set at the expected production rate before some gas had been produced. This would promote gas channeling and affect the oil production rate.

Gas was not produced continuously. The tiny amount of gas measured occasionally was considered to be the displaced air remaining in the connection tubes. The backpressure regulator was installed a horizontal distance of 120 cm and a vertical distance of 30 cm from the bottom of the core. Consequently, the value of the backpressure used was based on an estimate rather than on the optimized value from the numerical simulation. Moreover, the backpressure value was so high that it prevented the gas from being produced. The direct consequences of this might be solvent soaking to a certain extent, gas breakthrough being hard to detect and asphaltenes depositing in the core and further blocking the pores. This speculation is partially supported by the very slow decline of the injection pressure after turning off the tank valve and connecting the output to atmospheric pressure.

6.3.4 Oil Properties Measurement

As only a small amount of oil was recovered in Experiments #1 and #2, the produced oil properties were hard to measure. Hence the asphaltenes content and viscosity of the produced oil could not be determined and compared to the original oil properties.

An attempt was made to analyze the properties of the oil remaining in the core. However, the asphaltenes content obtained from the mixture of oil and sand actually included the asphaltenes contained in the oil and those sticking to the sand particles. This value would be constant because the asphaltenes deposits from the oil onto the sand grains. These two values could not be separated. However, a test was made through mixing the remaining oil in the core with water. The appearance performance was compared with that of the original oil (non-solvent diluted) in the water. The former case showed evidence of flocculation, while in the latter case, the oil stayed on the top of the water phase. This result demonstrated that asphaltene precipitation did occur in the core.

6.3.5 Recommendations for Future Experiments

1. A gas booster is needed for future experiments because the pressure in the propane cylinder may become lower than that needed in the later stage of the experiment.

2. A mass flow controller that can measure and control gas rates as low as 1 cm^3/min is needed.
3. The backpressure should be set lower than the value used in Experiment #2. The gas production rate should be controlled at the expected level at the beginning of the experiment.
4. The length of the connection tubes from the bottom of the core to the production container should be minimized.
5. An accurate digital scale (accuracy 0.001-0.01g) that can work on line is needed.

6.4 Summary

1. A VAPEX physical experiment for a reservoir permeability of 5 Darcies is hard to perform because the gas injection/production rate required is much lower than that for a high permeability experiment. Such rates are hard to measure and control both at the upstream end of the core and the downstream end because the lowest range of the flow meter for propane obtainable is 0 to 100 cm^3/min,while the optimized injection rate is 10 cm^3/min.
2. No significant blockage of flow through the porous medium was observed in both Experiments #1 and #2. That is, the pressure drops along the core in both Experiments #1 and #2 did not appear to be affected by asphaltenes deposition.
3. The results from Experiment #1 emphasized the importance of gas production pressure control.
4. The numerical model was demonstrated once again to be able to predict the oil production rate at the same level as in the experiment.
5. The performance of Experiment #2 could not be tracked properly because of the online weighing system and the high volume of the connection tubes.
6. High backpressure may have made it difficult to detect gas breakthrough in Experiment #2.
7. For Experiment #2, the injection pressure was difficult to release after turning off the tank valve and connecting the output to atmospheric pressure. This may indicate asphaltenes deposition.

7.0 CONCLUSIONS AND FUTURE WORK

The results presented in this study show that the numerical model constructed can reproduce the main features of the VAPEX process, and the asphaltenes precipitation was investigated both from a numerical and a physical perspective. The following conclusions can be drawn from this work:

1. VAPEX is easily modeled with STARS. STARS, which was used in the isothermal mode, is very fast.
2. The numerical simulation led to the same conclusions as the physical experiment. In particular, the effect of the well configuration, the operating pressure and the water saturation on the performance of VAPEX process was the same in both types of experiment.
3. A combination of operating pressure and gas rate control was critical for the optimal performance of the VAPEX process.
4. The numerical model constructed was able to history match the experimental results reported by Dr. Butler and the physical experimental results obtained in this study.
5. No significant blockage of flow through the porous medium was observed. That is, the pressure drops along the core in both Experiments #1 and #2 did not appear to be affected by asphaltene deposition.

In this study, it was not possible to conduct the experiments under optimal operating conditions. Focusing improvement on the overall methodology, the following future work is recommended:

- The equipment set-up need further development before one could perform the VAPEX process under optimal conditions, such as increasing the measurement accuracy of the equipment, introducing the multiphase backpressure etc..
- More experiments with varied operating conditions are necessary to investigate the conditions under which asphaltenes deposition occurs.

8.0 REFERENCES

Alberta Oil Sands Technology and Research Authority, (1998), " A Review of Analytical Methods for Bitumens and Heavy Oils", p. 101.

Baytex company, http://www.baytex.com

Bear, J., (1988), "Dynamics of Fluids in Porous Media", Dover Publications Inc., New York.

Boustani, A., (2002), "Investigation of Interfacial Mass Transfer in Vapour Extraction Process", M.Sc. Thesis, Department of Chemical and Petroleum Engineering, University of Calgary.

Burke, N.E., Hobbs, R.E. and Kashou, S. F., (1990), "Measurement and Modeling of Asphaltenes Precipitation", Journal of Petroleum Technology, November, pp. 1440-1456.

Butler, R. M. and Jiang, Q., (1997), "Improved VAPEX Performance Using Widely Spaced Horizontal Injectors and Producers", presented at the Seventh Petroleum Conference of the South Saskatchewan Section, Regina, Saskatchewan, 19-22 October.

Butler, R. M., Mcnab, G. S. and Lo, H. Y., (1979), " Theoretical Studies on the Gravity Drainage of Heavy Oil During In-Situ Steam Heating", presented at the 29th Canadian Chemical Engineering Conference, Sarnia, Ontario, 1-3, October.

Butler, R.M. and Mokrys, I.J., (1989), "The Rise of Interfering Solvent Chambers: Solvent Analog Model of Steam Assisted Gravity Drainage", AOSTRA Journal of Research, Vol.5, No.1, pp. 17-32.

Butler, R.M. and Mokrys, I.J., (1991), "A New Process (VAPEX) for Recovering Heavy Oils Using Hot Water and Hydrocarbon Vapour", Journal of Canadian Petroleum Technology, January-February 1991, Volume 30, No.1, pp. 97-106

Butler, R.M. and Mokrys, I., (1993a), "Closed-Loop Propane Extraction Method for the Recovery of Heavy Oils and Bitumens Underlain by Aquifers: The VAPEX Process", Paper No. 93-35, presented at the Fifth Petroleum

Conference of the south Saskatchewan section, the Petroleum Society of CIM, held with CANMET in Regina, Saskatchewan, 18-20 October.

Butler, R.M. and Mokrys, I.J., (1993b), "Recovery of Heavy Oils Using Vapourized Hydrocarbon Solvent: Further Development of the VAPEX Process", Journal of Canadian Petroleum Technology, June 1993, Volume 32, No. 6, pp.56-62.

Computer Modeling Group LTD manuals, STARS, GEM, version 2002, Calgary, Canada.

Coskuner, G. and Bentsen, R. G., (1990), " An Extended Theory to Predict the Onset of Viscous Instabilities for Miscible Displacements in Porous Media", Transport in Porous Media, 5, pp. 473-490.

Cuthiell, D. and Kissel, G., (2004), " Viscous Fingering Effects in Solvent Displacement of Heavy Oil", paper No. 2004-073, Canadian International Petroleum Conference, Calgary, Alberta, 8-10 June.

Cuthiell, D. and McCarthy C., (2003), " Investigation of the VAPEX Process Using CT Scanning and Numerical Simulation", Journal of Canadian Petroleum Technology, February, Volume 42, No.2, 41-50.

Das, S.K. and Butler, R.M., (1994a), " Investigation of VAPEX Process in a Packed Cell Using Butane as a Solvent", paper No. HWC 94-47, presented at the Society of Petroleum Engineers/Canadian Institute of Mining, Metallurgy & Petroleum /Canada Centre for Mineral and Energy Technology (SPE/CIM/ CANMET) International Conference in Horizontal Well Applications, Calgary, Alberta, 20-23 March, 1994.

Das, S.K. and Butler, R.M, (1994b), "Effect of asphaltenes deposition on the VAPEX process: A preliminary investigation using Hele-Shaw cell", The Journal of Canadian Petroleum Technology, June 1994, Volume 33, No.6.

Dauba, C., Quettier, L., Christensen, J., LeGoff, C. and Cordelier, P., (2002) "An Integrated Experimental and Numerical Approach to Assess the Performance of Solvent Injection into Heavy Oil", SPE 77459, presented at the SPE Annual Technical Conference and Exhibition held in San Antonio, Texas, 29 September.

Donnelly, J. K., (1997), " Application of Steam Assisted Gravity Drainage (SAGD) to Cold Lake", presented at the Joint Society of Petroleum Engineers

-Petroleum Society of Canadian Institute of Mining, Metallurgy & Petroleum 6th One-Day Conference on Horizontal Well Technology, Calgary, Alberta, 15 November.

Dumoré, J.M. (1964), " Stability Considerations in Downward Miscible displacements", SPE, 961, presented at 39th SPE Annual Fall Meeting, Houston, Texas, 11-14, October.

Fisher, B., Singhal, A. K., Goldman, J., Jackson, C. and Randall, L., (2002), " Insight from MRI and Micro Model Studies of Transport of Solvent into Heavy Oil", SPE 79024, presented at the 2002 SPE International Thermal Operations and Heavy Oil Symposium and International Horizontal Well Technology Conference, Calgary, Alberta, 4-7 November.

Gupta, A.K., (1986), "A Model for Asphaltenes Flocculation Using an Equation of State", M.Sc. Thesis, Department of Chemical and Petroleum Engineering, University of Calgary, June.

Hirschberg, A., deJong, L.N.J., Schipper, B.A., and Meijer, J.G. (1984), "Influence of Temperature and Pressure on Asphaltenes Flocculation", ACS Symposium Series, pp. 443-458.

Jha, K.N., Butler, R.M., Lim, G.B. and Oballa, V., (1995), "Vapour Extraction (VAPEX) Process for Recovery of Heavy Oil and Bitumen", presented at 6th UNITAR Heavy Crude & Tar Sands Int. Conf., Houston, Texas, pp. 12-17.

Jiang, Q., (1997), "Recovery of Heavy Oil and Bitumen Using VAPEX Process in Homogeneous and Heterogeneous Reservoirs", PhD Thesis, Department of Chemical and Petroleum Engineering, University of Calgary.

Jiang, Q. and Butler, R.M., (1996), " Experimental Studies Effects of Reservoir Heterogeneity on the VAPEX Process", Journal of Canadian Petroleum Technology, December, Volume 35, No. 10, 46-54.

Kokal, S.L., Najman, J., Sayegh, S.G., and George, A.E., (1992), "Measurement and Correlation of Asphaltenes Precipitation from Heavy Oils by Gas Injection", Journal of Canadian Petroleum Technology, Vol.31, No.4, April, pp.24-30.

Leontarieis, K.J. and Mansoori, G.A., (1988), "Asphaltenes Deposition: A Survey of Field Experiences and Research Approaches", Journal Petroleum Science and Engineering, Vol. 1, pp. 229-239.

Luhning, R. W., Das, S. K. and Fisher, L.J., (2003), "Full Scale VAPEX process-Climate Change Advantage and Economic Consequences", Journal of Canadian Petroleum Technology, February, Volume 42, No.2, 29-35.

Luhning, R. W. and Luhning C.P., (1999) "The VAPEX Process: non-Thermal Recovery of Bitumen and Heavy Oil for Improved Economics and Climate Change Advantage", presented at the Canadian Heavy Oil Association Conference, Calgary, Alberta, 13 April.

Mattax, C., (1990), "Reservoir Simulation", Monograph 13 (Society of Petroleum Engineers, U.S.A.)

Mehrotra, A. K. and Svreck. W.Y., (1986), "Viscosity of Compressed Athabasca Bitumen", Canadian Journal of Chemical Engineering, October, pp. 844-847.

Mokrys, I.J. and Butler, R.M., (1993), "In-Situ upgrading of heavy oils and bitumen by propane deasphalting: the VAPEX process", paper SPE 25452, presented at the Production Operations Symposium held in Oklahoma City, OK, U.S.A., 21-23 March .

Nghiem, L.X., Coombe, D. A. and Farouq Ali, S. M., (1998) " Compositional Simulation of Asphaltenes Deposition and Plugging", SPE 48996, 1998 SPE Annual Technical Conference and Exhibition, New Orleans, Louisiana, 27-30 September.

Nghiem, L.X., Hassam, M.S. and Nutakki, R., (1993), "Efficient Modelling of Asphaltenes Precipitation", SPE 26642, 68th Annual Technical Conference and Exhibition, Houston, Texas, 3-6 October.

Nghiem, L. X., Kohse, B. F. and Sammon, P. H., (2000a), "Compositional Simulation of the VAPEX Process", paper No. 2000-34, Canadian International Petroleum Conference, Calgary, Alberta, 6-8 June.

Nghiem, L. X., Sammon, P, H. and Kohse, B. F., (2000b), "Asphaltenes Precipitation: Phase Behaviour Modelling and Compositional Simulation",

SPE 59432, presented at the SPE Asia Pacific Conference on Integrated Modeling for Asset Management, Yokohama, Japan, 25-26 April 2000.

Nghiem, L. X., Sammon, P, H. and Kohse, B. F., (2001), "Modeling Asphaltenes Precipitation and Dispersive Mixing in the VAPEX Process", SPE 66361, presented at the SPE Reservoir Simulation Symposium held in Houston, Texas, 11-14 February.

Novosad, Z., and Costain, T.G., (1990), " Experimental and Modelling Studies of Asphaltenes Equilibria for a Reservoir Under CO2 Injection," paper SPE 20530, presented at the 1990 SPE Annual Technical Conference and Exhibition, New Orleans, Louisiana, 23-26 September.

Oduntan, A.R., Chatzis, I., Smith, J. and Lohi, A., (2001), "Heavy Oil Recovery Using the VAPEX Process: Scale-Up Issues", presented at the Canadian International Petroleum Conference, Calgary, Alberta, Canada, 12-14, June.

Perkins, T.K. and Johnston, O.C., (1963), "A Review of Diffusion and Dispersion in Porous Media," SPE Journal, pp. 70-80.

Rahnama, F., (2003), " Alberta's Reserves 2003 and Supply/Demand Outlook 2004-2013," EUB Statistical Series (ST) 2004-98

Shrivastava, V. K. and Nghiem, L. X., (2002), "A Novel Approach for Incorporating Physical Dispersion in Miscible Displacement", paper SPE 77724, SPE Annual Technical Conference and Exhibition, San Antonio, Texas, 29 September –2 October.

Shu, W.R., (1984), "A Viscosity Correlation for Mixtures of Heavy Oil, Bitumen and Petroleum Fraction: Society of Petroleum Engineering Journal, June, pp. 277-82.

Sigmund, P.H., (1976), "Prediction of Molecular Diffusion at Reservoir Conditions. Part 2—Estimating the effects of Molecular Diffusion and Convective Mixing in Multicomponent Systems", Journal of Canadian Petroleum Technology, July-September, pp. 53-62.

Singhal, A.K., Fisher, D. B., Fung, H. and Goldman J., (2002), "Compositional Changes During VAPEX Operations in Heavy Oil Pools", presented at Canadian International Petroleum Conference, Calgary, Alberta, 11-13 June, 2002.

Thomas, F. B., Bennion, D. B., Bennion, D. W., and Hunter, B. E. (1992), "Experimental and Theoretical Studies of Solids Precipitation From Reservoir Fluid", Journal of Canadian Petroleum Technology, Volume 31, No. 1, January, pp.22-31.

Wen, Y.W., Kantzas, A. and Wang, G. J., (2004), "Estimation of Diffusion Coefficients in Bitumen Solvent Mixtures Using X-Ray CAT Scanning and Low Field NMR", paper No. 2004-064, Canadian International Petroleum Conference, Calgary, Alberta, 8-10 June.

World Energyhttp://www.worldenergy.org/wec-geis/publications/default/tech_papers

Yazdani, A., and Maini, B., (2004), "Effect of Drainage Height and grain Size on the Convective Dispersion in the VAPEX Process: Experimental Study", SPE 89409, presented at the 2004 SPE/DOE Fourteenth Symposium on Improved Oil Recovery held in Tulsa, Oklahoma, U.S.A, 17-21 April.

Appendix A: Mathematical and Numerical Model

The following equations express all the relevant physical phenomena of the porous media fluid flow in mathematical form. They are adapted from the STARS manual. No aquifer is considered.

The conservation equation of flowing component i is:

$$V\frac{\partial}{\partial t}\left[\varphi_f\left(\rho_w S_w W_i + \rho_o S_o X_i + \rho_g S_g Y_i\right) + \varphi_{void} Ad_i\right] = \sum_{k=1}^{nf}\Big[T_w \rho_w W_i \Delta\Phi_w + T_o \rho_o W_i \Delta\Phi_o + T_g \rho_g W_i \Delta\Phi_g \Big] + V \sum_{k=1}^{nm}\left(s'_{ki} - s_{ki}\right) r_k + \sum_{k=1}^{nf}\Big[\varphi D_{wi} \rho_w \Delta W_i + \varphi D_{oi} \rho_o \Delta X_i + \varphi D_{gi} \rho_g \Delta Y_i \Big] + \delta_{iw} \sum_{k=1}^{nf} \rho_w q_{wk} W_i + \rho_o q_{ok} X_i + \rho_g q_{gk} Y_i \quad \text{[well layer k]}$$

The conservation eaquation of solid component i is:

$$V\frac{\partial}{\partial t}\left[\varphi_{void} c_i\right] = V \sum_{k=1}^{nm}\left(s'_{ki} - s_{ki}\right) r_k$$

The conservation equation of energy is:

$$V\frac{\partial}{\partial t}\left[\varphi_f\left(\rho_w S_w U_w + \rho_o S_o U_o + \rho_g S_g U_g\right) + \varphi_{void} c_{solid} U_{solid} + \left(1 - \varphi_{void}\right) U_m\right] = \sum_{k=1}^{nf}\Big[T_w \rho_w H_w \Delta\Phi_w + T_o \rho_o H_o \Delta\Phi_o + T_g \rho_g H_g \Delta\Phi_g \Big] + \sum_{k=1}^{nf} k\Delta T + V \sum_{k=1}^{nm} H_{rk} r_k + HL_o + HL_{convective} + HL_{constant}$$

The phase transmissibilities T_j are:

$$T_j = T\left(\frac{k_{rj}}{\mu_j r_j}\right) \qquad j = w, o, g$$

Upstream weighing scheme: the fluid mobility is based on the relative permeavility and viscosity data computed from fluid saturations and pressures in the upstream cell (n).

$$q = T_n\left(P_n - P_{n+1}\right)$$

Appendix B: Relative Permeability Curves

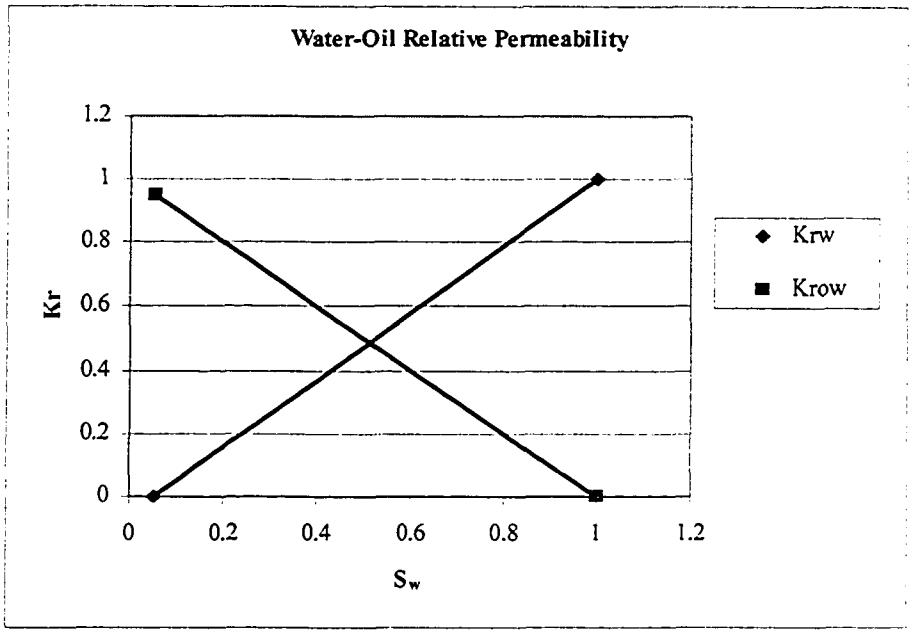

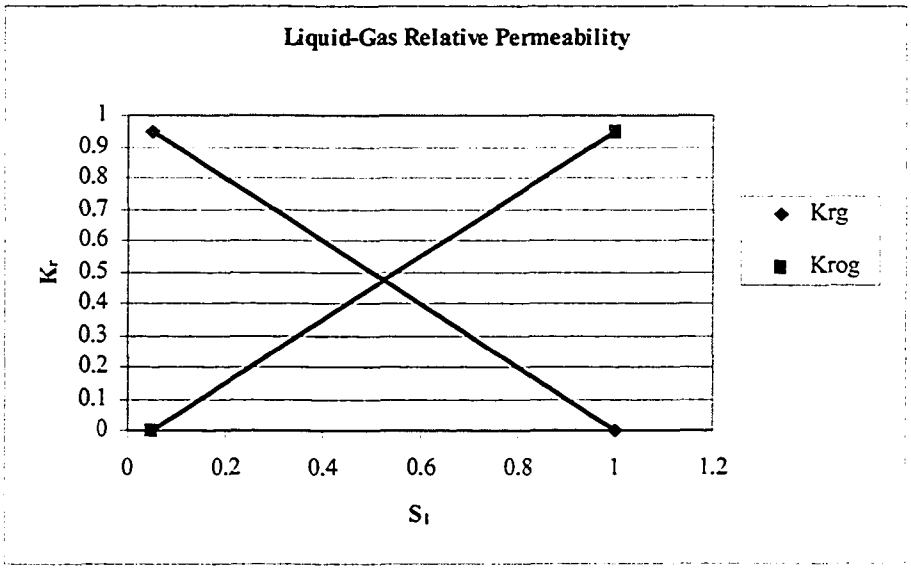

Figure B-1: Linear Relative Permeability Curves

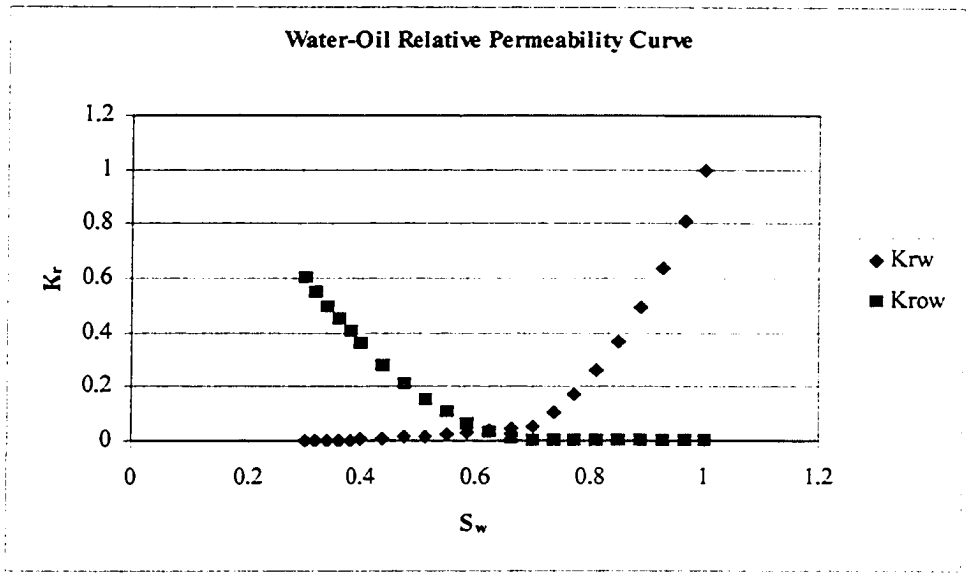

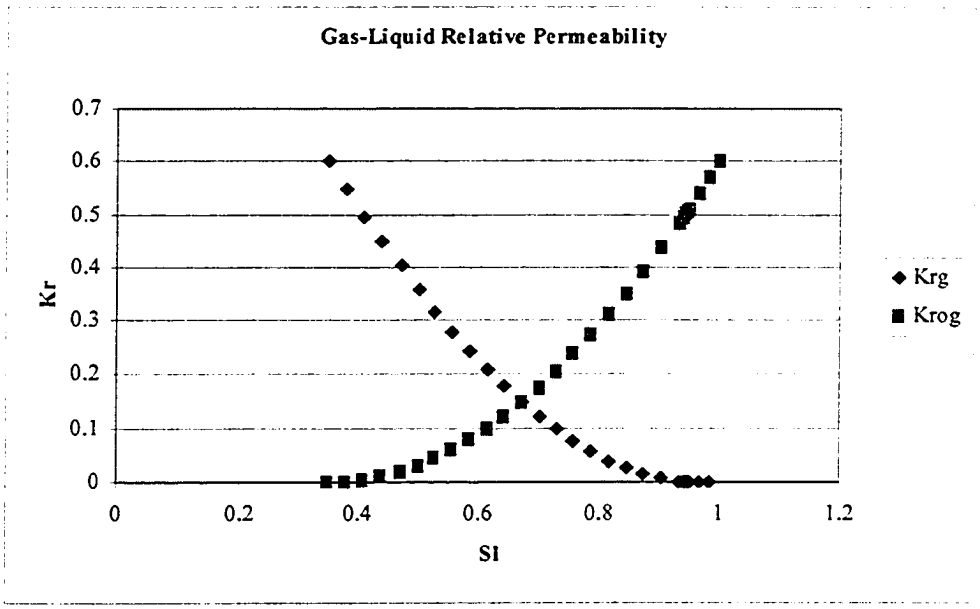

Figure B-2: Non-linear Relative Permeability Curves (after Donnelly, 1997)

Appendix C: Vapour Pressure of Propane

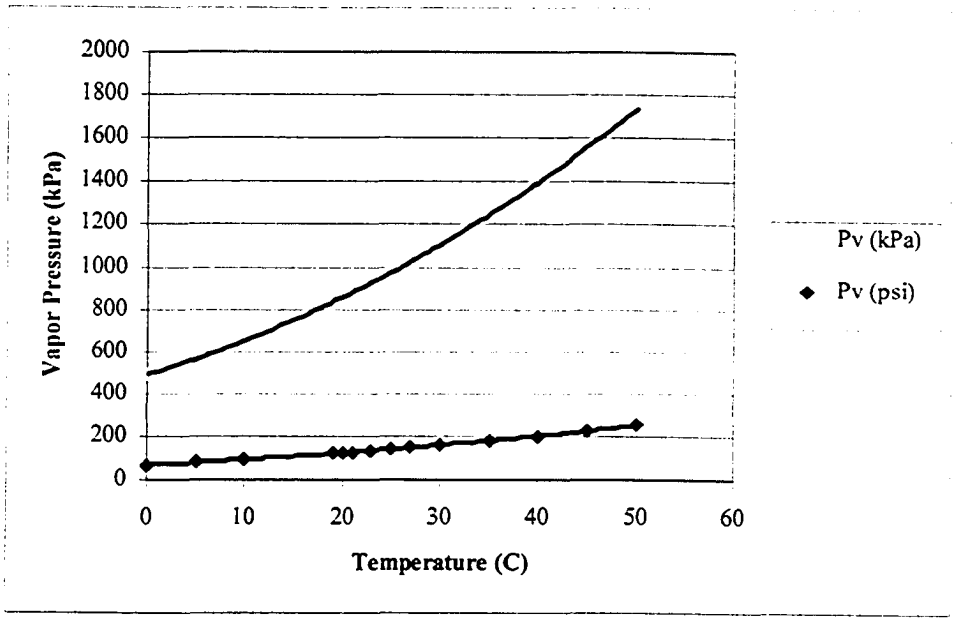

Figure C-1: Propane Vapour Pressure vs. Temperature

Appendix D: Reaction Model and Blocking Model

The material that follows has been adapted, for the reader's convenience, from the STARS manual.

Chemical reactions have traditionally been used almost exclusively in combustion processes. However, reactions may be used in any thermal or isothermal simulation if desired. Since reactions are treated as source/sink terms for each component and energy, they may be thought of as another way in which to link together the different components of a problem when rate is important. In particular, interphase mass transfer rates can be modelled, involving either well-defined components or "dispersed phase" components such as emulsion droplets.

CMG uses the reaction model to simulate asphaltenes precipitation during primary production. To use the reaction model, the user is just responsible for ensuring that the stoichiometric coefficients entered as data represent a mass-conserving set. A set of mass-conserving coefficients will satisfy: Sum of fluid component molecular mass (i)*stoichiometric coefficient of reacting componet (i)=sum of cmm (i)*stoichiometric coefficient of produced component.

Particles captured by the porous medium can cause permeability reductions (blockage) in a manner similar to equilibrium mass transfer to the rock (adsorption)

STARS offer the nonequilibrium blockage function to the permeability reductions (blockage) in a manner similar to equilibrium mass transfer to the rock.

The rate of propagation of many additives (surfactants, caustic, polymers) and in situ created species (fines, emulsions) are strongly

affected by their interaction with the rock matrix. These interactions can be chemical (e.g. ion exchange) or mechanical (e.g. blockage, straining capture) or some combination of mechanisms. The capture levels can depend on fluid concentrations, temperature and rock type (e.g. permeability).

STARS allows a phenomenological description of these phenomena, wherein a set of constant temperature adsorption isotherms (adsorption level as a function of fluid composition) are input. Their isotherms can be either in tabular form or in terms of the well known Langmuir isotherm correlation.

Permeability alteration often accompanies adsorption (especially if adsorption is of mechanical, blockage type). The simulator accounts for this via a region dependent resistance factor, which allows correlation of local permeability with local adsorption levels-it is assumed that only single-phase flow paths are altered. If the captured droplet is assumed to come from the oil phase then the oil phase effective permeability is

$$\frac{(absoluteperm)}{1+RRSFT*ccfac}*oilrelativeperm$$

where ccfac=max (0, cc-sldmin).

RRSFT: Flow restriction factor for the captured component.

In a manner similar to (equilibrium) adsorption blockage. Here cc is the concentration of captured oil droplets. If the captured droplet comes form the water or gas phases then the phase effective permeability is modified analogously.

The minimum solid concentration for blockage to start is given by sldmin. If cc is less than sldmin, no blockage occurs.

Appendix E: Data file for Model One

```
RESULTS SIMULATOR STARS
** Butler 2D VAPEX process is simulated

**============= INPUT/OUTPUT CONTROL================
**checkonly
*interrupt *stop
*title1 'Vapex 2D Corner Point Grid'
*inunit  lab  except 6 2  ** micro-m**2
*outprn *grid pres so sg  temp x viso kro krg rfg rfo  masdeno masdeng
*outsrf *grid pres sw so x viso rfg rfo
*outprn *well wellcomp  *outprn *iter *tss **newton
*outsrf *well downhole  **mass **comp
*wrst 10  *wprn *grid 10  *wprn *iter 1

** ============GRID AND RESERVOIR DEFINITION============
** actual size is 69.8x3.5x21.7
*grid *corner 15 1 6
*kdir *down        ** Two-dimensional grid
*di *ivar 15*4.65
*dj *con 3.5
*zcorn
0.0  28*0.0   0.0   0.0  28*0.0  0.0                                          **1 T
4.35 2*4.25 2*4.00  2*3.875 2*3.7 2*3.5 2*3.25  2*3.125 2*2.875 2*2.75  **1 B
2*2.5 2*2.4   2*2.225 2*2.0   2*1.8  1.52
4.35  2*4.25  2*4.00 2*3.875 2*3.7 2*3.5 2*3.25  2*3.125 2*2.875 2*2.75 **1 B
2*2.5 2*2.4   2*2.225 2*2.0   2*1.8  1.52
4.35 2*4.25  2*4.00 2*3.875 2*3.7 2*3.5 2*3.25  2*3.125 2*2.875 2*2.75  **2T
2*2.5 2*2.4   2*2.225 2*2.0   2*1.8 1.52
4.35 2*4.25  2*4.00 2*3.875 2*3.7  2*3.5 2*3.25  2*3.125 2*2.875 2*2.75  **2T
2*2.5 2*2.4   2*2.225 2*2.0   2*1.8 1.52
8.7   2*8.25 2*7.9 2*7.5 2*7.25 2*6.875 2*6.5 2*6.2  2*5.75 2*5.5 2*5.05  **2B
2*4.75 2*4.45 2*4 2*3.75  3.48
8.7   2*8.25 2*7.9 2*7.5 2*7.25 2*6.875 2*6.5 2*6.2  2*5.75 2*5.5 2*5.05  **2B
2*4.75 2*4.45 2*4 2*3.75  3.48
8.7   2*8.25 2*7.9 2*7.5 2*7.25 2*6.875 2*6.5  2*6.2  2*5.75 2*5.5 2*5.05 **3T
2*4.75 2*4.45 2*4 2*3.75  3.48
8.7   2*8.25 2*7.9 2*7.5 2*7.25 2*6.875 2*6.5  2*6.2  2*5.75 2*5.5 2*5.05 **3T
2*4.75 2*4.45 2*4 2*3.75  3.48
13.05  2*12.5 2*11.95 2*11.4 2*10.925 2*10.375  2*9.75 2*9.25 2*8.75    **3B
2*8.30  2*7.75  2*7.25  2*6.75  2*6.25  2*5.75  5.37
13.05  2*12.5 2*11.95 2*11.4 2*10.925 2*10.375  2*9.75 2*9.25 2*8.75    **3B
2*8.30  2*7.75  2*7.25  2*6.75  2*6.25  2*5.75  5.37
13.05  2*12.5 2*11.95 2*11.4 2*10.925 2*10.375 2*9.75 2*9.25 2*8.75    **4T
2*8.30  2*7.75  2*7.25  2*6.75  2*6.25  2*5.75  5.37
```

```
13.05  2*12.5 2*11.95 2*11.4 2*10.925 2*10.375 2*9.75 2*9.25 2*8.75    **4T
2*8.30  2*7.75  2*7.25  2*6.75  2*6.25  2*5.75  5.37
17.4   2*16.75 2*16 2*15.375 2*14.72 2*14.0  2*13.25 2*12.625  2*11.55 **4 B
2*11.2 2*10.45  2*9.75  2*9.125 2*8.45  2*7.75   7.2
17.4   2*16.75 2*16 2*15.375 2*14.72 2*14.0  2*13.25 2*12.625          **4 B
2*11.55 2*11.2 2*10.45  2*9.75  2*9.125 2*8.45  2*7.75   7.2
17.4   2*16.75 2*16 2*15.375 2*14.72 2*14.0  2*13.25 2*12.625 2*11.55  **5T
2*11.2 2*10.45  2*9.75  2*9.125 2*8.45  2*7.75   7.2
17.4   2*16.75 2*16 2*15.375 2*14.72 2*14.0 2*13.25 2*12.625 2*11.55  **5T
2*11.2 2*10.45  2*9.75  2*9.125 2*8.45  2*7.75   7.2
21.75  2*20.88 2*20.0 2*19.15 2*18.25 2*17.5  2*16.5 2*15.75 2*14.85  **5 B
2*14.0 2*13.15  2*12.35  2*11.5  2*10.75 2*9.875 9.04
21.75  2*20.88 2*20.0 2*19.15 2*18.25 2*17.5  2*16.5 2*15.75 2*14.85  **5 B
2*14.0 2*13.15  2*12.35  2*11.5  2*10.75 2*9.875 9.04
21.75  2*20.88 2*20.0 2*19.15 2*18.25 2*17.5  2*16.5 2*15.75 2*14.85  **6 T
2*14.0 2*13.15  2*12.35  2*11.5  2*10.75 2*9.875 9.04
21.75  2*20.88 2*20.0 2*19.15 2*18.25 2*17.5  2*16.5 2*15.75 2*14.85  **6 T
2*14.0 2*13.15  2*12.35  2*11.5  2*10.75 2*9.875 9.04
21.75 28*21.75  21.75 21.75  28*21.75 21.75                           **6 B
*por *con 0.391
*permi *con 1135
*permj *equalsi
*permk *equalsi
*vatype con 1
*end-grid
*prpor 915

** ============== FLUID DEFINITIONS ====================
*model 4 4 4   ** One aqueous and three oleic components
*compname 'WATER' 'LLOYD_O' 'ASPHALT' 'PROPANE'
**              -----  --------  --------  --------
*cmm             0        .450      .600      .0441
*molden          0       2.04e-3   1.6e-3    0.01151
*cp              0     1.944e-7  1.944e-7   1.151e-6
*pcrit           0        1000      1000       4246
*tcrit           0         500       500      96.65
*cpl1            0      1015.0    1015.0       89.3
*ev              0           0         0          0
*hvr             0           0         0    14960.0

** K VALUE CORRELATIONS
*KV1             0           0         0    1.459E6
*KV2             0           0         0          0
*KV3             0           0         0          0
*KV4             0           0         0   -2.548E3
*KV5             0           0         0     -331.3
```

```
** initial oil mu = 10000 cp (upgraded oil 2000 cp)
*AVISC          0.0             2.0E3       6.045E7             2.6
** Reference conditions
*prsr 101.3  *temr 20  *psurf 101.3  *tsurf 20

**============== ROCK-FLUID PROPERTIES====================
*rockfluid
*swt                                  ** Water-oil relative permeabilities
**  Sw        Krw      Krow
** -----    -------   -------
0.05      0.0       0.95
1.0       1.0       0.0

*slt  **noswc   **  Liquid-gas relative permeabilities

**  Sl        Krg      Krog
** ----     -------   ------
0.05      0.95       0.0
1.0       0.0        0.95

** ============== INITIAL CONDITIONS ====================
*initial
*pres *con 847.2
*sw *con .001
*temp *con 20
** actual asph content is 15.6 wt %
*mfrac_oil 'LLOYD_O' con 0.844
*mfrac_oil 'ASPHALT' con 0.156

** ============== NUMERICAL CONTROL ====================
*numerical
** All these can be defaulted. The definitions
** here match the previous data.
*dtmax 2.5    *upstream klevel
*bakflosw on
*rangecheck off
*norm      press 200  satur 0.2  temp 10   x 0.2  y 0.2
*converge  press 0.2  satur 0.02  temp 0.5  x  0.002  y 0.002
*rangecheck on
*converge totres normal

** ============== RECURRENT DATA ====================
*run
*time 0  dtwell 0.1
well 1 'INJTR'      ** Well list
well 2 'PRODN'
```

```
producer 2
operate min bhp 100.0
operate max bhg 5.0
operate max bhl 10.6
geometry j .11 .3687 1 0  ** rw,cc,ff,ss
perf  2  **  i j k
1 1 5  5000.0
injector mobweight 1
incomp gas   .0    0   .0    1.
tinjw 20.0
operate bhp 848.2
perf 1  ** i j k  wi
15 1 1 5000
*time 10.0
producer 2
operate max bhl 10.6
operate max bhg 50.0
*time 13.0
*time 25.0
*time 46.0
*time 66.0
*time 100
*time 140
*time 200
*time 260
*time 319
*time 397
*time 480
*time 540
*stop
```

Appendix F: Data file for Cartesian Grid

```
RESULTS SIMULATOR STARS
** Butler 2D VAPEX process is simulated

**============ INPUT/OUTPUT CONTROL====================
**checkonly
*interrupt *stop
*title1 'Vapex 2D Cartesian Grid'
*inunit lab except 6 2 ** micro-m**2
*outprn *grid pres so sg temp x viso kro krg rfg rfo masdeno masdeng
*outsrf *grid pres sw so x viso rfg rfo
*outprn *well wellcomp *outprn *iter *tss **newton
*outsrf *well downhole **mass **comp
*wrst 10 *wprn *grid 10 *wprn *iter 1

**===========GRID AND RESERVOIR DEFINITION===============
** actual size is 69.8x3.5x21.7
*grid *cart 15 1 5
*kdir *down ** Two-dimensional grid
*di *ivar 15*4.65
*dj *jvar 3.5
*dk *kvar 5*4.35
*por *con 0.391
*permi *con 1135
*permj *equalsi
*permk *equalsi
*vatype con 1
*end-grid
*prpor 915
** ============== FLUID DEFINITIONS ====================
*model 4 4 4 ** One aqueous and three oleic components
*compname 'WATER' 'LLOYD_O' 'ASPHALT' 'PROPANE'
**          -----   --------  --------  --------
*cmm          0        .450      .600      .0441
*molden       0       2.04e-3   1.6e-3    0.01151
*cp           0      1.944e-7  1.944e-7   1.151e-6
*pcrit        0        1000      1000       4246
*tcrit        0        500       500       96.65
*cpl1         0       1015.0    1015.0     89.3
*ev           0          0         0          0
*hvr          0          0         0       14960.0

** K VALUE CORRELATIONS
*KV1          0          0         0       1.459E6
*KV2          0          0         0          0
```

```
*KV3            0           0           0           0
*KV4            0           0           0      -2.548E3
*KV5            0           0           0        -331.3
** initial oil mu = 10000 cp (upgraded oil 2000 cp)
*AVISC      0.0         2.0E3     6.045E7          2.6
** Reference conditions
*prsr 101.3  *temr 20  *psurf 101.3  *tsurf 20

**============== ROCK-FLUID PROPERTIES====================
*rockfluid
*swt                              ** Water-oil relative permeabilities
**  Sw       Krw      Krow
** -----    -------   -------
0.05      0.0       0.95
1.0       1.0       0.0

*slt  **noswc   **  Liquid-gas relative permeabilities
**  Sl       Krg      Krog
** ----     -------   ------
0.05      0.95      0.0
1.0       0.0       0.95

** ============== INITIAL CONDITIONS ======================
*initial
*pres *con 847.2
*sw *con .001
*temp *con 20
** actual asph content is 15.6 wt %
*mfrac_oil 'LLOYD_O' con 0.844
*mfrac_oil 'ASPHALT' con 0.156

** ============== NUMERICAL CONTROL ====================
*numerical
** All these can be defaulted.  The definitions
** here match the previous data.
*dtmax 2.5    *upstream klevel
*bakflosw on
*rangecheck off
*norm      press 200  satur 0.2  temp 10   x 0.2  y 0.2
*converge  press 0.2  satur 0.02  temp 0.5  x  0.002  y 0.002
*rangecheck on
*converge totres normal

** ============== RECURRENT DATA ======================
*run
*time 0  dtwell 0.1
```

```
well 1 'INJTR'      ** Well list
well 2 'PRODN'
producer 2
operate min bhp 100.0
operate max bhg 5.0
operate max bhl 10.6
geometry j .11 .3687 1 0  ** rw.cc.ff.ss
perf  2  **  i j k
1 1 5  5000.0
injector mobweight 1
incomp gas    .0    0    .0    1.
tinjw 20.0
operate bhp 848.2
perf 1  ** i j k  wi
15 1 1 5000
*time 10.0
producer 2
operate max bhl 10.6
operate max bhg 50.0
*time 13.0
*time 25.0
*time 46.0
*time 66.0
*time 100
*time 140
*time 200
*time 260
*time 319
*time 397
*time 480
*time 540
*stop
```

Appendix G: Data File for Reaction Model (Model Two)

```
RESULTS SIMULATOR STARS
** Butler 2D VAPEX process is simulated

**============ INPUT/OUTPUT CONTROL ====================
**checkonly
*interrupt *stop
*title1 'Vapex 2D Corner Point Grid'
*inunit lab except 6 2 ** micro-m**2
*outprn *grid pres so sg temp x viso kro krg rfg rfo masdeno masdeng
*outsrf *grid pres sw so x viso rfg rfo
*outprn *well wellcomp *outprn *iter *tss **newton
*outsrf *well downhole **mass **comp
*wrst 10 *wprn *grid 10 *wprn *iter 1

** ============GRID AND RESERVOIR DEFINITION=============
** actual size is 69.8x3.5x21.7
*grid *corner 15 1 6
*kdir *down        ** Two-dimensional grid
*di *ivar 15*4.65
*dj *con 3.5
*zcorn
0.0  28*0.0   0.0   0.0  28*0.0  0.0                                    **1 T
4.35  2*4.25  2*4.00  2*3.875 2*3.7  2*3.5 2*3.25  2*3.125 2*2.875 2*2.75**1 B
2*2.5 2*2.4   2*2.225 2*2.0   2*1.8  1.52
4.35  2*4.25  2*4.00  2*3.875 2*3.7 2*3.5 2*3.25  2*3.125 2*2.875 2*2.75 **1 B
2*2.5 2*2.4   2*2.225 2*2.0   2*1.8  1.52
4.35 2*4.25  2*4.00  2*3.875 2*3.7 2*3.5 2*3.25  2*3.125 2*2.875 2*2.75  **2T
2*2.5 2*2.4   2*2.225 2*2.0   2*1.8 1.52
4.35 2*4.25  2*4.00  2*3.875 2*3.7  2*3.5 2*3.25  2*3.125 2*2.875 2*2.75  **2T
2*2.5 2*2.4   2*2.225 2*2.0   2*1.8 1.52
8.7   2*8.25 2*7.9 2*7.5 2*7.25 2*6.875 2*6.5 2*6.2 2*5.75 2*5.5 2*5.05  **2B
2*4.75 2*4.45 2*4 2*3.75  3.48
8.7   2*8.25 2*7.9 2*7.5 2*7.25 2*6.875 2*6.5 2*6.2 2*5.75 2*5.5 2*5.05  **2B
2*4.75 2*4.45 2*4 2*3.75  3.48
8.7   2*8.25 2*7.9 2*7.5 2*7.25 2*6.875 2*6.5 2*6.2  2*5.75 2*5.5 2*5.05 **3T
2*4.75 2*4.45 2*4 2*3.75  3.48
8.7   2*8.25 2*7.9 2*7.5 2*7.25 2*6.875 2*6.5 2*6.2  2*5.75 2*5.5 2*5.05 **3T
2*4.75 2*4.45 2*4 2*3.75  3.48
13.05  2*12.5 2*11.95 2*11.4 2*10.925 2*10.375 2*9.75 2*9.25 2*8.75    **3B
2*8.30  2*7.75  2*7.25  2*6.75  2*6.25  2*5.75  5.37
13.05  2*12.5 2*11.95 2*11.4 2*10.925 2*10.375 2*9.75 2*9.25 2*8.75    **3B
2*8.30  2*7.75  2*7.25  2*6.75  2*6.25  2*5.75  5.37
13.05  2*12.5 2*11.95 2*11.4 2*10.925 2*10.375 2*9.75 2*9.25 2*8.75    **4T
2*8.30  2*7.75  2*7.25  2*6.75  2*6.25  2*5.75  5.37
```

```
13.05  2*12.5 2*11.95 2*11.4 2*10.925 2*10.375 2*9.75 2*9.25 2*8.75      **4T
2*8.30  2*7.75  2*7.25  2*6.75  2*6.25  2*5.75  5.37
17.4    2*16.75 2*16 2*15.375 2*14.72 2*14.0 2*13.25 2*12.625  2*11.55  **4 B
2*11.2 2*10.45  2*9.75  2*9.125 2*8.45  2*7.75    7.2
17.4    2*16.75 2*16 2*15.375 2*14.72 2*14.0  2*13.25 2*12.625           **4 B
2*11.55 2*11.2 2*10.45  2*9.75  2*9.125 2*8.45  2*7.75    7.2
17.4    2*16.75 2*16 2*15.375 2*14.72 2*14.0  2*13.25 2*12.625 2*11.55  **5T
2*11.2 2*10.45  2*9.75  2*9.125 2*8.45  2*7.75    7.2
17.4    2*16.75 2*16 2*15.375 2*14.72 2*14.0 2*13.25 2*12.625 2*11.55   **5T
2*11.2 2*10.45  2*9.75  2*9.125 2*8.45  2*7.75    7.2
21.75   2*20.88 2*20.0 2*19.15 2*18.25 2*17.5  2*16.5 2*15.75 2*14.85   **5 B
2*14.0 2*13.15  2*12.35  2*11.5  2*10.75 2*9.875 9.04
21.75   2*20.88 2*20.0 2*19.15 2*18.25 2*17.5  2*16.5 2*15.75 2*14.85   **5 B
2*14.0 2*13.15  2*12.35  2*11.5  2*10.75 2*9.875 9.04
21.75   2*20.88 2*20.0 2*19.15 2*18.25 2*17.5   2*16.5 2*15.75 2*14.85   **6 T
2*14.0 2*13.15  2*12.35  2*11.5  2*10.75 2*9.875 9.04
21.75   2*20.88 2*20.0 2*19.15 2*18.25 2*17.5  2*16.5 2*15.75 2*14.85   **6 T
2*14.0 2*13.15  2*12.35  2*11.5  2*10.75 2*9.875 9.04
21.75 28*21.75  21.75 21.75  28*21.75 21.75      **6 B
*por *con 0.391
*permi *con 1135
*permj *equalsi
*permk *equalsi
*vatype con 1
*end-grid
*prpor 915
** ============== FLUID DEFINITIONS ======================
*model 6 5 5 1    ** One aqueous and three oleic components
*compname 'WATER' 'PROPANE' 'LLOYD_O' 'C31A+' 'C31B+' 'ASPHALT'
**            ----------  ------------  --------------  ---------  ---------   ------------
*cmm          0          .0441          .450        .600     .600   .600**MW oil 473.4
*molden       0   0.01151   2.04e-3   1.6e-3    1.6e-3  ** oil .972 g/cm3: prop .892
g/cm3
*cp           0  1.151e-6  1.944e-7  1.944e-7  1.944e-7
*pcrit        0      4246      1000      1000      1000
*tcrit        0     96.65       500       500       500
*cpl1         0      89.3    1015.0    1015.0    1015.0
*ev           0         0         0         0         0
*hvr          0    4960.0         0         0         0
SOLID_DEN  'ASPHALT'  0.02088 0 0
** K VALUE CORRELATIONS
*KV1      0    1.459E6    0          0         0
*KV2      0       0       0          0         0
*KV3      0       0       0          0         0
*KV4      0   -2.548E3    0          0         0
*KV5      0    -331.3     0          0         0
```

```
** initial oil mu = 10000 cp (upgraded oil 2000 cp)
*AVISC    0.0    2.6     2.0E3    6.045E7  6.045E7       ** 26.0
** Reference conditions
*prsr 101.3  *temr 20  *psurf 101.3  *tsurf 20
** Asphaltene Precipitation via Nonequilibrium Reaction Approach
**  reaction describes irreversible asphaltene deposition:
**  stoichiometry defines flocculation as converted solution component
**  which stays in liquid phase
*STOREAC  0      0        0        0       1       0
**STOREAC 0      1        0        0     0.9265    0  ** Propane Reaction
*STOPROD  0      0        0        0       0       1
*RPHASE    0     0        0        0     2       0  ** Compnt reaction phase
*RORDER    0     0        0        0     1       0  ** Compnt reaction order
*FREQFAC  0.0004   ** value chosen has unit of (min)-1
*EACT 0            ** Activation energy (J/gmol)
*RENTH 0           ** Reaction enthalpy (J/gmol)
**RXEQFOR 5   1.997E+6   -5.1e-4   32.64e-0   0   0     **  Forward reaction
equilibrium modifier  (correlation)
*blockage *o 'ASPHALT'  ** eff. perm   flow restr factor
20          2.50e+4
200         2.50e+4
**==============ROCK-FLUID PROPERTIES ==================
*rockfluid
*swt                                  ** Water-oil relative permeabilities
**  Sw       Krw      Krow
** -----    -------   -------
0.05      0.0       0.95
1.0       1.0       0.0

*slt  **noswc   **  Liquid-gas relative permeabilities
**  Sl       Krg      Krog
** ----     -------   ------
0.05      0.95      0.0
1.0       0.0       0.95
**DISPI_GAS 'PROPANE' con 30      **5E-5 m2/s.
**DISPJ_GAS 'PROPANE' con 30      **dispersion effect of Propane considered
**DISPK_GAS 'PROPANE' con 30

** ============== INITIAL CONDITIONS ====================
*initial
*pres *con 847.2
*sw *con .001                 ** So by difference
*temp *con 20
** actual asph content is 15.6 wt %
*mfrac_oil 'LLOYD_O' con 0.844
*mfrac_oil 'C31B+' con 0.156
```

```
** ============== NUMERICAL CONTROL ==================
*numerical
** All these can be defaulted. The definitions
** here match the previous data.
*dtmax 2.5   *upstream klevel
*bakflosw on
*rangecheck off
*norm      press 200  satur 0.2  temp 10   x 0.2  y 0.2
*converge  press 0.2  satur 0.02  temp 0.5  x  0.002  y 0.002
*rangecheck on
*converge totres normal
** ============== RECURRENT DATA ====================
*run
*time 0  dtwell 0.1
well 1 'INJTR'     ** Well list
well 2 'PRODN'
producer 2
operate min bhp 100.0
operate max bhg 5.0
operate max bhl 10.6
geometry j .11 .3687 1 0  ** rw,cc,ff,ss
perf  2  **  i j k
1 1 5  5000.0
injector mobweight 1
incomp gas   0    1   0    0    0
tinjw 20.0
operate bhp 848.2
perf 1  ** i j k  wi
15 1 1 5000
*time 10.0
producer 2
operate max bhl 10.6
operate max bhg 50.0
*time 13.0
*time 25.0
*time 46.0
*time 66.0
*time 100
*time 140
*time 200
*time 319
*time 397
*time 480
*time 540
*stop
```

Appendix H: Core Flooding Numerical Model

```
RESULTS SIMULATOR STARS
**  Butler 2D VAPEX process is simulated

**==========INPUT/OUTPUT CONTROL==================
**checkonly
*interrupt *stop
*title1 'Experiment'
*title2 'Vapex 2D Cartesian Grid'
*inunit  lab  except 6 2  ** micro-m**2
*outprn *grid pres so sg  temp x viso kro krg  rfg rfo  masdeno masdeng
*outsrf *grid pres sw so x viso rfg rfo
*outprn *well wellcomp  *outprn *iter *tss **newton
*outsrf *well downhole  **mass **comp
*wrst 10  *wprn *grid 10  *wprn *iter 1

**==========GRID AND RESERVOIR DEFINITION ==========
** actual size is 4.5*4.5*34cm
*grid *cart 63 1 34
*kdir *up         ** k=1 at bottom of reservoir
*di *ivar 63*0.07143
*dj *con 4.5
*dk *kvar 34*1.0
 *por *con 0.331
*permi *con 5
*permj *equalsi
*permk *equalsi
*vatype con 1
*end-grid
*prpor 915

** ============== FLUID DEFINITIONS ======================
*model 4 4 4   ** One aqueous and three oleic components
*compname  'WATER'  'LLOYD_O'  'ASPHALT'  'PROPANE'
**         -----   --------  --------  --------
*cmm       0      .450      .600      .0441    **MW oil 473.4
*molden    0    2.04e-3   1.6e-3  0.01151     ** oil .972 g/cm3; prop .892 g/cm3
*cp        0    1.944e-7  1.944e-7   1.151e-6
*pcrit     0      1000      1000       4246
*tcrit     0      500       500      96.65
*cpl1      0     1015.0    1015.0      89.3
*ev        0       0         0          0
*hvr       0       0         0     14960.0
** K VALUE CORRELATIONS
*KV1       0       0         0      1.459E6
```

```
*KV2      0       0       0       0
*KV3      0       0       0       0
*KV4      0       0       0     -2.548E3
*KV5      0       0       0     -331.3
** initial oil mu = 10000 cp (upgraded oil 2000 cp)
*AVISC     0.0     2.0E3     6.045E7       2.6       ** 26.0
** Reference conditions
*prsr 101.3  *temr 20  *psurf 101.3  *tsurf 20

**==============ROCK-FLUID PROPERTIES ====================
*rockfluid
*swt                                  ** Water-oil relative permeabilities
**  Sw       Krw      Krow
** -----    -------   -------
  0.05      0.0       0.95
  1.0       1.0       0.0
*slt  **noswc   **  Liquid-gas relative permeabilities
**  Sl       Krg      Krog
** ----     -------   ------
  0.05      0.95      0.0
  1.0       0.0       0.95

**============== INITIAL CONDITIONS ======================
*initial
*pres *con 810              ** 689kPa gauge + 88kPa barometric p: Psat=838kPa
*sw *con .001                ** So by difference
*temp *con 20
** actual asph content is 15.6 wt %
*mfrac_oil 'LLOYD_O' con 0.844
*mfrac_oil 'ASPHALT' con 0.156

** ============== NUMERICAL CONTROL ====================
*numerical
** All these can be defaulted.  The definitions
** here match the previous data.
**dtmax 2.5    *upstream klevel
**bakflosw on
**rangecheck off
**norm      press 200  satur 0.2  temp 10   x 0.2  y 0.2
**converge  press 0.2  satur 0.02  temp 0.5  x  0.002  y 0.002
**rangecheck on
*converge totres normal

** ============== RECURRENT DATA ======================
*run
*time 0  dtwell 0.1
```

```
   well 1 'INJTR'     ** Well list
   well 2 'PRODN'
   producer 2
   operate min bhp 809.99
   geometry k .11 .235 1 0  ** rw.cc.ff.ss
   perf  2  **  i j k
              32 1 1  5000.0
   injector mobweight 1
   incomp gas   .0    0   .0    1.
   tinjw 20.0
   operate bhp 812.0
   operate stg 5
   perf 1  ** i j k  wi
         32 1 34 5000
*time 10.0
*time 20
*time 30.0
*time 45.0
*time 60.0
*time 100
*time 150
*time 200
*time 240
*time 300.0
*time 360
*time 400
*time 480
*time 600
*time 720
*time 840.0
*time 960
*time 1080
*time 1200
*time 1320
*time 1380
*time 1440
*time 1680
*time 1920
*time 2160
*time 2400
*time 2880
*time 4320
*time 5760
*time 7200
*time 10080
*stop
```

Appendix I: Propane Flow Meter Calibration Curve

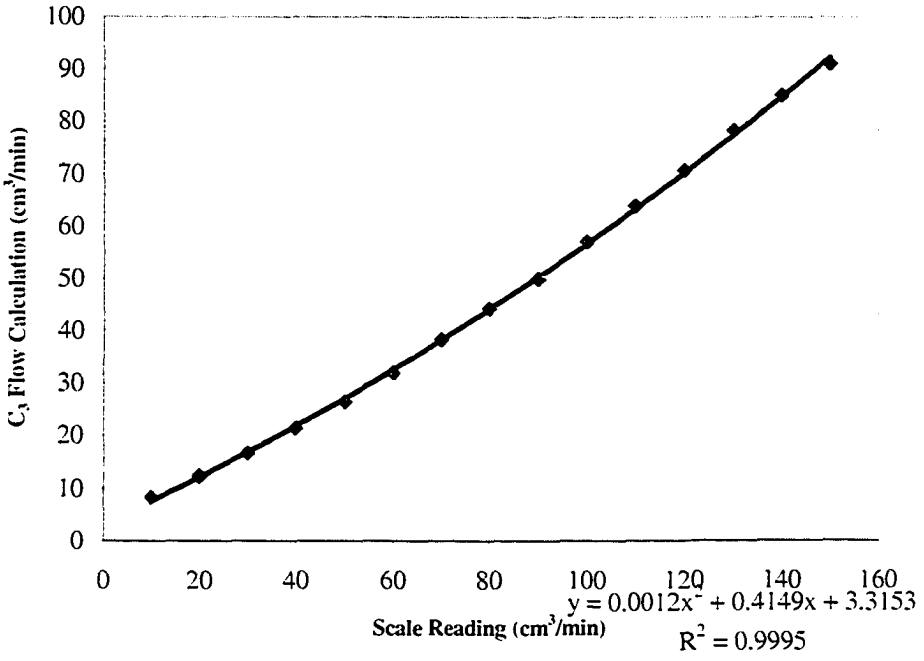

Figure I-1: Propane Flow Meter Calibration Curve